TRIBHUVAN UNIVERSITY

INSTITUTE OF ENGINEERING

PULCHOWK CAMPUS

THESIS NO: M-29-MSMDE-2018-2021

Comparative Study of Air Performance of Fully Ducted Damper for HVAC based on Different Blade Profiles

by

Gaurav Paudel

A THESIS

SUBMITTED TO

THE DEPARTMENT OF MECHANICAL AND AEROSPACE ENGINEERING

IN PARTIAL FULFILLMENT OF THE REQUIREMENTS FOR

THE DEGREE OF MASTER OF SCIENCE IN MECHANICAL SYSYTEMS DESIGN ENGINEERING

DEPATRMENT OF MECHANICAL AND AEROSPACE ENGINEERING

LALITPUR, NEPAL

MARCH, 2021

TRIBHUVAN UNIVERSITY

INSTITUTE OF ENGINEERING

PULCHOWK CAMPUS

DEPARTMENT OF MECHANICAL AND AEROSPACE ENGINEERING

The undersigned certify that they have read, and recommended to the Institute of Engineering for acceptance, a thesis entitled " **Comparative Study of Air Performance of Fully Ducted Damper for HVAC based on Different Blade Profiles** " submitted by Gaurav Paudel in partial fulfillment of the requirements for the degree of Master of Science in Mechanical Systems Design and Engineering.

____

Supervisor, Vishwa Prasanna Amatya
Associate Professor
Department of Mechanical and Aerospace Engineering

____

Supervisor, Dr. Nawraj Bhattarai
Associate Professor
Department of Mechanical and Aerospace Engineering

____

External Examiner, Roshan Thapa
Managing Director
C-zone HVAC Inc., Bishalnagar, Kathmandu

____

Committee Chairperson, Dr. Nawraj Bhattarai
Associate Professor
Department of Mechanical and Aerospace Engineering

Date

ABSTRACT

Volume control damper is a device for controlling and regulating the airflow into an indoor atmosphere and is one of the different fittings in a Heating Ventilation and Air Conditioning system. Airfoil damper blade is a best suited blade among the different damper blades in use, viz. airfoil, triple-V and flat.

A comparative air performance analysis was done between same thickness blades, one is conventional airfoil and NACA0010, other being reduced thickness of airfoil shape of conventional airfoil and NACA0006 for different air velocities.

Computational Fluid Dynamics analysis of all four cases were done in Ansys software as per American National Standards Institute and Air Movement and Control Association Standard 500D configuration 5.3. Pressure drop from conventional airfoil was compared with the data available in the American Society of Heating Refrigerating and Air-conditioning Engineers duct fitting database for different air velocities.

From the analysis of four different airfoil profile, it was found out that 4-digit NACA0010 airfoil has least pressure drop of all, and hence is the best suited profile for the damper among the damper profiles considered in the analysis. Also, superiority of 4-digits NACA airfoil profile is observed to that of conventional airfoil with respect to their total pressure drop.

ACKNOWLEDGEMENTS

I owe my sincere gratitude to my supervisors, Assoc. Prof. Dr. Nawraj Bhattarai and Assoc. Prof. Vishwa Prasanna Amatya. Without out their continuous support, encouragement and guidance, this work would not have completed on time. I would like to express my sincere thanks to Assistant Prof. Hari Bahadur Dura, Deputy Head, Department of Mechanical and Aerospace Engineering, Pulchowk Campus for his guidance in completion of this work. Also, I would like to present my gratitude to Assistant Prof. Kamal Darlami, Department of Mechanical and Aerospace Engineering, Pulchowk Campus, for suggesting for different input in the analysis.

I would like to thank professors, lecturers, staffs, and friends from Department of Mechanical and Aerospace Engineering, Pulchowk Campus for their support. I would like to thank my parents, relatives, and friends for their moral support in completion of this work.

Finally, I would like to appreciate every individual directly or indirectly involved in the completion of my thesis.

Sincerely

Gaurav Paudel

TABLE OF CONTENTS

LIST OF TABLES

LIST OF FIGURES

LIST OF ABBREVIATIONS

HVAC	Heating Ventilation and Air Condition
IAQ	Indoor Air Quality
AHU	Air Handling Unit
ASHRAE	American Society of Heating, Refrigeration and Air-conditioning Engineers
PTTFE	polytetrafluorethylene
AMCA	Air Movement and Control Association
ANSI	America National Standards Institute
RABA	Robust air balancing
CFD	Computational Fluid Dynamics
VAV	Variable Air Volume
NACA	National Advisory Committee of Aeronautics

CHAPTER ONE: INTRODUCTION

1.1 Background

HVAC system has been designed with the purpose of providing healthy and comfortable indoor atmosphere which can be achieved by controlling temperature, pressure, moisture, and indoor air quality (IAQ) (Ntourai, 2015). Temperature and moisture can be controlled by either cooling or heating the indoor air. To maintain the humidity level to the human comfort level, humidifier and/or dehumidifier can be used. Pressure can be controlled by the use of damper in the line of incoming air from the atmosphere (Ntourai, 2015). Air handling unit (AHU) can be used to supply required level of fresh air into the system.

HVAC system is broadly classified in two: Self-contained unitary system and centralized system. Unitary system has all conditioning parameters functioned in a single package and is limited to small space conditioning. While centralized system has its sub-systems/terminals to function its respective task and is generally used in large space conditioning.

Problem in the HVAC system includes system parameters variation, interaction between climatic parameters, variable conditions, intense non-linear factors, model uncertainty. These factors have to be considered while designing any of the HVAC systems. Schematic diagram of typical HVAC is shown in Figure 1-1 (Xu, 2012).

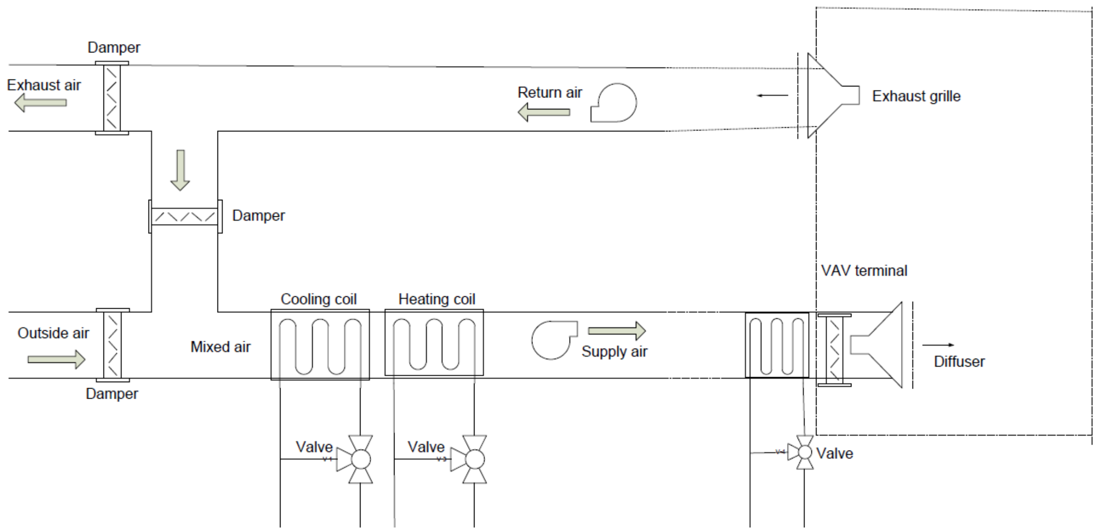

Figure 1-1 Schematic diagram of typical HVAC

The purpose of AHU in HVAC system is to maintain the air quality of the conditioned space. Indoor air quality (IAQ) of the HVAC system can be achieved through the use of dampers and fans. They control the flow of air inward and outward of the conditioned space. According to the American Society of Heating, Refrigerating and Air-conditioning Engineers (ASHRAE), over a 70-year lifespan in a developed region, indoor air constitutes around 65% of the total lifetime exposure, whereas outdoor air makes up the rest. It is therefore necessary to consider the IAQ along with temperature control of indoor environment which, if compromised, will have adverse effect on human health due to their long exposure.

Damper is a device which is used to control and regulate the flow rates in an Air-conditioning and mechanical ductwork system (Montgomery, 2009). It controls air flow pressure as per the signal transmitted from the sensor measuring the air flow pressure in the room to the actuator attached to the damper (Belimo, 1995). It is one of the prominent elements in AHU for pressurization of the indoor environment of any system. In static balancing to the design requirements of air flow network, dampers are commonly used (Laurence, 2009).

Damper is broadly classified into two in terms of blade orientation: parallel blades damper and opposed blade damper. Opposed blade damper gives better control over parallel blade damper of same size and has higher loss among the two (ASHRAE, 2017).

Following factors are considered while selecting a damper for stable and accurate control (Laurence, 2009):

1. Importance of duct length as controller for full static pressure regain is influenced adversely immediately downstream of damper.
2. Ability of damper in mixing two air streams at two different temperature level and to prevent total air volume flow stratification ahead of next section of system.

Dampers are made up of galvanized steel or extruded aluminum. Generally, aluminum is used for outdoor damper for it is resistant to oxidation. Stainless steel is used in corrosive atmosphere. Frames and blades of a damper must be heavy enough to operate without wrapping and twisting. Shaft bearing should be permanently lubricated bronze, stainless steel, or polytetrafluoroethylene (PTFE) to minimize friction.

The pressure losses due to the operation of the damper are the losses which occur across the damper and the leakage of air through the damper.

According to (AMCA, 2007), there are eight main damper installation cases:

1. AMCA Figure 5.1, entrance, ducted downstream only
2. AMCA Figure 5.2, exit, ducted upstream only
3. AMCA Figure 5.3, fully ducted
4. AMCA Figure 5.4, wall entrance
5. AMCA Figure 5.5, exit, wall mounted
6. Wall mounted, either ducted or connecting large spaces or plenums
7. Ducted, like AMCA Figure 5.3, with realistic short runs of duct before and after the damper
8. Damper is at right angles to airflow

Of all these configurations, ANSI/AMCA 500-D damper is considered for study with 12×12 inch damper size. Recommended two-blades for 12×12 inch damper is used. ANSI/AMCA configuration 5.3 is shown in Figure 1-2. Long distance before and after the damper is maintained for good airflow profile and for less total pressure loss. If damper is close to the next element of AHU of HVAC, this brings high pressure loss and poor predictability in the system.

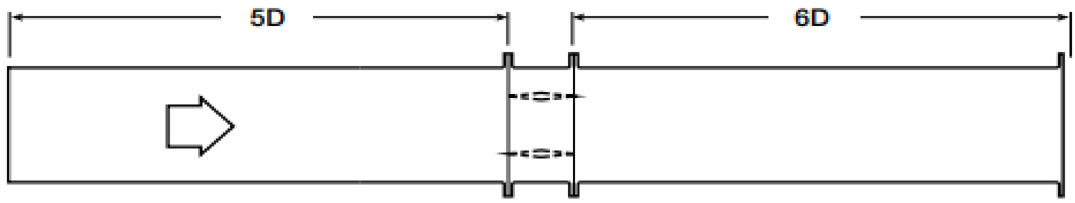

Figure 1-2 ANSI/AMCA 500D standard configuration 5.3 for fully ducted damper

(source: Greenheck)

Where, $D = \sqrt{\frac{4WH}{3.14}}$ and

W and H denote width and height of the damper

Long distance before and after the damper is maintained for good airflow profile and for less total pressure loss. If damper is close to the next element of AHU of HVAC, this brings high pressure loss and poor predictability in the system

Damper is required in HVAC system in order to positively pressurize the indoor environment and air flow control of the system.

Importance of pressurization of indoor environment is highlighted below (ASHRAE, 2017):

1. Pressurization maintains good indoor air quality (IAQ) by preventing outdoor air infiltration, protecting structure from entrance of moisture which can freeze and crack stone joints and promote mold and bacteria growth.
2. Outdoor air infiltration causes draft and IAQ is compromised.
3. Outdoor infiltration causes undue pressure on door and creates problem for people with disabilities. Just in case, it violates the American with Disability Act, 1990 in USA.

1.2 Objectives

Objective of this research is separated into main and specific objectives. Main objective is a gist of this research and specific objective sets different objectives to achieve the main objective of the research

1.2.1 Main objective

To make comparative analysis of different blade profiles of a damper.

1.2.2 Specific objective

Specific objectives of the study are undermentioned:

1. To simulate pressure loss characteristics of different blade profiles for different airflow velocities
2. To evaluate theoretical pressure loss characteristics of different blade profiles for different airflow velocities and blade numbers
3. To compare simulated result with theoretical result and analysis them

1.3 Assumptions

Assumptions that are made during this research are undermentioned:

1. Air flow is fully developed
2. Density and viscosity is constant

3. Inlet turbulence intensity is constant with the value of 5%
4. Roughness of wall and airfoil profile is smooth

1.4 Structure

Chapter one has explained briefly about the HVAC and in detail about damper which is one of the elements of HVAC. Objective of the research is mentioned here. In chapter two, relevant literature to this research are explained briefly which includes articles, manufactures brochures, loss mechanism and fluid parameters. Methodology involved to achieve the results for this research are explained in detail in chapter three. Results of the research can be seen in chapter four along with the interpretations of the result. Chapter five draws the conclusion and suggest scope of work in future.

CHAPTER TWO: LITERATURE REVIEW

2.1 Commercial Dampers

Of many manufacturers of dampers in certified list of Air Movement and Control Association (AMCA) International, Inc., some of the products are undermentioned.

2.1.1 Johnson Controls

As per the catalogue issued by Johnson Controls for VD-1630 Galvanized Steel Damper on February 2015, a low leak, galvanized steel damper with airfoil blades for higher velocity and pressure HVAC systems has been designed for standard operating condition of -40°C to 93°C. Blades used were double skin aerofoil shape of galvanized steel and nominal width of 6-inch. Blades were constructed of rollformed galvanised steel. Testing for air performance was done as per the AMCA standard 500D configurations 5.3 for standard air density of $1.201\frac{kg}{m^3}$ with all data corrected to standard conditions (Johnson Controls, 2015).

2.1.2 Greenheck

As per the catalogue issued by Greenheck Fan Corporation for VCD-33 Low Leakage Airfoil Control Damperr on December 2020, medium to high pressure and velocity systems low leakage damper with galvanised steel aerofoil blades was designed for the temperature range of -40°C to 121°C. Two skins of 20 ga.(1mm) were used as blade thickness and 5-inch width of blades. Testing for air performance was done as per the AMCA standard 500D configurations 5.3 for standard air density of $1.2\frac{kg}{m^3}$ with all data corrected to standard conditions (Greenheck, 2020).

2.1.3 Louvers & Dampers

As per the catalogue issued by Louvers & Dampers for model L517- L518 on September 2018, double skin aerofoil shape galvanized steel model width of 6⅝" operating up to maximum temperature of 200°F(93.3°C) was designed. Testing for air performance was done as per the AMCA standard 500D configurations 5.3 for standard air density of $0.075\frac{lb}{ft^3}$ with all data corrected to standard conditions (Louvers & Dampers, 2018).

2.1.4 Ruskin

As per the catalogue issued by Ruskin for CD60, class 1A leakage rated of AMCA for control damper with high performance in February 2015, one-piece aerofoil shape Galvanized steel damper of thickness 14 gauge with width of typically 6 inch was designed for the temperature range of -58°C to 135°C. Testing for air performance was done as per the AMCA standard 500D configurations 5.3 for standard air density of $0.075\frac{lb}{ft^3}$ with all data corrected to standard conditions (Ruskin, 2015).

Similarly, as per the catalogue issued by Ruskin for CD50 high performance low leakage extruded aluminum aerofoil Class 1A leakage rated control damper in February 2005, 6063T5 heavy gage extruded aluminum with width of 6 inch aerofoil shape damper blade was designed for then temperature range of -58°C to 135°C. Testing for air performance was done as per the AMCA standard 500D configurations 5.3 for standard air density of $0.075\frac{lb}{ft^3}$ with all data corrected to standard conditions (Ruskin, 2005).

2.2 Mechanism of losses

Factors affecting the flow by reducing the efficiency of turbomachinery is known as loss. It is important to understand the origin of flow loss and to properly understand physic of the flow. Primarily, there are three types of losses viz. losses due to profile, losses due to endwall and losses due to tip leakage and are dependent.

Losses due to profile are the losses that are generated in the boundary layers of a blade which is farther from the end wall for the flow in 2D. Tests of cascade in 2D and calculation of boundary layer determines the losses due to profile. Normally, losses that arises in trailing edge is considered as the losses due to profile (Denton, 1993).

Generation of secondary flow due to annulus layer of boundary which passes through the rows of blade partly contributes to development of endwall indirectly due to cumulative effects of various factors. Due to difficulties in distinguishing losses due to profile and losses due to tip leakage from the losses due to endwall, some of the times all the losses are considered to be losses due to endwall for those which are indistinguishable.

Losses due to tip leakage are the losses that is developed due to flow leakage on the blades tip. Shrouded or unshrouded nature of blade determines the loss mechanism of losses due to tip leakage. Usually, compressor with unshrouded blade has very strong interaction between losses due to leakage and losses due to endwall and are not differentiated by some methods.

Ligrani (2012) on his research “Aerodynamic Losses in Turbines with and without Film Cooling, as Influenced by Mainstream Turbulence, Surface Roughness, Airfoil Shape, and Mach Number” has studied the effects of a various physical phenomena on the turbine aerofoil aerodynamic performance for compressible and high speed flows with distributions of Mach number for either subsonic or transonic condition. Numerical results and experimental results of comparison are from investigation in a span of 32 years. He had considered the variation of intensity of free turbulence, roughness of surface Mach number at exit as these variations affects losses of integrated and local total pressures, local kinetic energy deficits, deficits of local Mach number, area averaged coefficients of loss, loss of mass averaged total pressures, coefficient of omega losses, parameters of second law loss and distribution for symmetric aerofoil of loss of integrated aerodynamics (Ligrani, 2012).

Primarily, projected losses in damper of HVAC are:

1. Pressure loss
2. Turbulence
3. Surface roughness
4. Geometry

2.2.1 Pressure Loss

The pressure loss that arises due to a damper is a function of a number of geometric, inherent construction methods and structural configurations. Factors affecting pressure drop in damper are as follows (Laurence, 2009):

1. Ratio of open free area of damper to area of the duct or wall
2. Losses due to entrance or exit effects
3. Velocities of flows
4. Flow profile before and after the damper
5. Shapes and geometry of the damper frame edges

6. Type of blade
7. Aspect ratio

Legg (1986), on his research on “Characteristics of single and multi-blade dampers for ducted air systems”, experimentally found that over the wide blade angles range, it is found that a linear relationship between the blade angle and the logarithm of the loss coefficient. To come up with the conclusion, he has tested different blade sizes, shapes and configurations. To validate his test results, he compared his results with other authors’ published test results. Based on the study, he has considered his work will be a matter of consideration for sizing of damper in order to achieve constant pressure drop in the damper (Legg, 1986).

Fanyong et al. (2019), on their research on “A robust air balancing method for dedicated outdoor air system” proposed a robust air balancing (RABA) method depending on a model of data driven. The method that is proposed includes three parts viz. developing a mathematical model depending on pressure balance at steady state for duct, training using algorithm for robust air balancing learning for model parameters and using the damper characteristic curve to find out damper positions. The proposed method performance produces more accurate prediction of pressure difference in comparison to existing method (Jing method) which was validated by laboratory test results. RABA method was found out to be better than Jing method which was known by evaluating damper position and static pressure (Fanyong, 2019).

Charles et al. (2003), on their research on “Pressure Loss Characteristics of Thin Single-Blade Flat Dampers for Square Airflow branch Ducts” studied experimentally thin single blade flat damper for its pressure loss characteristics in square branch ducts with damper width ratios range from 0.5 to 1.414 in the turbulent region. They also studied the interactions between the shaft and damper blade. They found that rectangular and circular shafts having obstruction area less than or equal to 0.16 have no relation with the pressure loss characteristics. But pressure loss characteristics depends on the blade angle of damper. They validate the result by comparing with the measurements by Legg (1986). (Charles Y.S. H. and Lam, 2003)

Annabattula (2008), on her research on “A Cfd model to predict pressure loss coefficient in circular with a motorized damper” has used computational fluid dynamics (CFD) Star CD package in determination of pressure loss coefficient of circular damper for a circular duct to evaluate distribution of pressure and the air flow in the duct. A three-dimensional CFD model was developed, and simulation was performed for five different positions of the damper from partially opened to completely opened position. The standard k-ε model with high Reynolds number was used. Simulation of duct was also done for different flow conditions for various Reynolds number. Pressure loss coefficient was evaluated using the code that generated the pressure drop across the damper (Annabattula, 2008).

Godwine et al. (2014), on their research on "A review of recent developments and technological advancements of variable-air-volume (VAV) air-conditioning systems" reviewed modelling and simulation of VAV, strategies of control and tools of optimization, the airflow characteristics of VAV systems. They also reviewed faults of some common VAV systems and their detection and diagnosis. Even, analysis and energy use and VAV air-conditioning systems current application. They pointed out that control of damper position and static pressure will control airflow in VAV sysytems (Godwine, 2014).

2.2.2 Turbulence

Importance of viscosity and inertia of flow determines if the flow is either laminar or turbulent. Reynold's number is the ratio of inertial force to viscous force. For the boundary layer with rough surface of a conduit, at lower Reynold's number itself, flow transition occurs to fully turbulent flow. Conversely, for the boundary layer with smooth surface of the conduit and carefully designed boundary conditions, flow will be laminar even in higher Reynold's number. Eddies of turbulency leads to velocity fluctuations (Bahrami, 2009).

Flow will have distinct shape in location attached to the solid boundary which is known as boundary layer. In the boundary layer, fluid velocity tends to zero which is an important feature of the boundary layer and is known as no slip condition which means velocity of fluid is as par the velocity at boundary. This condition is occurred due to the viscosity of the fluid. Here, fluid is attached to the boundary of the solid. The more the viscosity is, the more will be the resistance of the fluid resisting flow.

Turbulence occurs due to instability produced by shear in the boundary layer. Turbulence and shear are directly related. Theories and experiment prove that turbulence in boundary layer has pronounced shape of velocity profile. Vertical momentum transport is controlled by viscosity near the boundary and by turbulence away from the boundary which are the characteristics of velocity profile. Turbulence will create fluctuation in the density of velocity profile.

Flow is irregular and unsteady for higher Reynold's number, but the flow is predictable and steady when it is averaged over the time. For characteristics length, average velocity and Reynold's number, range of Reynold's number is as follows:

$0 < Re < 1$: flow is laminar with high viscosity and creeping motion
$1 < Re < 100$: flow is laminar and is dependent on Reynold's number
$100 < Re < 1000$: flow is laminar, and theory of boundary layer theory is useful
$1000 < Re < 10000$: transition of flow to turbulence
$10000 < Re < 1000000$: flow is turbulent and is moderately dependent in Reynold's number
$1000000 < Re < \infty$: flow is turbulent and is slightly dependent on Reynold's number

In this research, flow velocities considered are all in the region of turbulence.

2.2.3 Surface Roughness

Shorter frequencies in comparison with troughs of surfaces of real object is known as surface roughness (Denton, 1993). For operating aerofoil surfaces, surface roughness is a basic feature. Longer service time, natural collections and manufacturing processes will enhance surface roughness.

For fluid dynamics and heat transfer, surface roughness has larger impact. Surface roughness has higher consequences in the development of flow beyond critical value of Reynold's number and also enhance boundary layer as it goes from laminar to turbulence. Considering the frame material as galvanised steel, it is assumed that effective roughness as0.00592in (ASHRAE, 2017). For airfoil as 6063 T5 extruded aluminium, roughness is considered as 0.0015in from M and K Metals.

2.2.4 Geometry

Airflow is restricted by blocking the duct in a damper. Type of frame, type of blade profile, linkage, comer brace changes the free area slightly. In the case of round damper, only prominent blockade is due to the blade profile.

Opposed blade and parallel blade orientations are two common variants of control dampers. With respect to linkage mechanism, parallel blade dampers are also called single acting damper and opposed blade dampers are also called double acting dampers. Linkage in damper can be allocated individually to each blade profile but are most of the times to a side in the frame itself (Laurence, 2009).

Blade profile can be of varied height in a damper. Commonly one damper blade is larger than that of other. Damper shaft is usually mounted in the middle of the damper blade profile, but there are cases that damper shaft are unbalanced in the blade profile. Flow characteristics is varied depending in mounting variations.

Blade seals which are used for the purpose of reducing leakage extends beyond the profile of the blade and its consequences can be seen in the flow primarily at initial 15° of opening. Flow characteristics difference is observed as different way of sealing is done. Linkage of high quality dampers are repeatable and are better in quality.

Experiments regarding airflow in and around the damper are very little. Theoretical analysis is based on data of thick wall orifice and airstream blockade. Hard data is obtained primarily from the manufacturers' test data. Study of effects with respect to different irregular flow profile of damper is yet to observed.

Sinisa et al. (2015), on their research on "Air torque position damper energy consumption analysis" has studied the air torque position damper energy consumption which depends on structure of it. Air torque position damper is a device for flow measurement, otherwise it is flow control device in HVAC. They made a comparison of energy consumption among four types of damper having non-cascading blades viz. with two opposed blades, with two parallel blades, with two blades of which one is measuring, and the other is fixed in horizontal position and with one blade. It was found that the third one is the energy efficient for same measurement accuracy level as per American National Standard Institute (ANSI) standard test. Straight line ducting was made before and after the damper for the test. They also developed the mathematical model for these four arrangements of damper (Sinisa, 2015).

Becelaere et al. (2003) have conducted experiment for triple V and airfoil blade profiles for different ANSI/AMCA standard 500D arrangements and have their results in "Flow resistance of modulating characteristics of control damper (RP-1157), final report" (Becelaere, 2004)

2.3 Fluid parameters involved in a damper

Fluid parameters that need consideration in a damper are:

1. Density
2. Viscosity
3. Temperature
4. Reynold’s number
5. Speed of sound

2.3.1 Density

Quantity of matter that is contained in unit volume of the substance is called density. When the density of the substance is nearly constant, flow is called as incompressible flow. But, when density varies by more than 5 percent, the flow is called as compressible flow. Mach number for this case is 0.3 at room temperature. In this research, calculation is made for corrected density of $1.201\frac{kg}{m^3}$ as per ANSI/AMCA 500D.

2.3.2 Viscosity

Internal resistance to flow of the fluid is known as viscosity. Newtonian fluid has rate of deformation of fluid proportional to the shear stress. Commonly, ratio of dynamic viscosity to the density of fluid is used and is known as kinematic viscosity. In this research, viscosity value for density $1.201\frac{kg}{m^3}$ is $1.8189\frac{kg}{m-s}$ which is considered with reference to heat and mass transfer data book (Kothandaraman, 2014). In general, the viscosity of a fluid mainly depends on temperature. Viscosity of fluid is directly proportional to the temperature for liquid and is inversely related to temperature for gases.

2.3.3 Temperature

Temperature is the measure of hotness and coldness of a system. According to the thermodynamics perspective, temperature is the measure of internal energy of a system. For density of $1.201\frac{kg}{m^3}$, temperature is assumed to be 21°C.

2.3.4 Velocity

Highly viscous flow of the fluid at lower velocity is laminar flow and flow of fluid at high velocity is termed as turbulent flow. The intermediate range of the flow between laminar and turbulent flows is known as transitional flow. Reynold's number is a main factor that determines whether the flow is laminar or turbulent. Also it determines if the flow is steady or unsteady, with fluid properties remaining unchanged.

2.3.5 Speed of sound

Introduction of disturbances in the fluid at some finite velocity is due to the consequences of compressibility of the fluid. Velocity at which propagation of disturbance occurs is known as speed of sound. As the Mach number for the different velocities taken into consideration in the research are less than 0.3, airflow is assumed to be incompressible.

Mee et al. (1992) on their research "An Examination of the Contributions to Loss on a Transonic Turbine Blade in Cascade" experimentally measured transonic blades of turbine for linear cascade loss. Measurement in detail for rear part of suction blade surface boundary layer and wake transverse data examination were done to determine boundary layer individual components and to determine losses in mixing and in shock. It was concluded through result that overall losses in regimes of various Mach number are significantly affected by each component (Mee, 1992).

2.4 Problem statement

Airflow control and pressurization in HVAC is maintained by positioning of damper blades as per the flow velocity. To obtain efficiency in the result, blade profile plays an important role. This study is basically focused on comparative study of different blade profiles to obtain efficiency in the damper performance.

CHAPTER THREE: RESEARCH METHODOLOGY

Research methodology flow chart is undermentioned in Figure 3-1 and are explained.

\

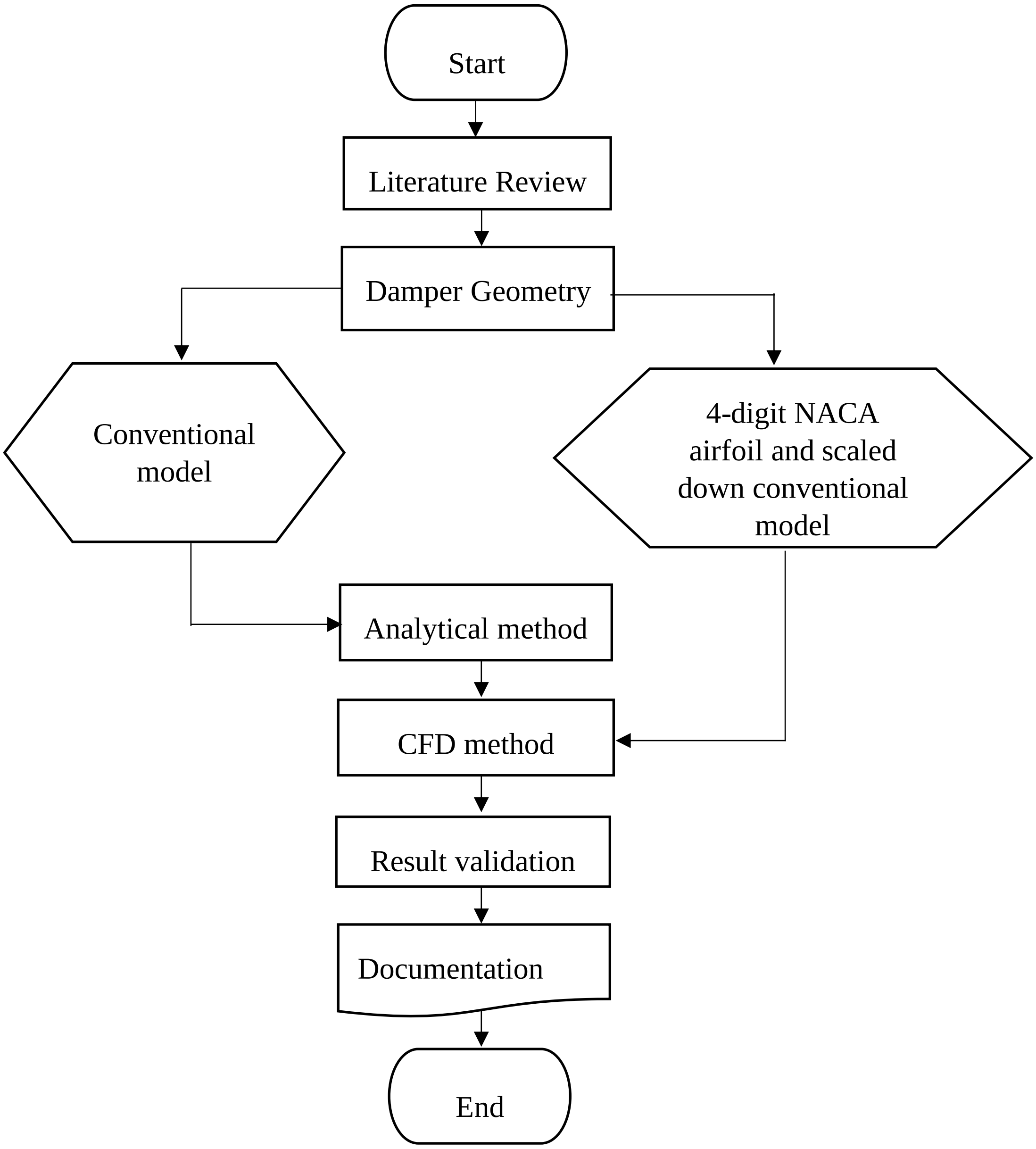

Figure 3-1 Flow chart of Research Methodology

3.1 Damper Geometry

Basic model of damper includes frame, blade, axle, jackshaft, side seal, linkage, and blade seal. For motorized damper, actuator is also a part of the damper.

3.1.1 Conventional model

Normally, available variety of damper blades are flat, triple V (3V) and aerofoil. But latter two types of blades are prominently used in damper with aerofoil blades being highly efficient. Models of aerofoil damper blade considered are similar to that of airfoil blade researched by Becelaere er al. (2004). Length and width of blade for analysis are 12 inches and 6 inches respectively.

3.1.2 Airfoil as dampers

In order to study if there is any scope for enhancing the performance of damper, this study primarily focuses on development of new model of damper blades. In this research, some of the 4-digit NACA symmetric airfoils have been purposed for the study. Reason behind selecting symmetric airfoils as damper blades is that they produce less lift and more drag in comparison to asymmetric airfoils. Also, there is more concern in the research regarding airflow control and indoor pressurization than lift. Length and width of blade for analysis are 12 inches and 6 inches, respectively.

Proposed model of damper blades for the research are:

1. Conventional airfoil
2. NACA0010
3. Conventional airfoil with reduced thickness of 0.36 in
4. NACA0006

Figure 3-2 shows the model profiles as proposed. All dimensions in the figure are in inches.

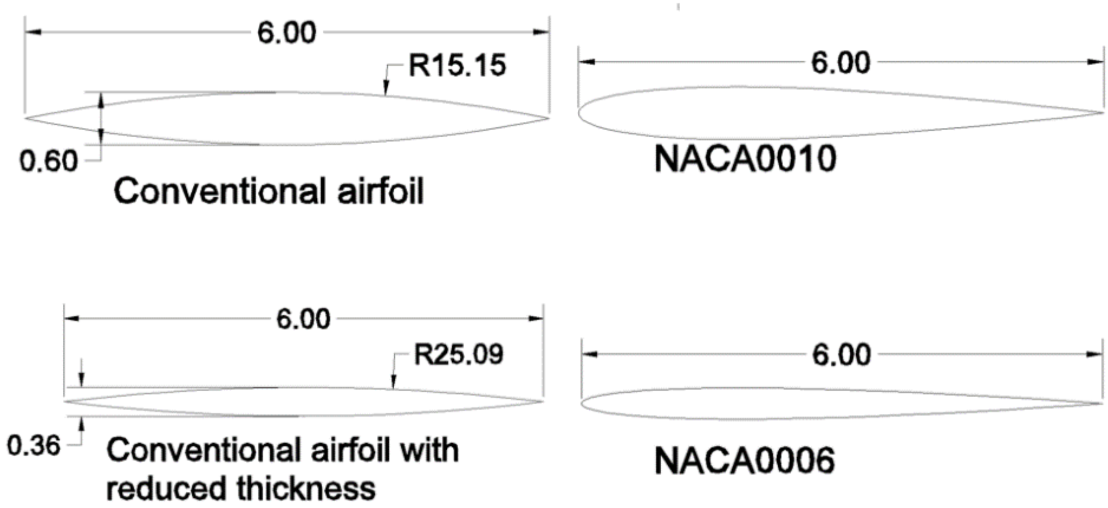

Figure 3-2 Proposed damper blades

3.2 CFD Methods

Flow chart of CFD method is shown in Figure 3-3.

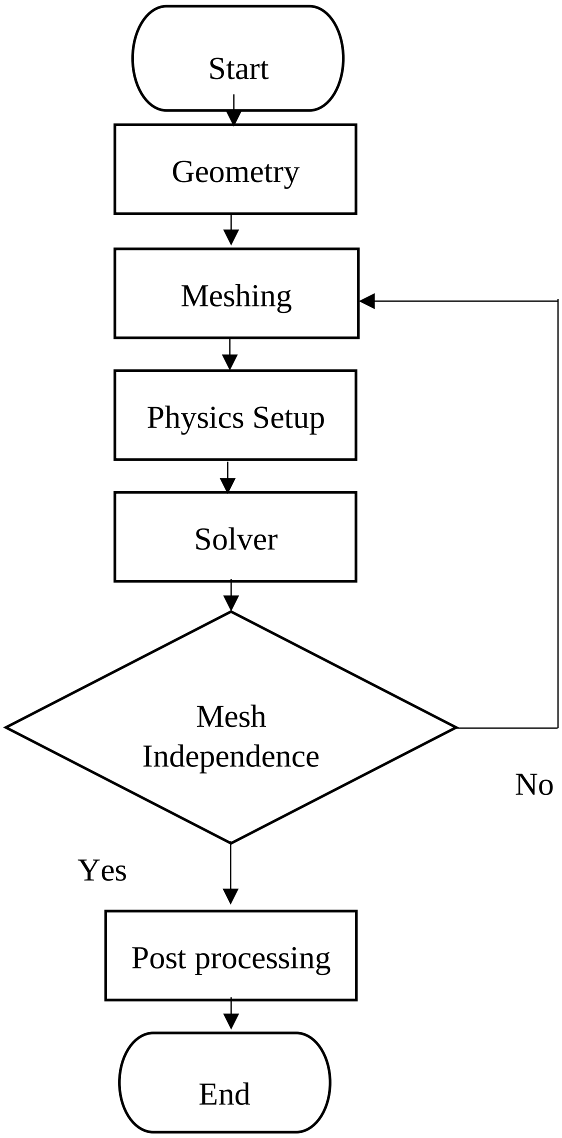

Figure 3-3 Flow chart for CFD analysis

3.2.1 Geometry

Geometry of the model for purposed blade and conventional aerofoil blades was first developed in Autodesk Autocad 2017 for the size of 12”×12” and was imported in DesignModeler in Ansys Fluent. Fill tool was used to define air domain and Boolean operation was performed to subtract blade profile from air domain. In order to reduce computational time, symmetric profile is cut using symmetry tool in symmetric plane. Figure 3-4 shows the geometry of conventional airfoil profile in DesignModeler.

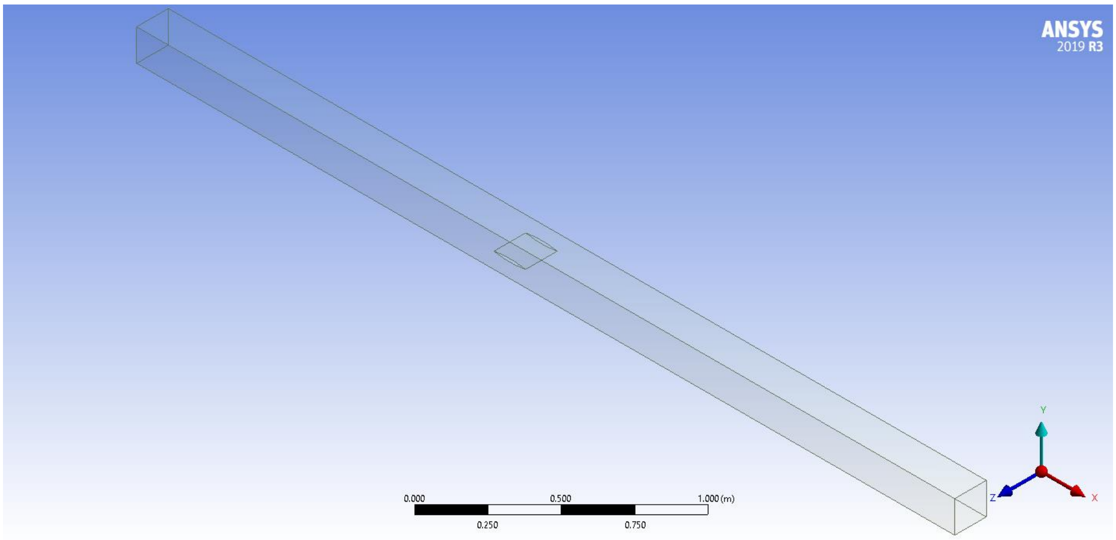

Figure 3-4 Geometry of conventional airfoil profile

3.2.2 Meshing

After geometry was made, meshing was done. Patch conforming method was applied on air domain and faces and edges on airfoil-air domain interface were refined. Name was selected as inlet, outlet, symmetric plane, airfoil and wall for the respective surface and fluid body is set as air domain. Mesh independency tests were performed for each physics set up for 1% imbalance consecutive tests with increase in test elements by 1.5 times the preceding one. Figure 3-5 shows a refined mesh of conventional airfoil at 500 fpm.

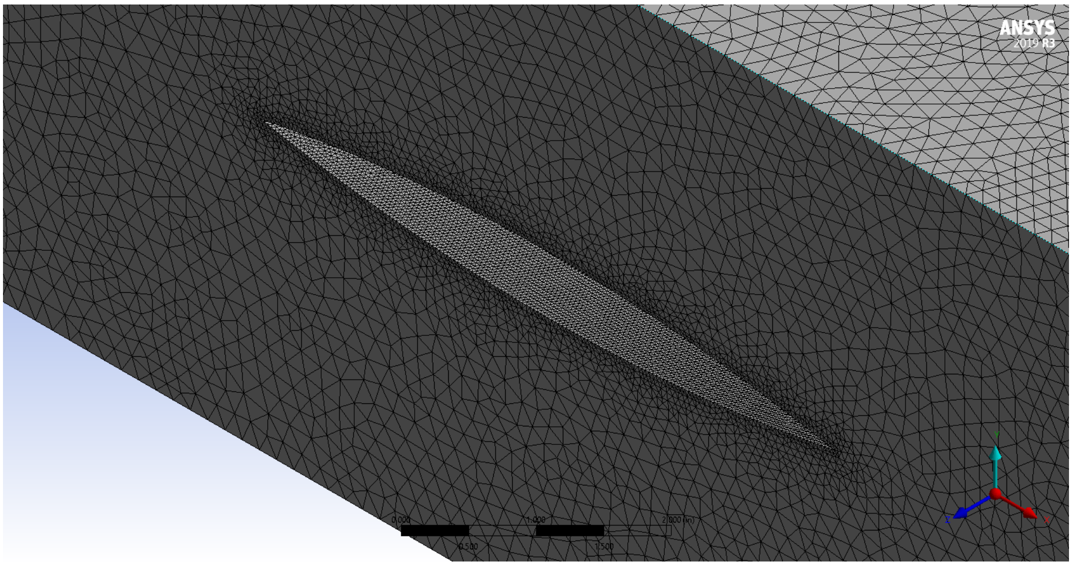

Figure 3-5 Refined mesh of conventional airfoil at 500 fpm

3.2.3 Physics Setup

Once meshing was done, parameters were set in fluent. Standard k-epsilon model with standard wall treatment was set. Then, material was selected as air of density $1.201\frac{kg}{m^3}$ as per ANSI/AMCA 500D fig 5.3. The viscosity is set as $1.8189 \times 10^{-5}\,\frac{kg}{m-s}$ from property value at one atmospheric pressure corresponding to $1.201\frac{kg}{m^3}$.

Next, boundary condition at inlet is set for velocity of 500fpm and increased in step of 500 to 3000fpm for next simulations. Boundary conditions and their respective values are tabulated in table 3-1. Same boundary conditions are applied in other cases as well other than varying velocity at inlet.

Table 3-1 Boundary conditions and values for 500 fpm conventional airfoil

S. N	Name	Boundary Condition	Boundary Value
1	Inlet	Velocity	500fpm
2	Outlet	Gauge Pressure	0 in w. g
3	Wall	No slip	Roughness height of 0.00591 in
4	airfoil	No slip	Roughness height of 0.0015 in

3.2.4 Solver

Solver used for the numerical analysis was pressure based with absolute velocity formulation at steady state condition. Here, hybrid initialization of solution was done.

3.2.5 Post processing

Once simulation is done, result of pressure drop between a plane 1 D before damper and outlet was calculated as mass flow averaged total pressure for surface integral as per ASHRAE standard 120 and ANSI/AMCA 500D. Pressure measurement point on ANSI/AMCA 500D configuration 5.3 as per ASHRAE standard 120 is shown in Figure 3-6.

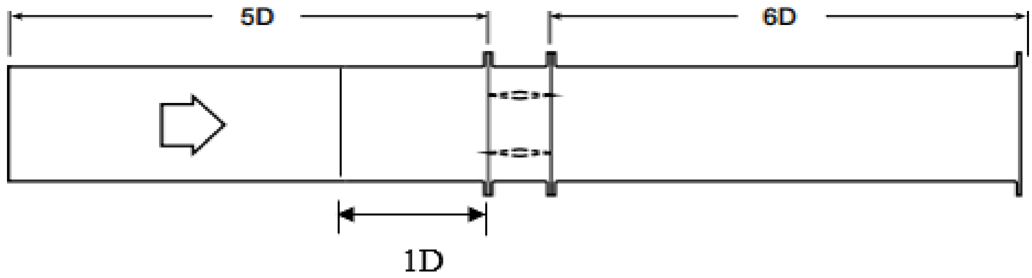

Figure 3-6 ASHRAE STANDARD 120 application on ANSI/AMCA 500D

3.3 Analytical Method

For the purpose of validation of the simulation, ASHRAE duct fitting database is referenced. In the database, airfoil damper data are based in the airfoil selected in the research “Flow resistance characteristics of the airflow control dampers” by Becelaere et al. (2004). Simulated airfoil blade selected is as par the conventional blade profile selected for the analysis.

Pressure drop data is available for different velocities for the conventional airfoil damper of size 12”×12” using ASHRAE Duct fitting Database v6.0.

3.4 Result Validation

Evaluating air performance of a damper is basically finding out of pressure drop of the damper for different velocities. ANSI/AMCA has standardized that manufacturers have to test for pressure drop to get certified for the air performance of the damper. To validate the result, pressure drop results obtained from the simulation of the conventional blade profile is compared with the analytical result of the same profile.

3.5 Software

Simulation software used in this research was Ansys. It uses computer based numerical techniques to solve the physics problem. Of different analysis system available in Ansys, fluid flow (fluent) was used as research is based on the air (fluid) performance.

CHAPTER FOUR: RESULT AND DISCUSSION

4.1 Mesh Independency study

Mesh independency studies in computational fluid dynamics is done to avoid the results as a consequence of mesh resolution rather to rely on physics and boundary conditions used. Solution of mesh independency is based on selected mesh to solve turbulence model and fluid flow to evaluate the physics of the problem. Mesh independency study is an important parameter to solve CFD problem in evaluating balance between density of mesh and final solution which is an initial step to know the accuracy of the result. Mesh independency is confirmed if there is 1% imbalance for increase in elements by one and half times.

Mesh independent study of NACA0010 at 3000fpm is Figure 4-1.

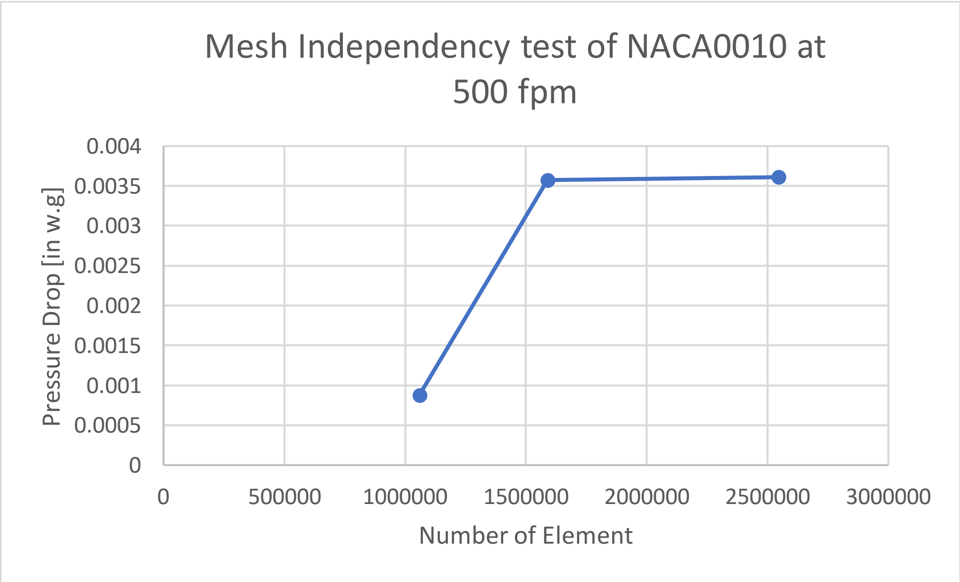

Figure 4-1 Mesh independent study of NACA0010

4.2 Validation of Result

Results of CFD analysis and pressure data of 12” ×12” airfoil blade damper obtained from Ashrae duct fitting database for the conventional airfoil used by Becelaere et al.(2004) is tabulated in table 4-1.

Table 4-1 Results of CFD analysis and ASHRAE duct fitting database of conventional airfoil

Velocity (fpm)	Total pressure drop (in w.g) from CFD software	Total pressure drop (in w.g) from ASHRAE Duct fitting Database	Percentage Variation (%)
500	0.00361	0.00281	-28.5
1000	0.01030	0.01122	8.20
1500	0.02147	0.02525	15.0
2000	0.03678	0.04489	18.1
2500	0.05627	0.07014	19.8
3000	0.08088	0.10100	20.0

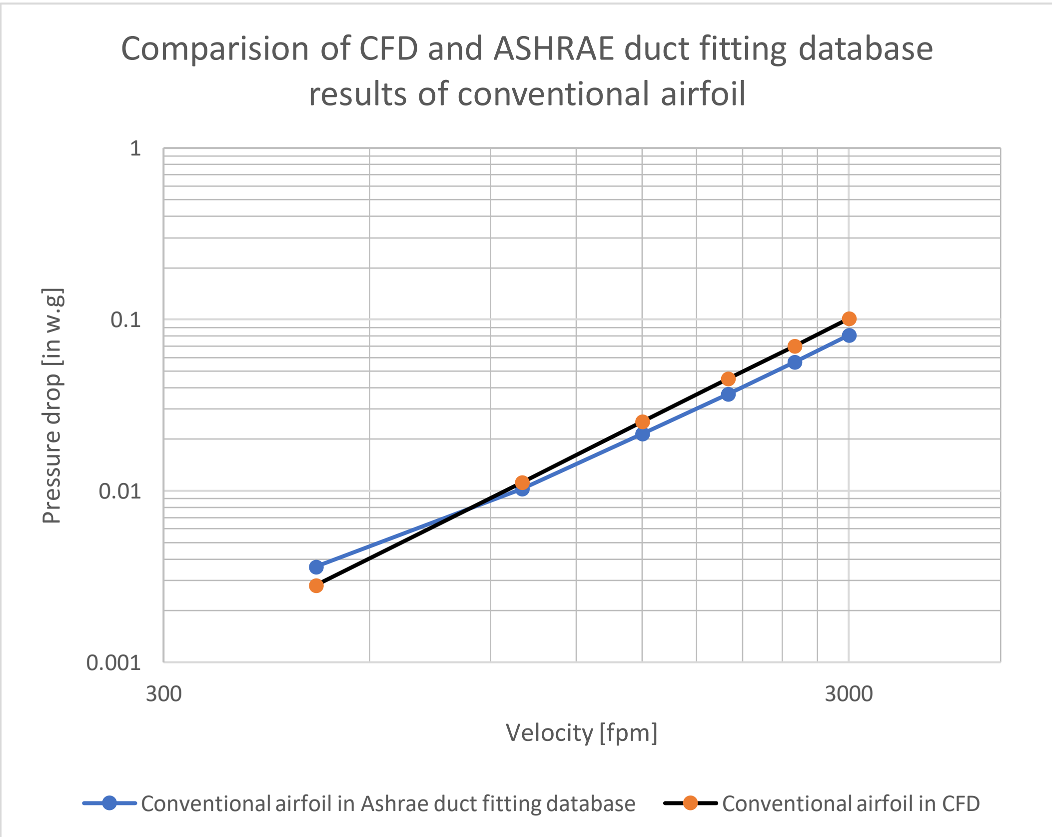

Figure 4-2 Logarithmic chart of CFD and ASHRAE duct fitting database results of conventional airfoil

Table 5-2 CFD results of all the simulations performed

Velocity (fpm)	For the thickness of 0.6 in			For the thickness of 0.36 in		
	Pressure drop (in w.g)		Percentage variation (%)	Pressure drop (in w.g)		Percentage variation (%)
	Conventional	NACA0010		Conventional with reduced thickness	NACA0006	
500	0.00361	0.00195	46.0	0.00382	0.00382	0.00
1000	0.01030	0.00624	39.4	0.01012	0.01007	0.49
1500	0.02147	0.01313	38.8	0.02110	0.02093	0.81
2000	0.03678	0.02254	38.7	0.03614	0.03578	0.10
2500	0.05627	0.04098	27.2	0.05537	0.05471	1.19
3000	0.08088	0.04834	40.2	0.07784	0.07765	0.24

Result of CFD and data of airfoil blade damper from ASHRAE duct fitting database has ±30 % variation. Percentage variation of total pressure drop from ASHRAE duct fitting database to CFD analysis is negative at 500fpm but is positive in all other velocities considered. This variation could be probably due to extrapolation inaccuracies in lower velocity. Graphical representation of total pressure drop in table 4-1 is represented in Figure 4-2. It can be seen that CFD analysis result of conventional airfoil result has higher total pressure drop than that of ASHRAE duct fitting database with the exception for 500fpm velocity.

4.3 Total Pressure Drop

CFD results of all the simulations performed is tabulated in table 5-2. It can be seen that NACA0010 blade outpass all other three blades with its least pressure drop from logarithmic chart is presented in Figure 4-3.

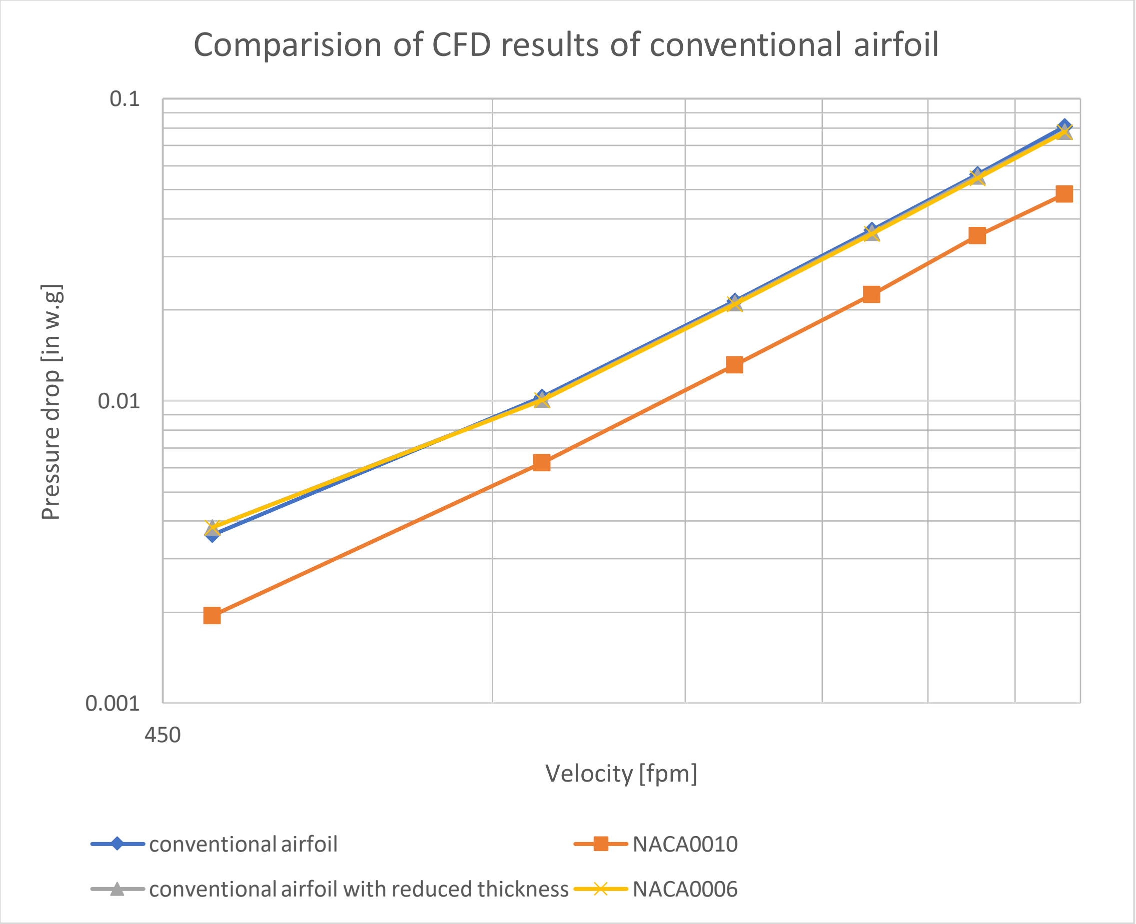

Figure 4-3 Logarithmic chart of CFD results of all the simulations performed

4.4 Turbulence Intensity

Turbulence intensity contour for different velocities for conventional blade profiles is given in Figure 4-4.

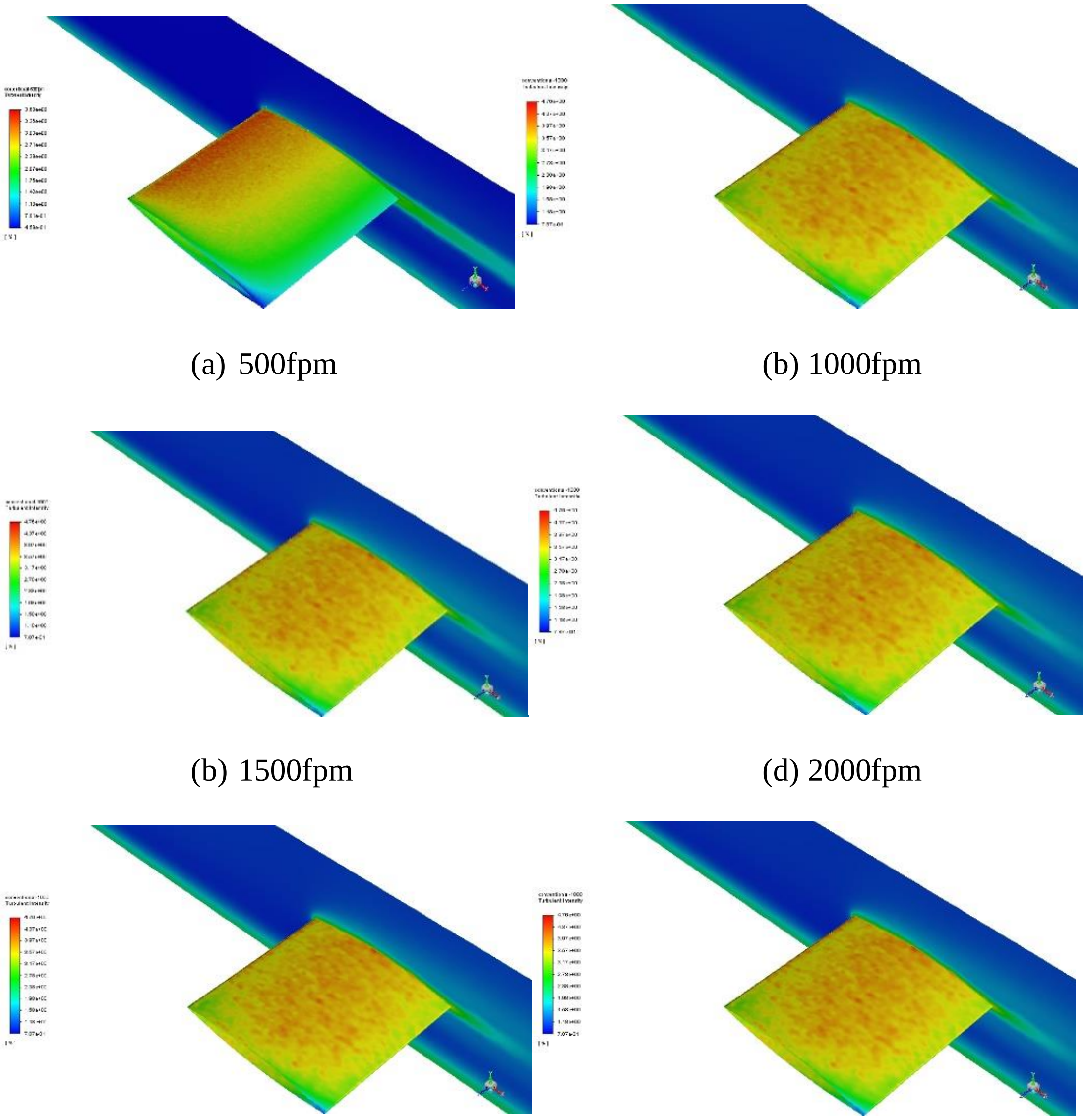

(a) 500fpm (b) 1000fpm

(b) 1500fpm (d) 2000fpm

(e) 2500fpm (f) 3000fpm

Figure 4-4 Turbulence intensity contour for different velocities for conventional blade profiles

From the figure 4-4, it is found that turbulence intensity is higher in higher velocities. Turbulence intensity range for 3000fpm is 2.36-12.0%, while it is 0.459-3.69% in 500fpm velocity for conventional airfoil. It can be seen that trailing edge of airfoil for 500fpm has lower turbulence intensity than that in leading edge. But for 3000fpm, higher turbulence intensity is spread all over the profile. For enlarged plot of given cases and other profiles turbulence intensity, refer appendix A.

4.5 Pressure Losses

Total pressure drop contour for different velocities for conventional blade profiles is given in Figure 4-5.

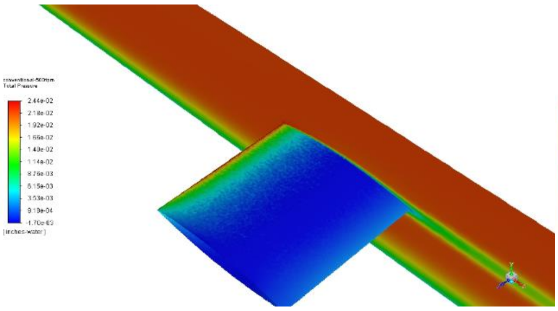

(a) 500fpm

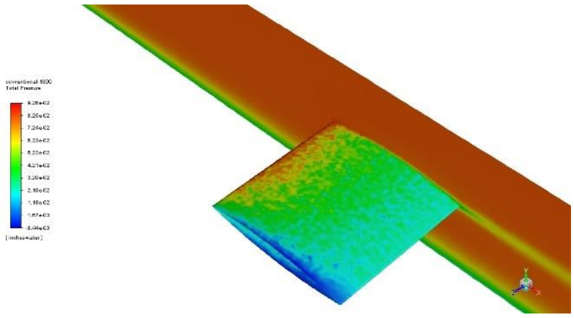

(b) 1000fpm

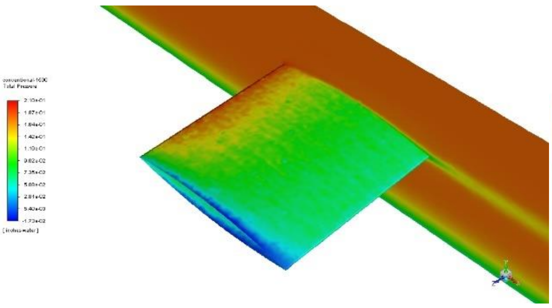

(c) 1500fpm

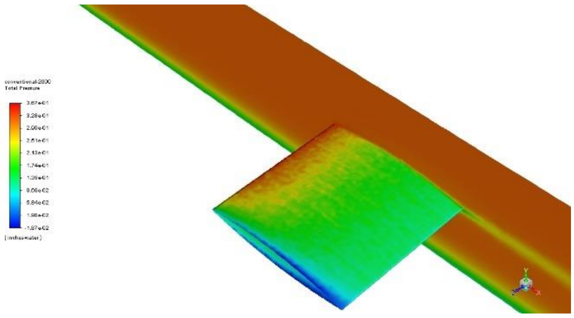

(d) 2000fpm

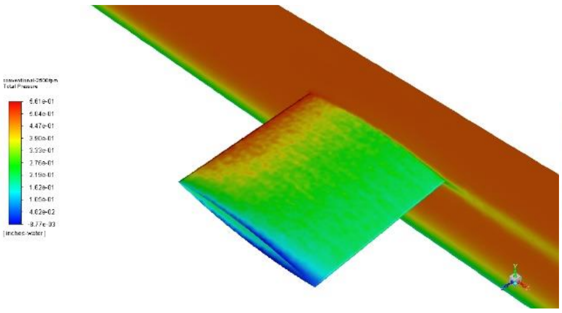

(e) 2500fpm

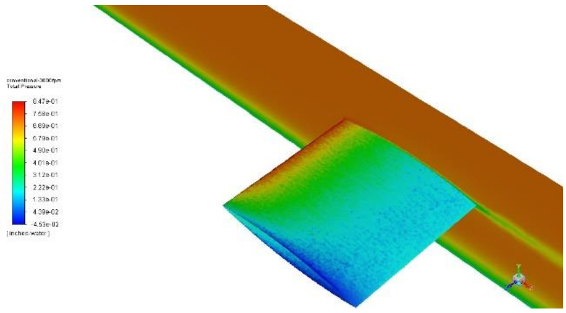

(f) 3000fpm

Figure 4-5 Total pressure drop contour for different velocities for conventional blade profiles

From the figure 4-5, it is found that total pressure drop is higher in leading edge than that in trailing edge. Also, total pressure drop is negative short after leading edge in 500 fpm, but it is positive throughout in 3000fpm exception being on wall side of the profile. Total pressure drop range from -0.0017 to 0.0244 in w.g for 500fpm, while 3000fpm has it range from -0.0453 to 0.847 in w.g. For enlarged plot of given cases and other profiles total pressure, refer appendix B.

4.6 Velocity Vector

Velocity vector for different velocities for conventional blade profiles is given in Figure 4-5

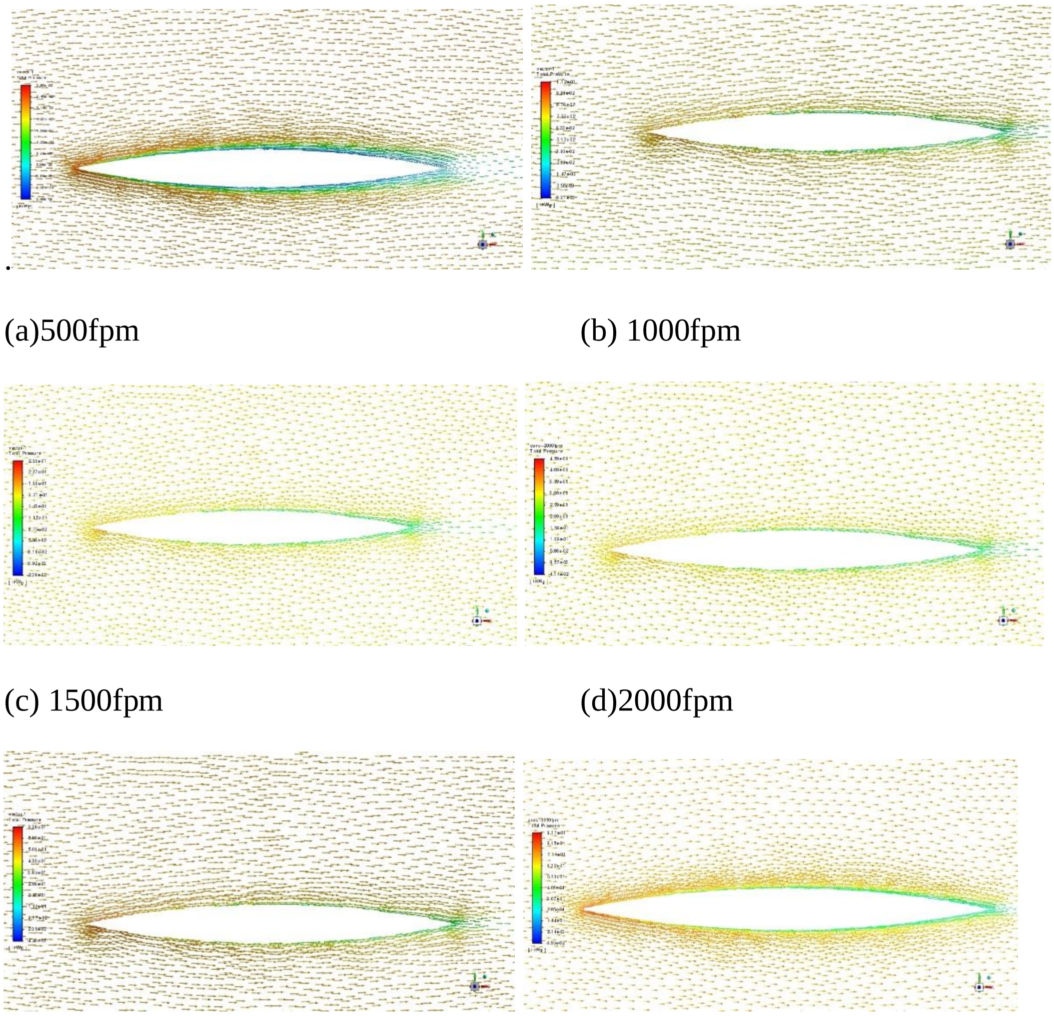

(a)500fpm (b) 1000fpm

(c) 1500fpm (d)2000fpm

(e) 2500fpm (f) 3000fpm

Figure 4-6 Velocity vector for different velocities for conventional blade profiles

Velocity vector coloured with total pressure has higher value of total pressure at leading edge and lower values at trailing edge of 500fpm as seen from the colour legends. As the velocity increases, higher values of total pressure moves towards trailing edge covering the airfoil and lower total pressure values are confined in the proximity leading edge. the For enlarged plot of given cases and other profiles velocity vector, refer appendix C.

CHAPTER FIVE: CONCLUSION AND FUTURE RECOMMENDATION

5.1 Conclusion

1. From the analysis of four different airfoil profile, it is found out that 4-digit NACA0010 airfoil has least pressure drop of all. Hence it can be concluded that NACA0010 is best suited profile for the damper among the damper profiles considered in the analysis.
2. It is found that NACA0010 has less pressure drop than the conventional damper profile and is the same case with respect to NACA0006 and conventional damper profile reduced to the thickness of 0.36 in. Here, it can be distinguished the superiority of 4-digit NACA profiles with conventional profiles of blade for the purpose of use in HVAC dampers.

5.2 Suggestion for future

1. There is the scope for the analysis of profiles used as damper blade in this research for different blade angle positions to find the pressure loss coefficient.
2. Different damper sizes can also be analysed for their pressure drop calculations.

REFERENCES

Abdel-Rahman, A. a. (1997). Surface roughness effects on flow over aerofoils. *Wind Engineering, 21*(3).

AMCA. (2007). *ANSI/AMCA Standard 500-D Laboratory methods of Testing Dampers for Rating.* Air Movement and Control Association International, Inc.

Annabattula, P. (2008). *A Cfd model to predict pressure loss coeffifficient in circular ducts with a motorized damper.* UNLV Retrospective Theses & Dissertations. doi:http://dx.doi.org/10.25669/paqq-wgwd

ASHRAE. (2017). *ASHRAE Fundamentals.* American Society of Heating, Ventilation and Air-conditioning Engineers.

Bahrami, M. (2009). Fluid mechanics-viscous flow in ducts.

Becelaere, R. V. (2004). RP-1157 - FLOW RESISTANCE AND MODULATING CHARACTERISTICS OF CONTROL DAMPERS. *ASHRAE Research Project Report*.

Belimo. (1995). *Damper application guide 1.* Belimo Aircontrols (USA), Inc.

Charles Y.S. H. and Lam, H. N. (2003). Pressure Loss Characteristics of Thin Single-Blade Flat Dampers for Square Airflow Branch Ducts. *HVAC&R Research, 9*(3), 327-345. doi:DOI: 10.1080/10789669.2003.10391073

Denton, J. D. (1993). Loss Mechanisms in Turbomachines. *The 1993 IGTI Scholar Lecture. 115*, pp. 621-656. American Society of Mechanical Engineers.

Fanyong, C. C. (2019). A robust air balancing method for de dicate d outdoor air system. *Energy & Buildings, 202*. doi:https://doi.org/10.1016/j.enbuild.2019.109380

Farinaz, B. N. (2018). Review of control techniques for HVAC systems-Nonlinearity approaches based on fuzzy cognitive maps. *Energies 2018*.

Godwine, S. O. (2014). A review of recent developments and technological advancements of variable-air-volume (VAV) air-conditioning systems. *Renewable and Sustainable Energy Reviews, 59*, 784-817. doi:https://doi.org/10.1016/j.rser.2015.12.328

Greenheck. (2020). *Model VCD-33 Low Leakage Airfoil Control Damper.* Greenheck Fan Corporation. Retrieved from www.greenheck.com.

Johnson Controls. (2015). *VD-1630 Galvanised Steel Damper.* ANSI/AMCA Standard 500-D Laboratory methods of Testing Dampers for Rating. Retrieved from www.johnsoncontrols.com

Kothandaraman, C. a. (2014). *Heat and mass transfer data book.* New Age International Ltd.

Laurence, G. F. (2009). *Dampers and Airflow Control.* American Society of Heating, Refrigerating and Air-Conditioning Engineers, Inc.

Legg, R. C. (1986). Characteristics of single and multi-blade dampers for ducted air systems. *7*(4). doi:doi:10.1177/014362448600700402

Ligrani, P. (2012). Aerodynamic Losses in Turbines with and without Film Cooling, as Influenced byMainstreamTurbulence, Surface Roughness, Airfoil Shape, andMach Number. *International Journal of Rotating Machinery, 2012*. doi:doi:10.1155/2012/957421

Louvers & Dampers. (2018). *Model L517 - L518 Steel Control Damper.* Louvers & Dampers. Retrieved from www.louvers-dampers.com

Mee, D. B. (1992). Examination of the contribution to loss on a transonic turbine blade in cascade. *Journal of turbomachinery, 114*(1).

Montgomery, R. a. (2009). *Fundamentals of HVAC Control Systems.* American Society of Heating, Refrigerating and Air-Conditioning Engineers, Inc.

Munson, B. Y. (2009). *Fundamentals of fluid mechanics.* John Wiley and sons, Inc.

Ntourai, I. a. (2015). *Modelling and Control of a multi-zone HVAC-system.* Aalborg University, Esbjerg Campus, Energy Department. SAMCO maritime.

Ruskin. (2005). *CD50 LOW LEAKAGE CONTROL DAMPER.* Kansas City: RUSKIN. Retrieved from www.ruskin.com

Ruskin. (2015). *CD60 AMCA CLASS 1A LEAKAGE RATED, HIGH PERFORMANCE CONTROL DAMPER.* Kansas City: RUSKIN. Retrieved from www.ruskin.com

Sinisa, B. D. (2015). Air torque position damper energy consumption analysis. *Energy and Buildings, 99*, 131-139.

Wang, S. (2001). *Handbook of air conditioning and refrigeration* (second ed.). McGraw-Hill companies, Inc.

Xu, G. (2012). *HVAC system study: a data-driven approach.* University of Iowa, Graduate College. Iowa Research Online. Retrieved from https://doi.org/10.17077/etd.g4aewujp

PUBLICATION

Paudel G., Amatya V. P., Bhattarai N. and Dura, H. B. (2021), Comparative Study of Air Performance of Fully Ducted Damper for HVAC based on Different Blade Profiles, IOE Graduate Confrerence, 2021, 9 (Accepted for oral presentation)

APPENDIX A: TURBULENCE INTENSITY CONTOUR PLOT OF DIFFERENT PROFILES FOR DIFFERENT VELOCITIES

A1: Turbulence intensity contour plot of conventional airfoil for different velocities

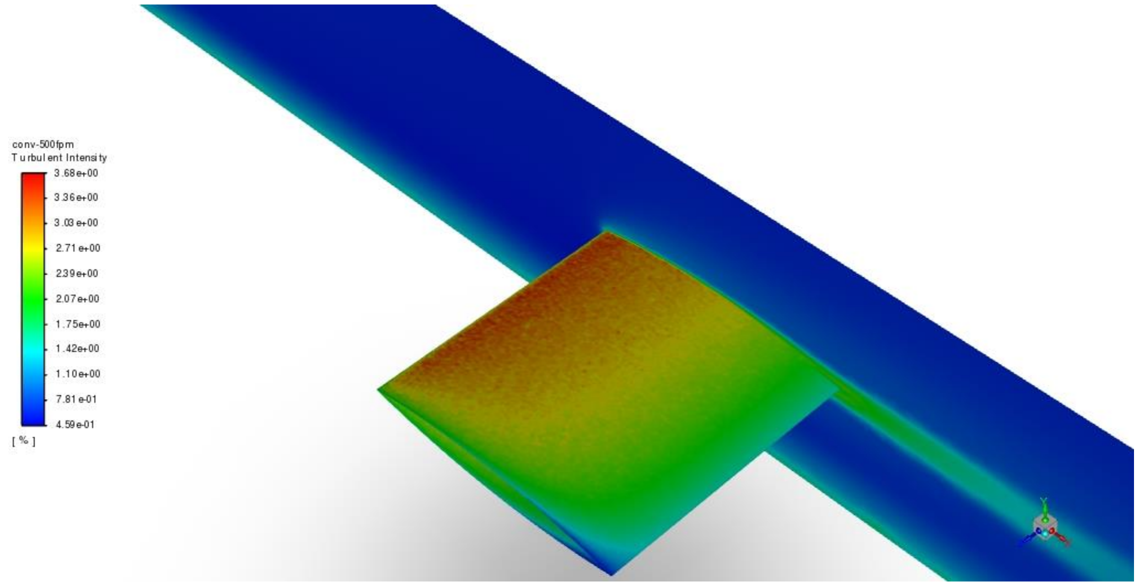

(a) 500fpm

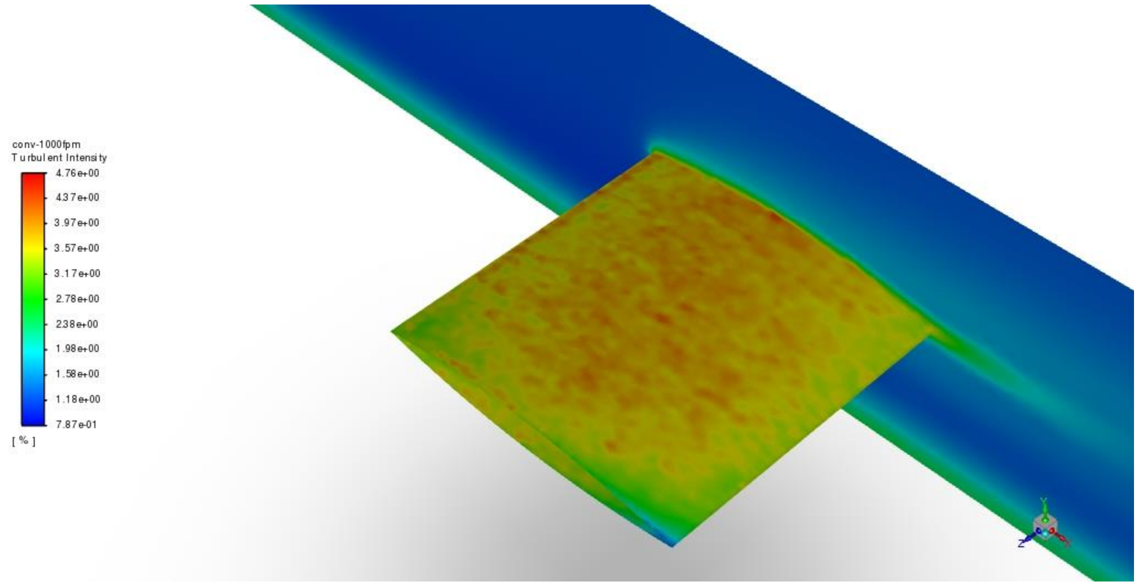

(b) 1000fpm

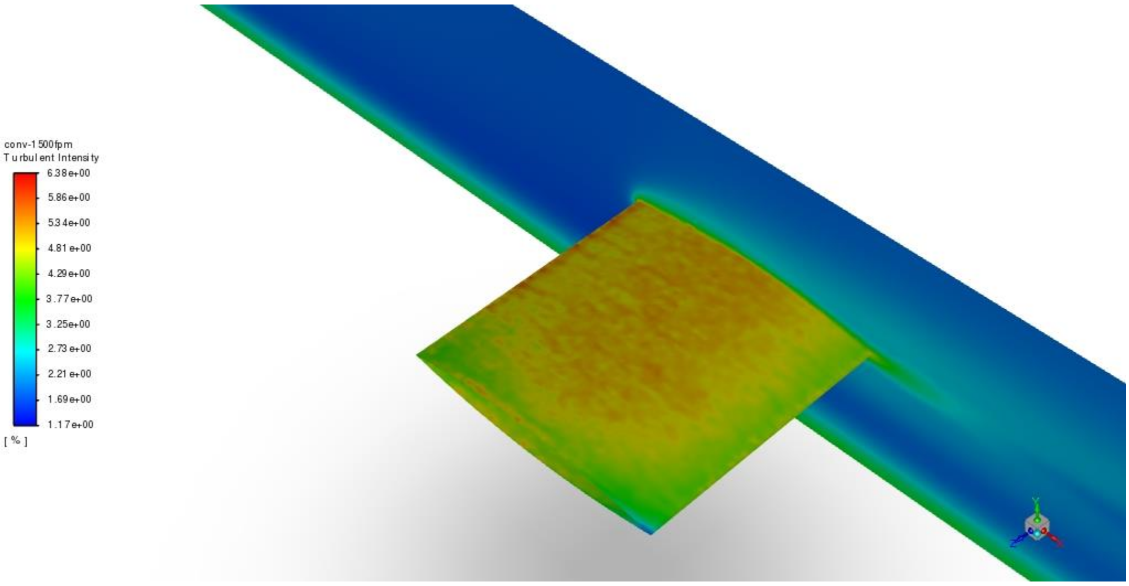

(c) 1500fpm

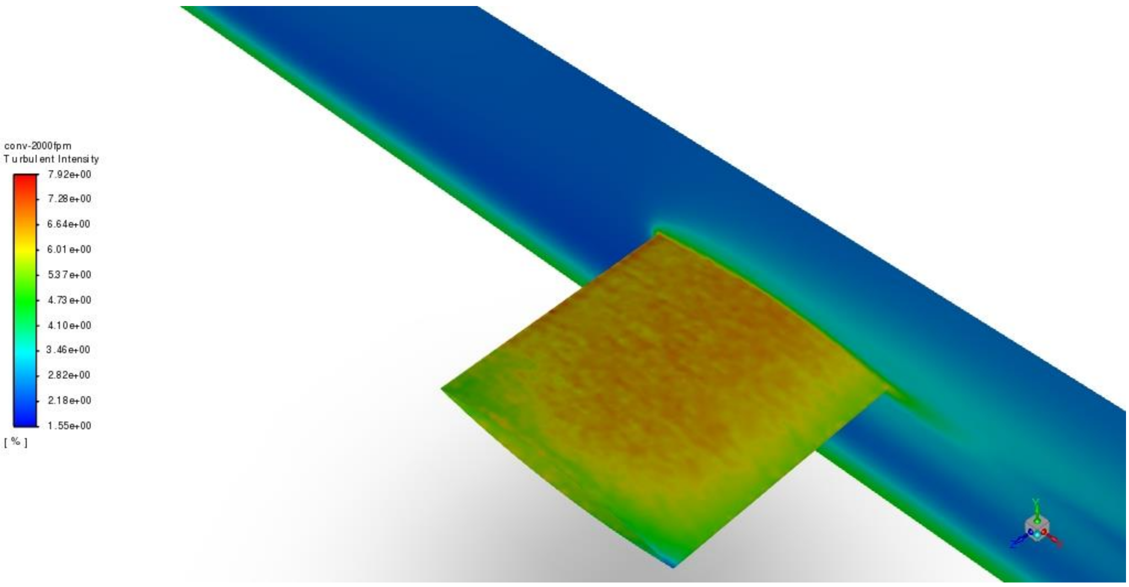

(d) 2000fpm

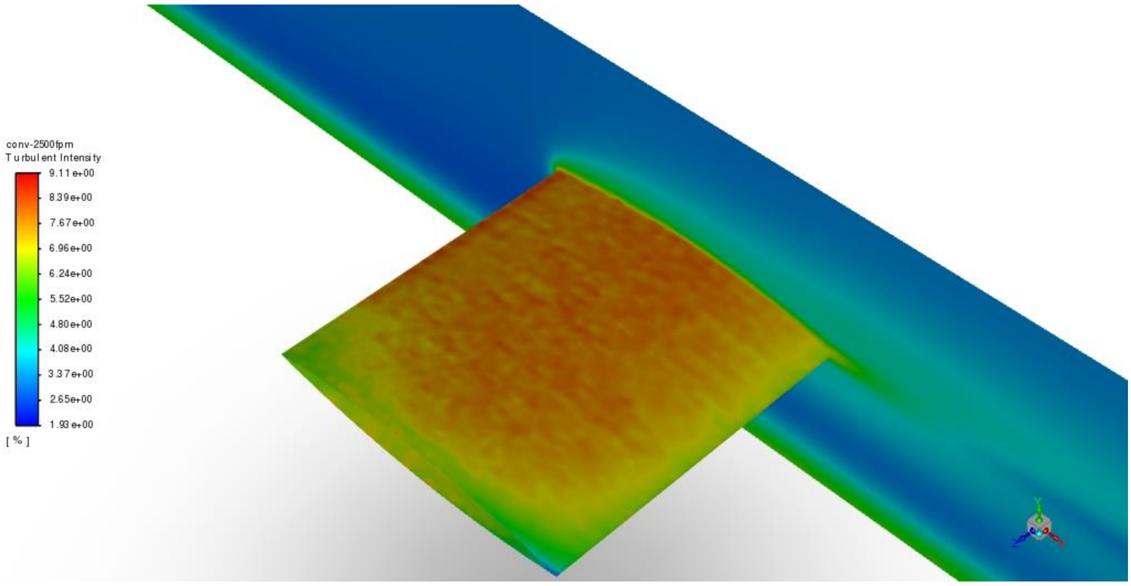

(e) 2500fpm

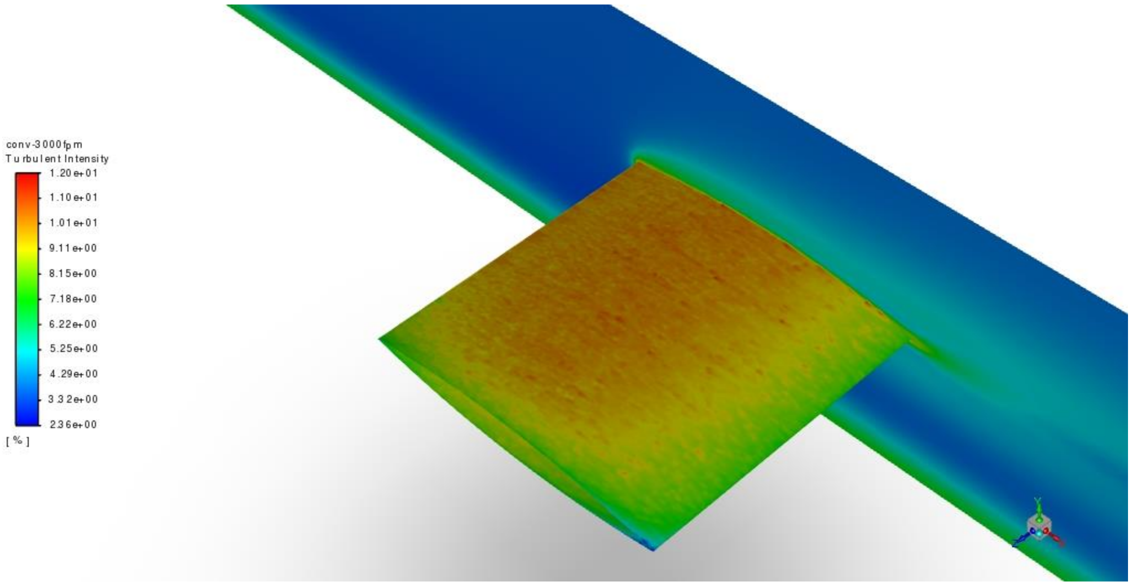

(f) 3000fpm

A2: Turbulence intensity contour plot of NACA0010 airfoil for different velocities

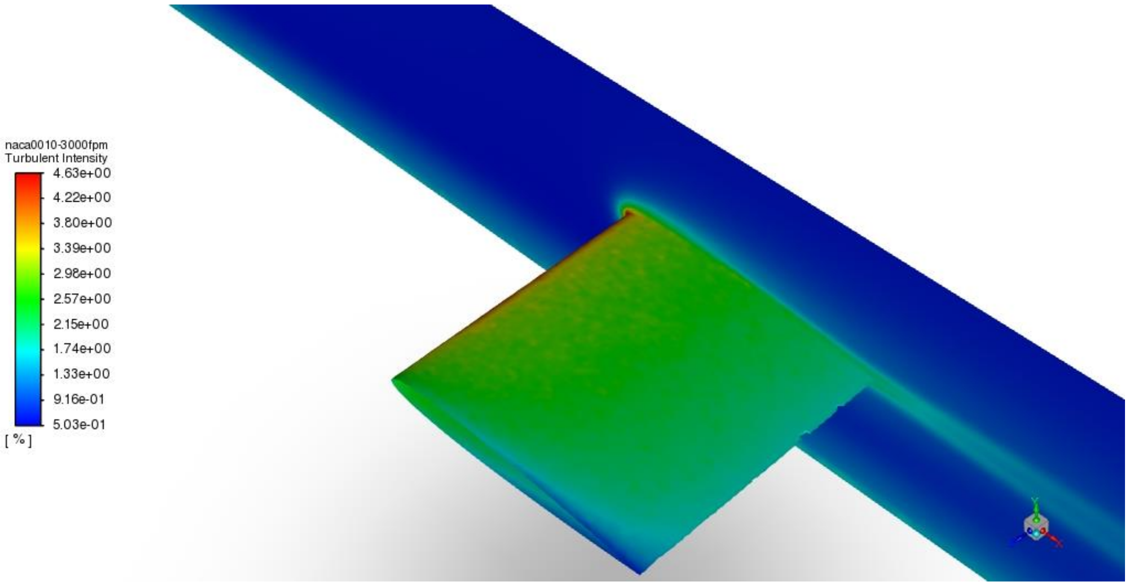

(a) 500fpm

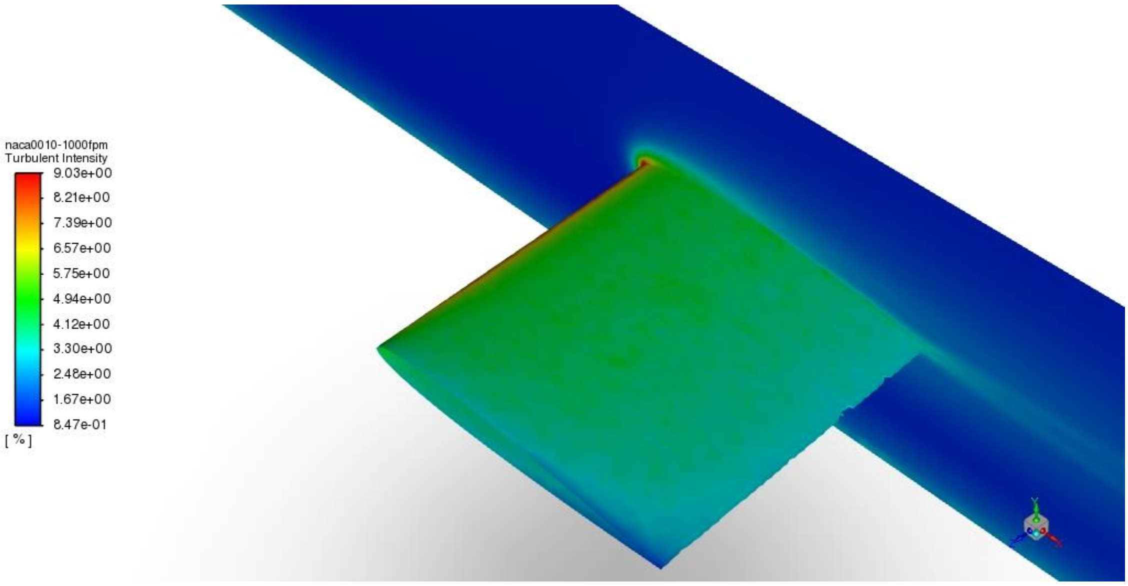

(b) 1000fpm

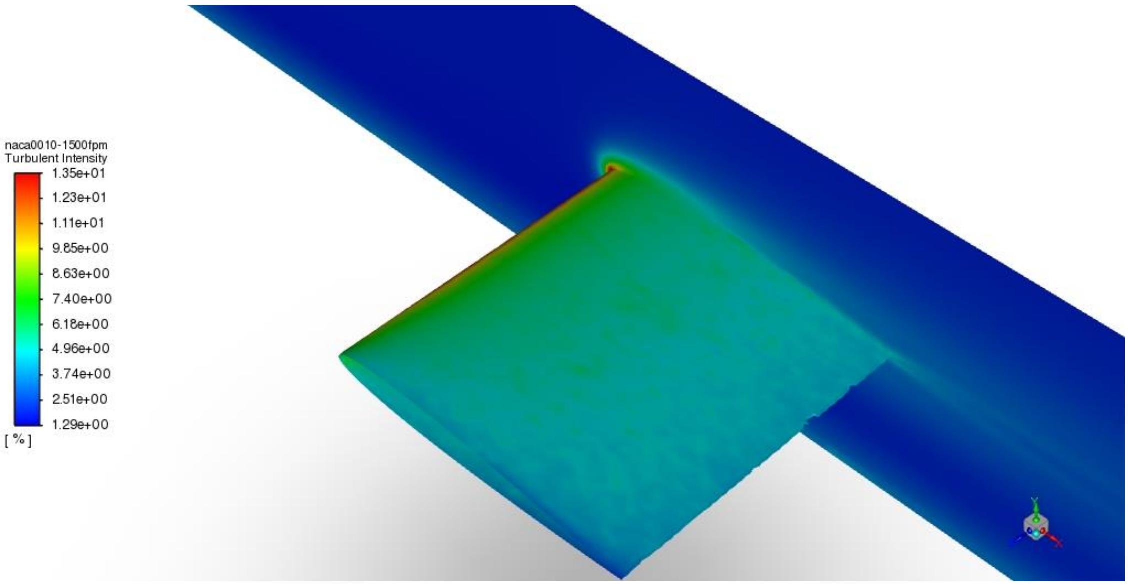

(c) 1500fpm

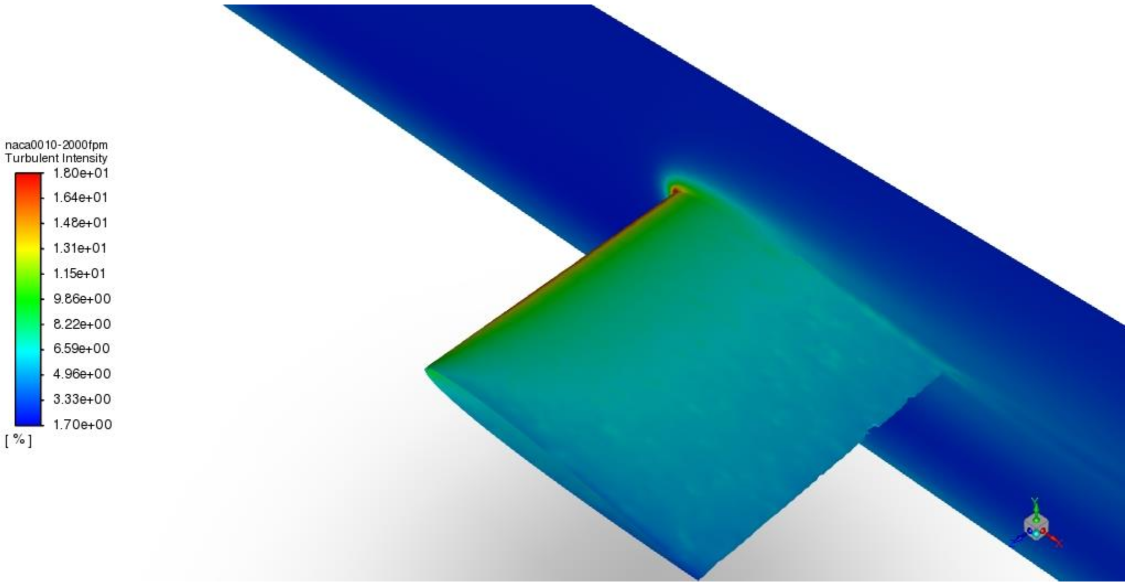

(d) 2000fpm

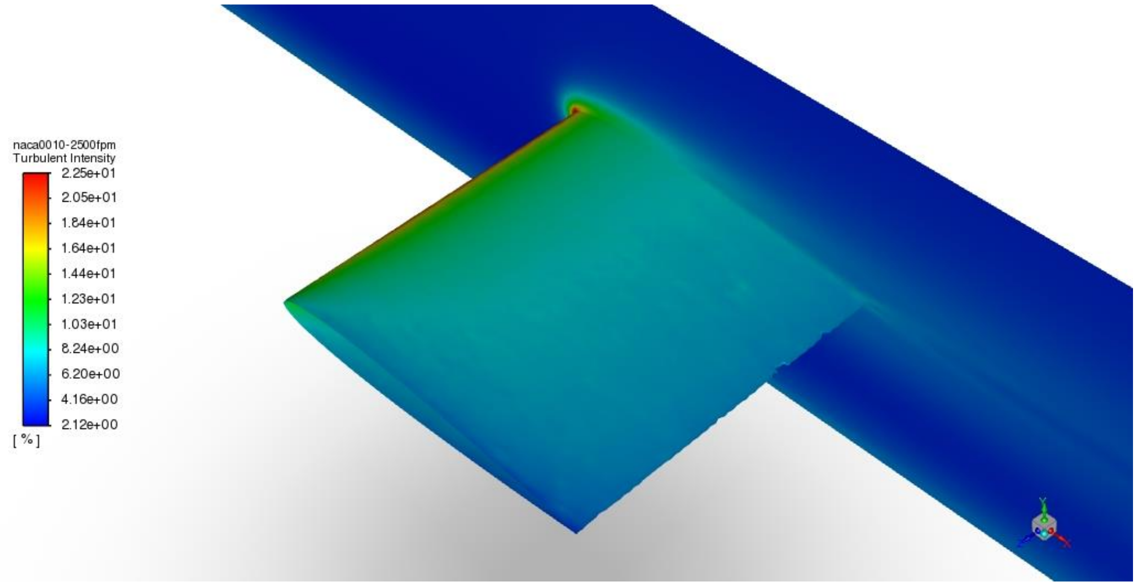

(e) 2500fpm

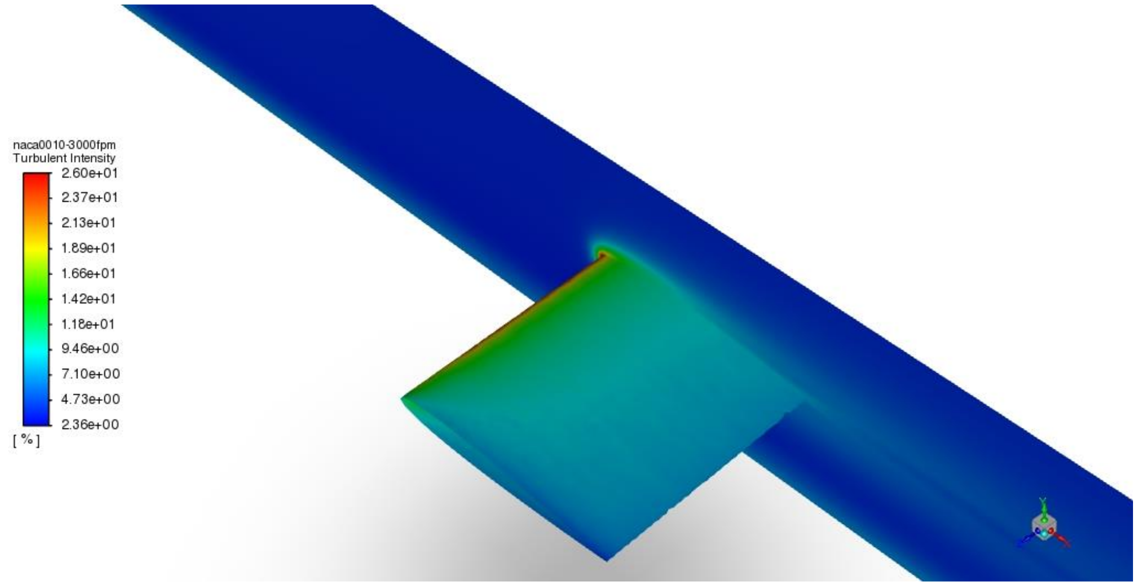

(f) 3000fpm

A3: Turbulence intensity contour plot of conventional airfoil with reduced thickness for different velocities

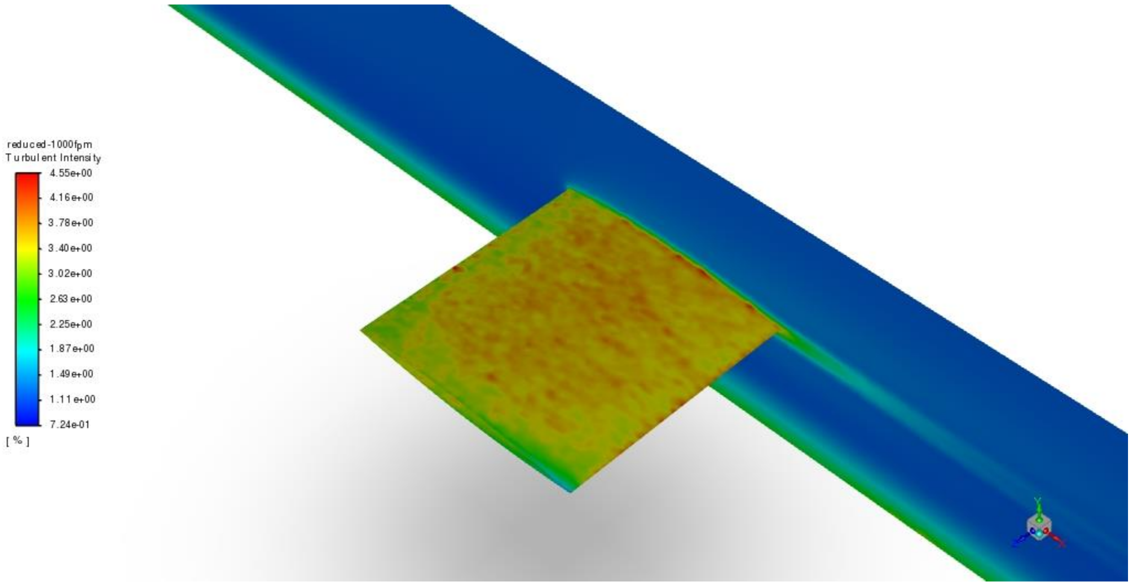

(a) 500fpm

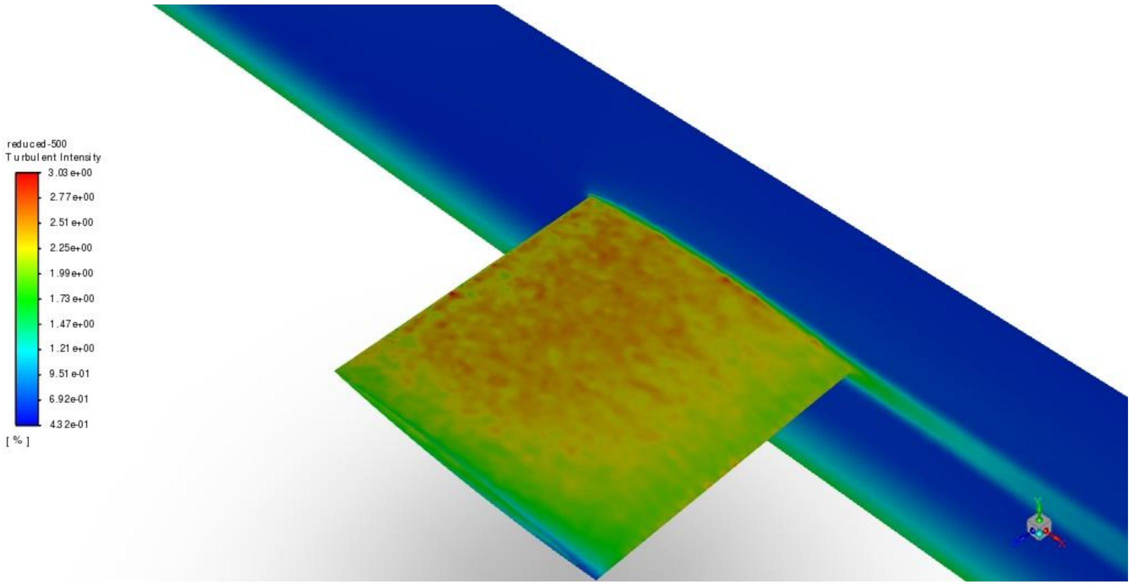

(b) 1000fpm

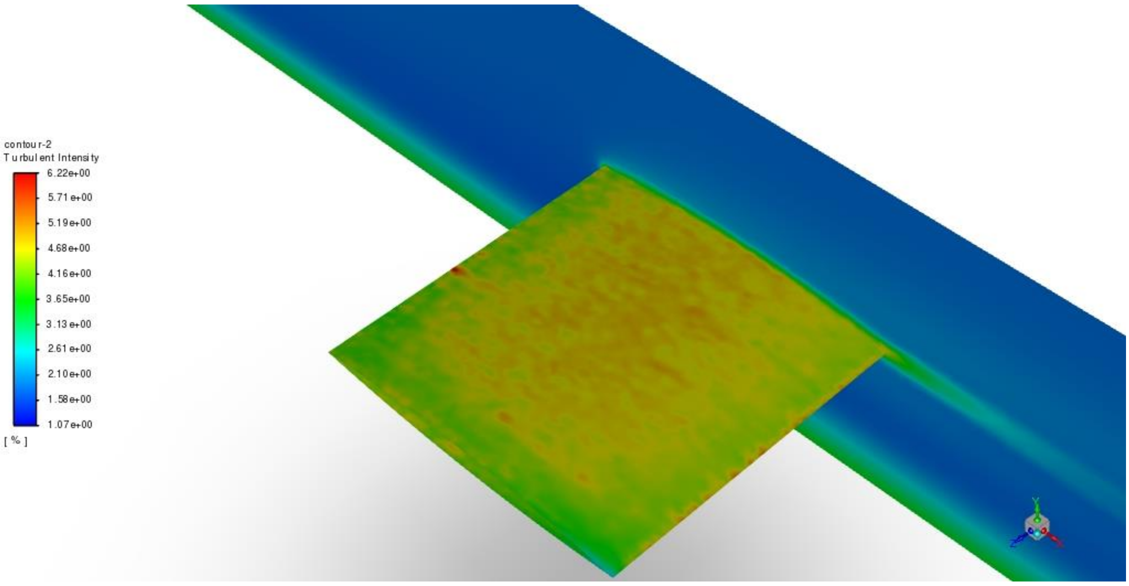

(c) 1500fpm

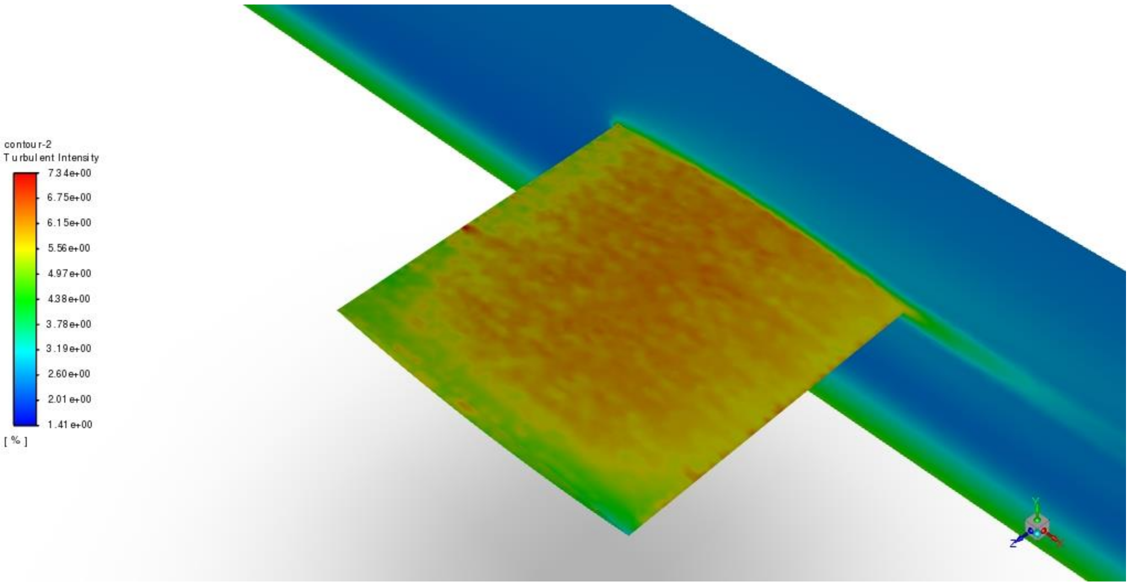

(d) 2000fpm

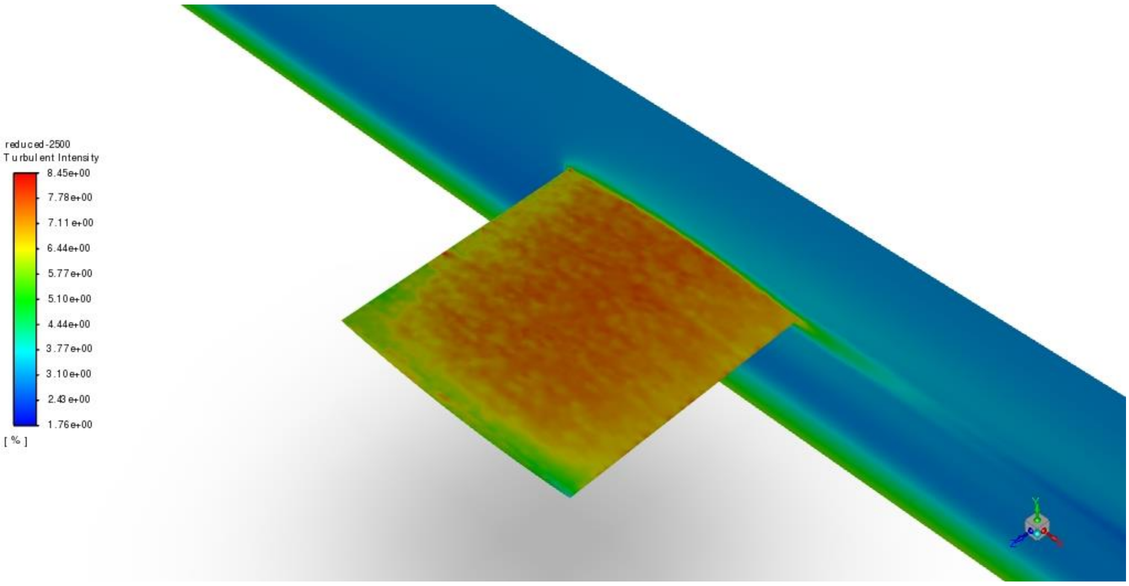

(e) 2500fpm

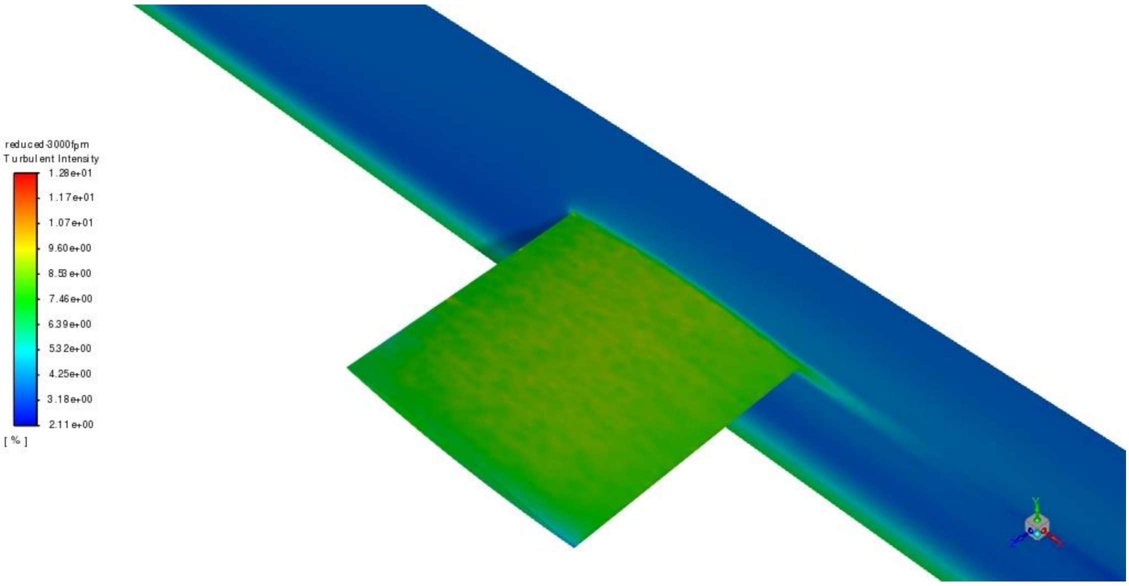

(f) 3000fpm

A4: Turbulence intensity contour plot of NACA0006 airfoil for different velocities

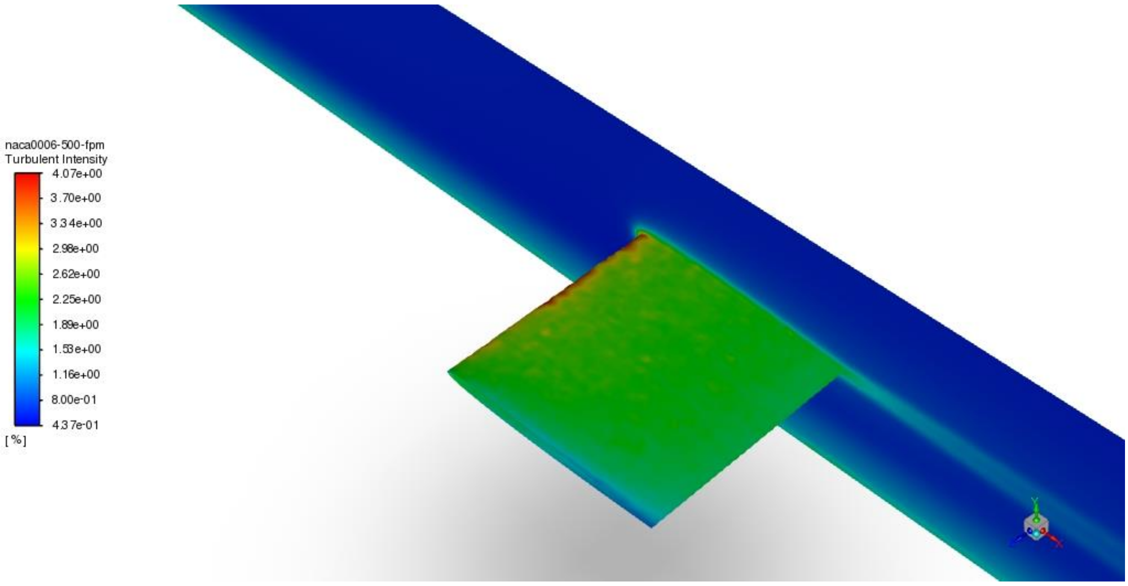

(a) 500fpm

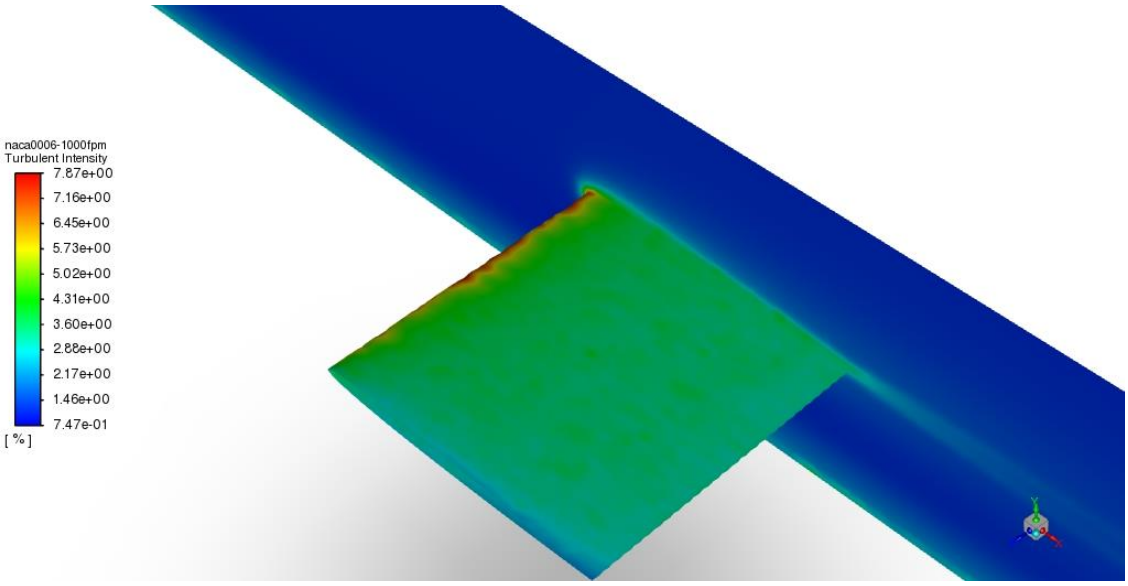

(b) 1000fpm

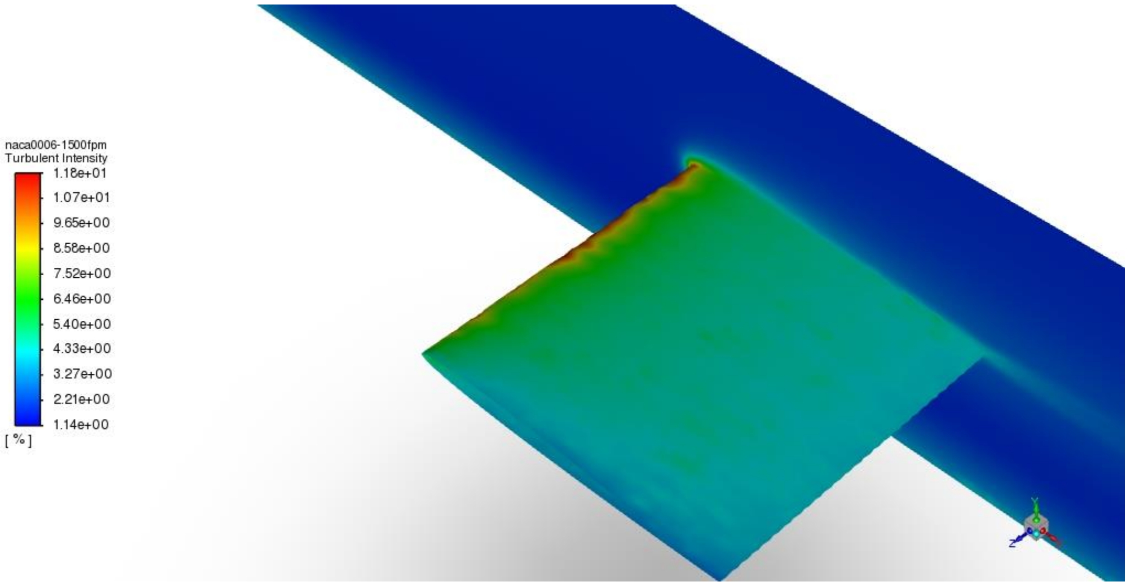

(c) 1500fpm

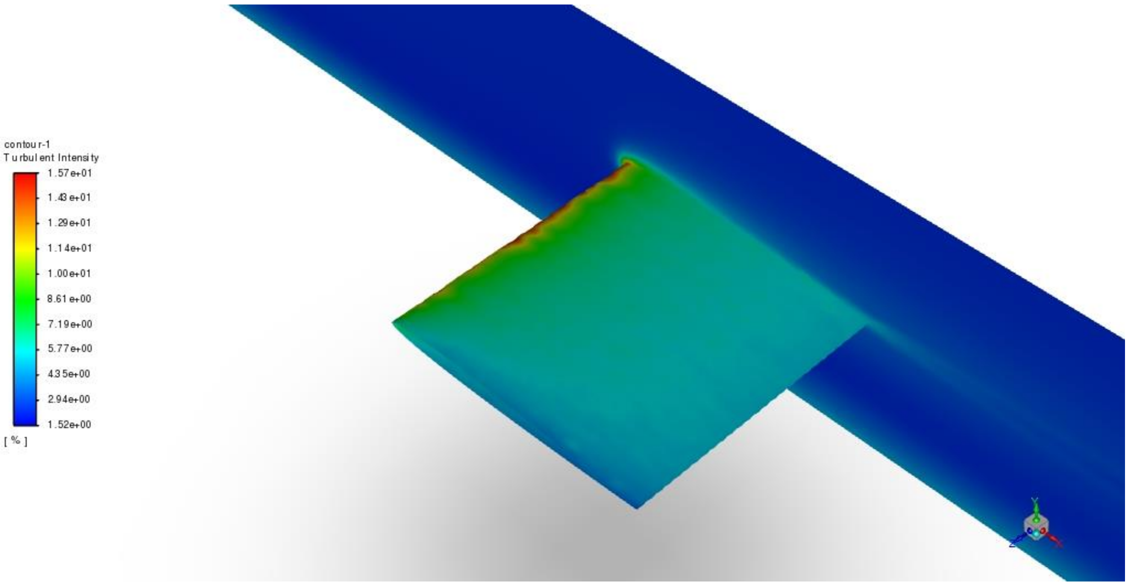

(d) 2000fpm

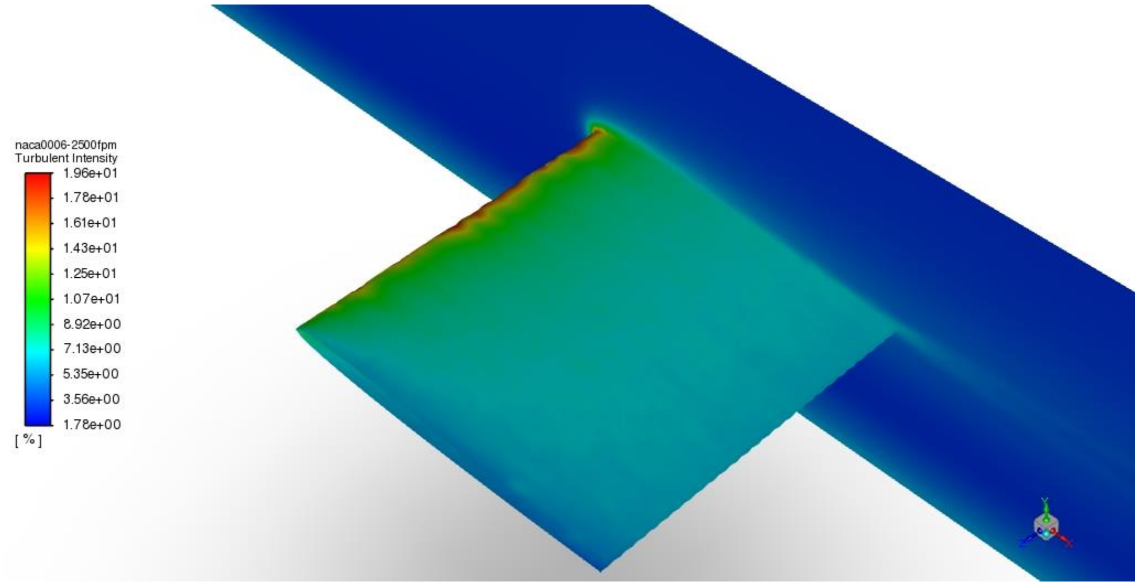

(e) 2500fpm

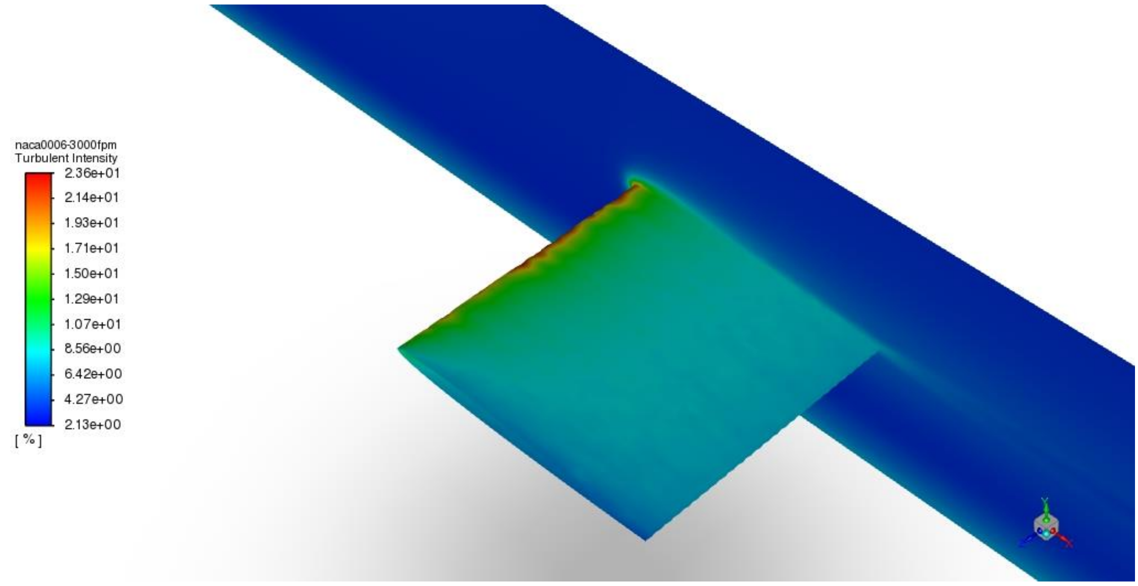

(f) 3000fpm

APPENDIX B: TOTAL PRESSURE CONTOUR PLOT OF DIFFERENT PROFILES FOR DIFFERENT VELOCITIES

B1: Total Pressure contour plot of conventional airfoil for different velocities

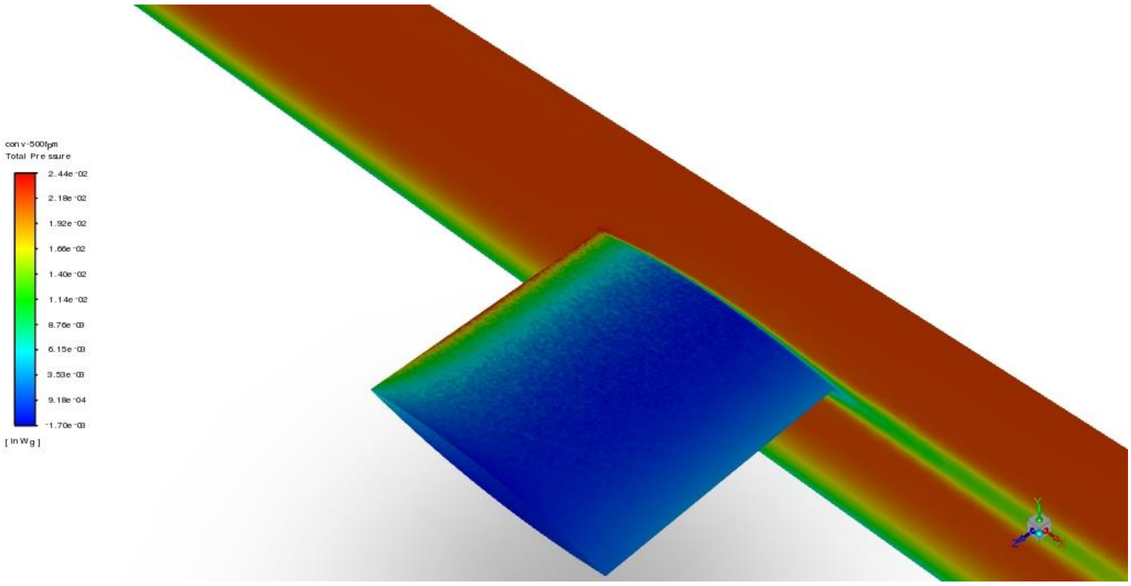

(a) 500fpm

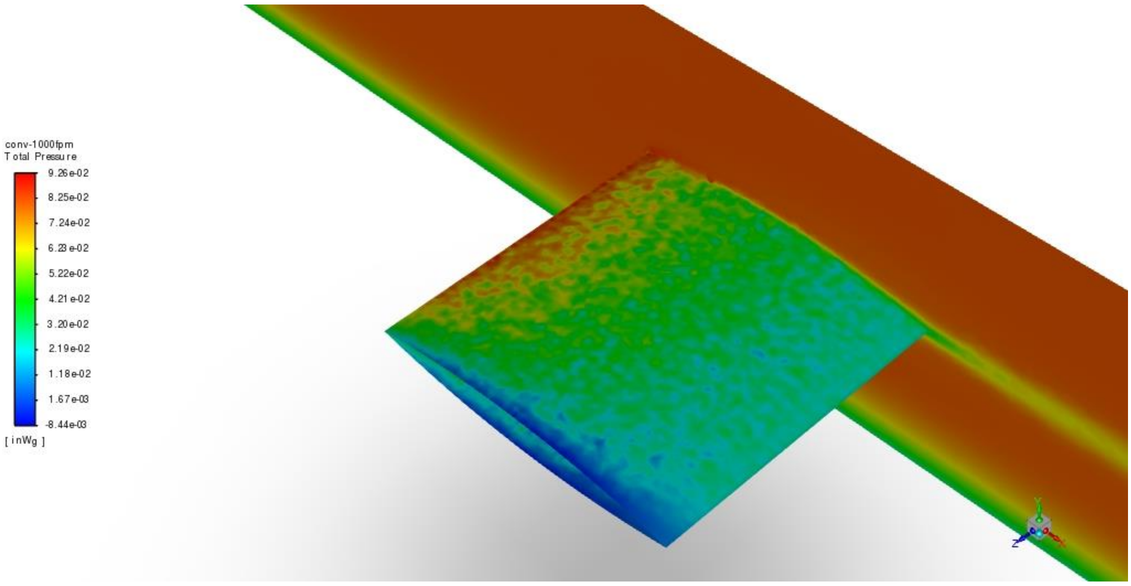

(b) 1000fpm

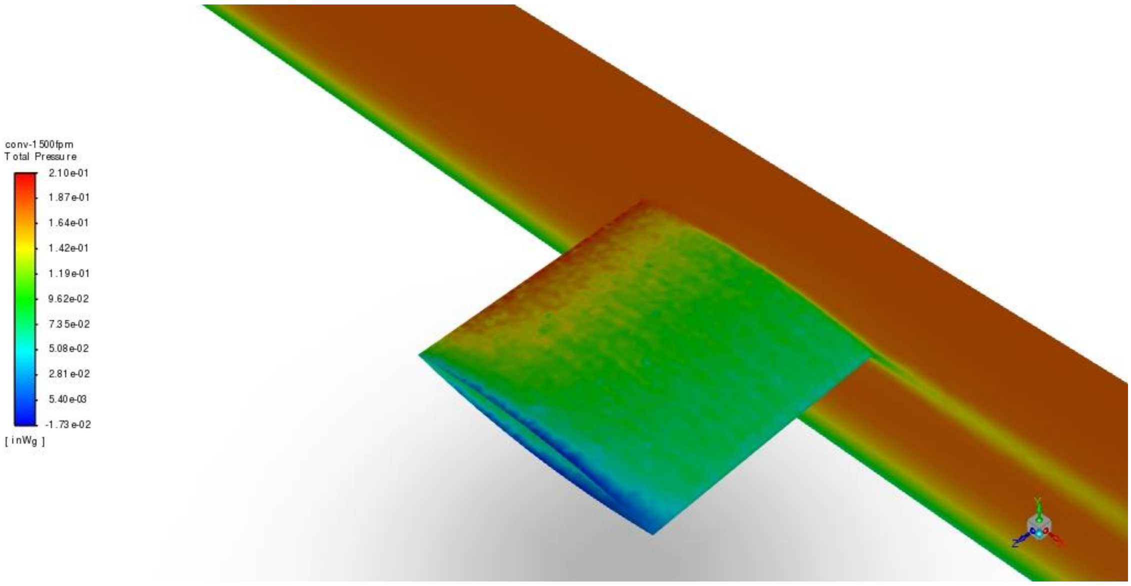

(c) 1500fpm

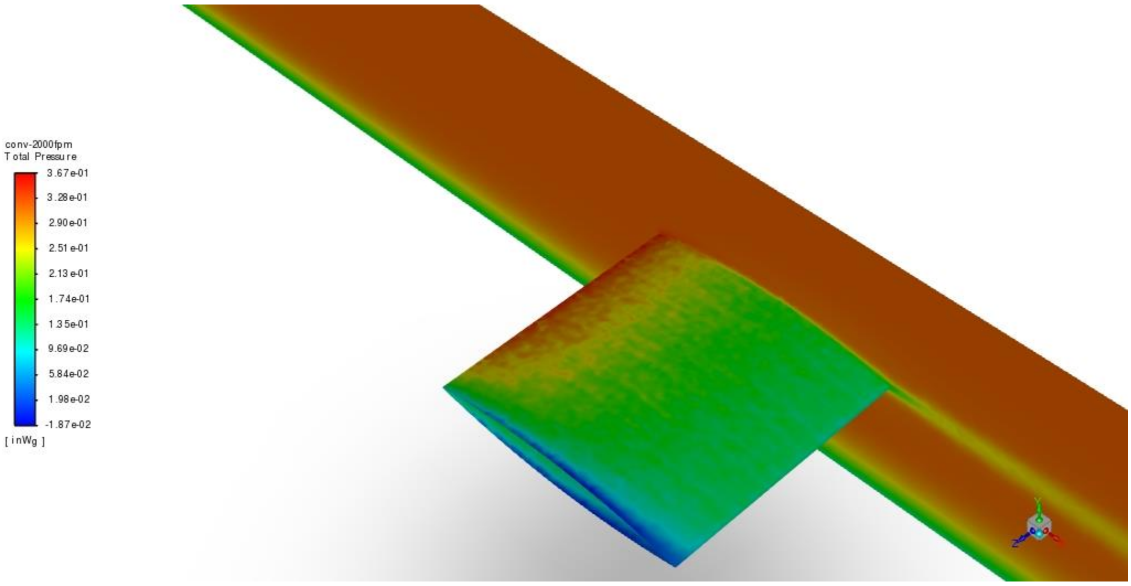

(d) 2000fpm

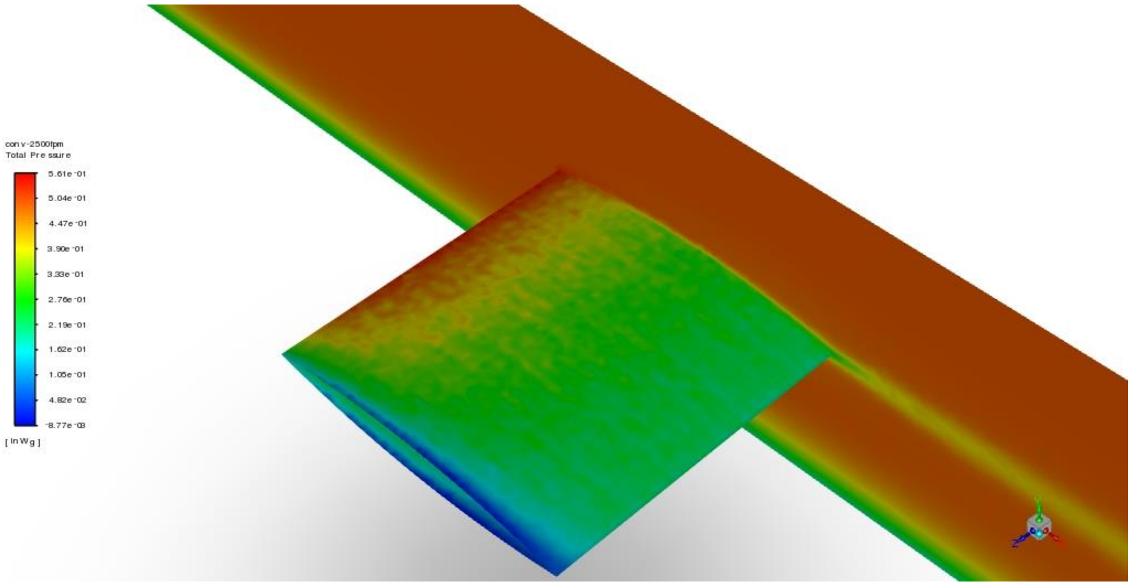

(e) 2500fpm

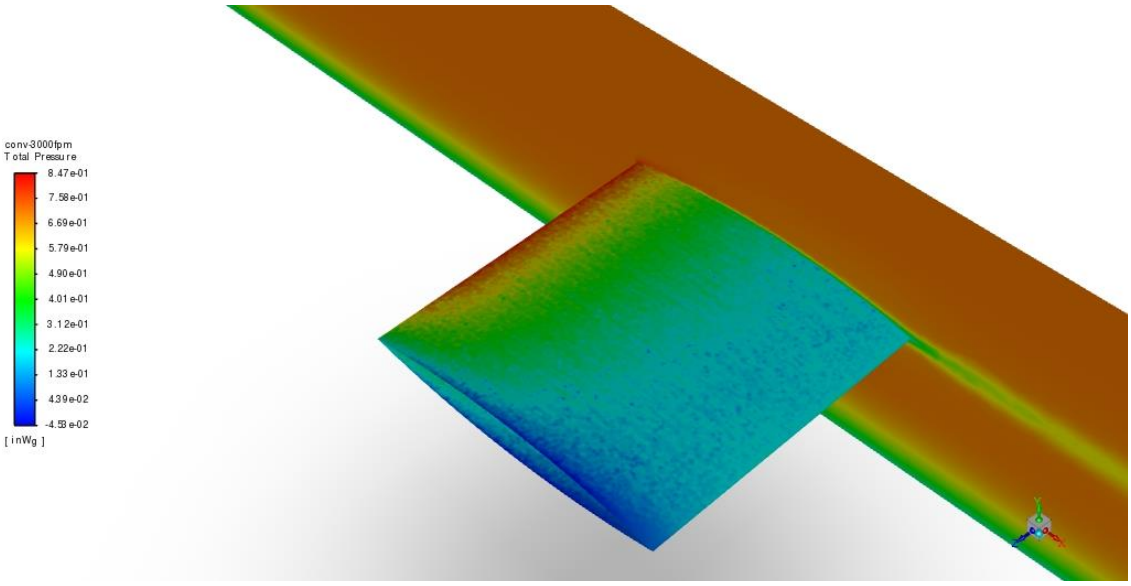

(f) 3000fpm

B2: Total Pressure contour plot of NACA0010 airfoil for different velocities

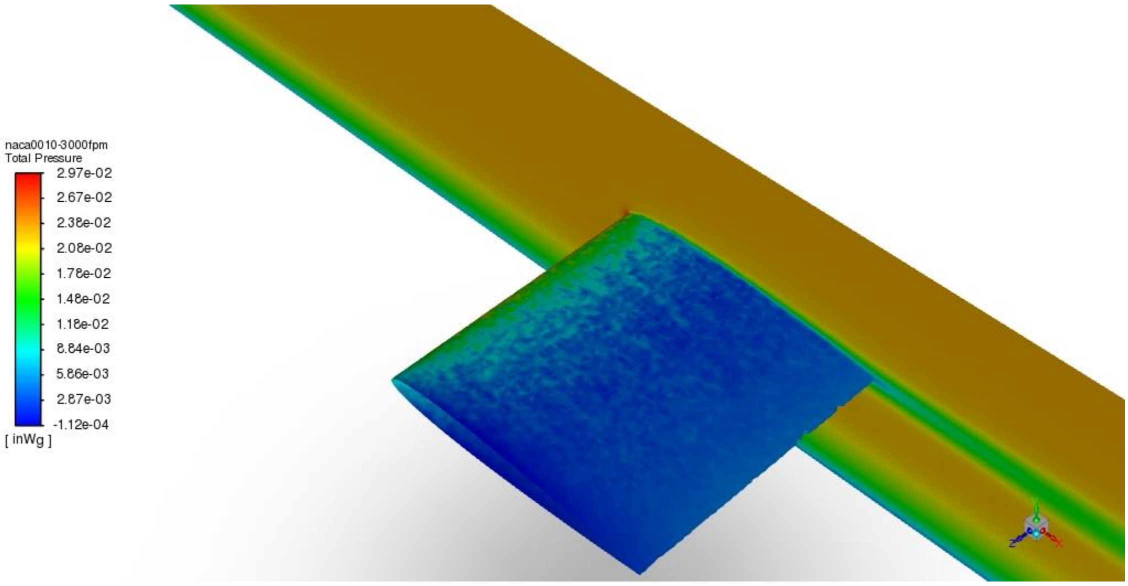

(a) 500fpm

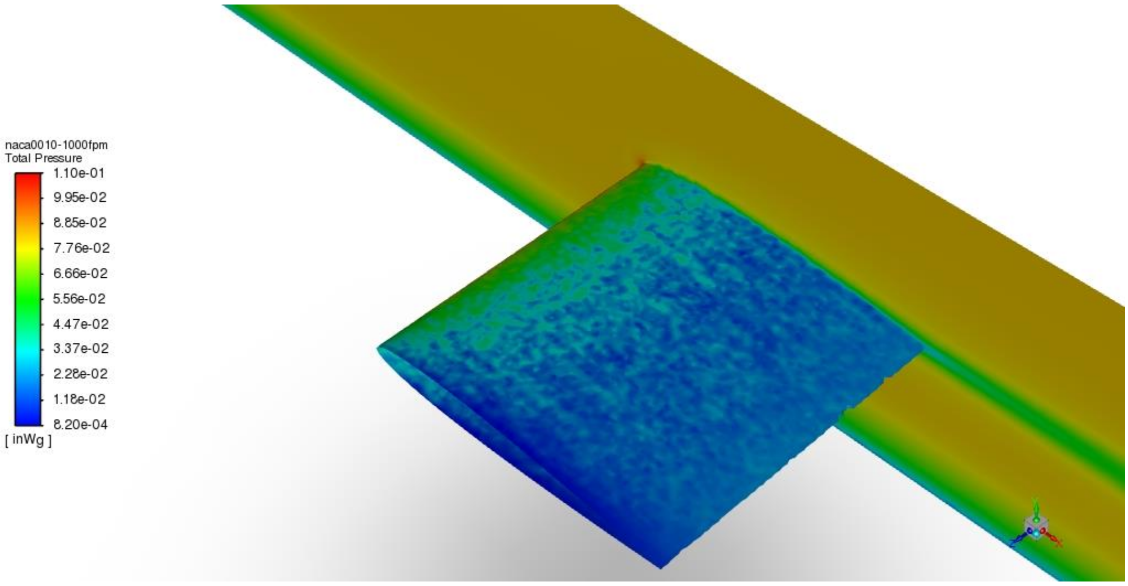

(b) 1000fpm

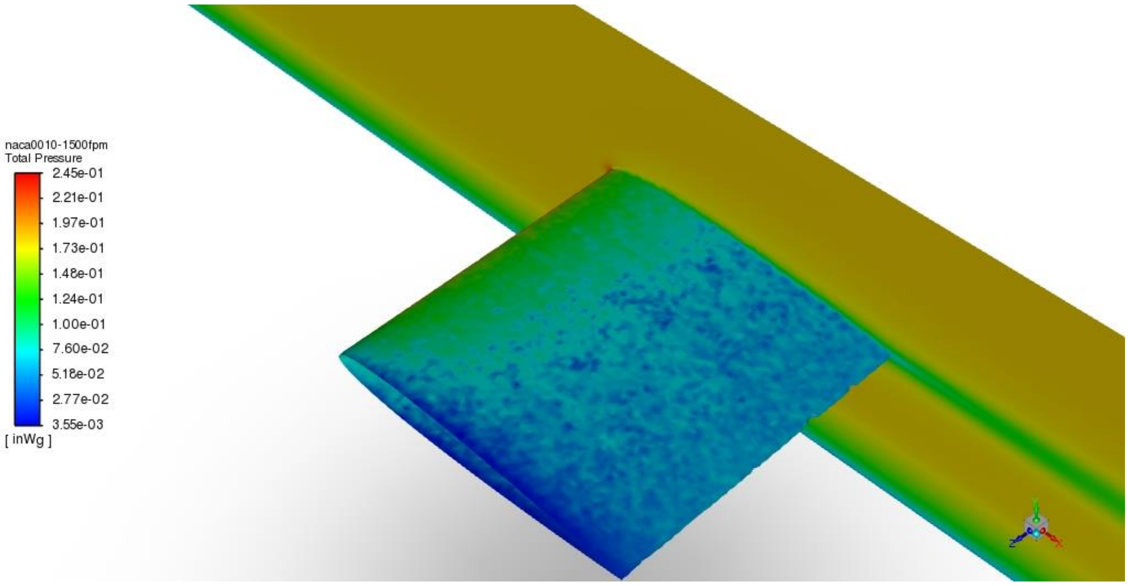

(c) 1500fpm

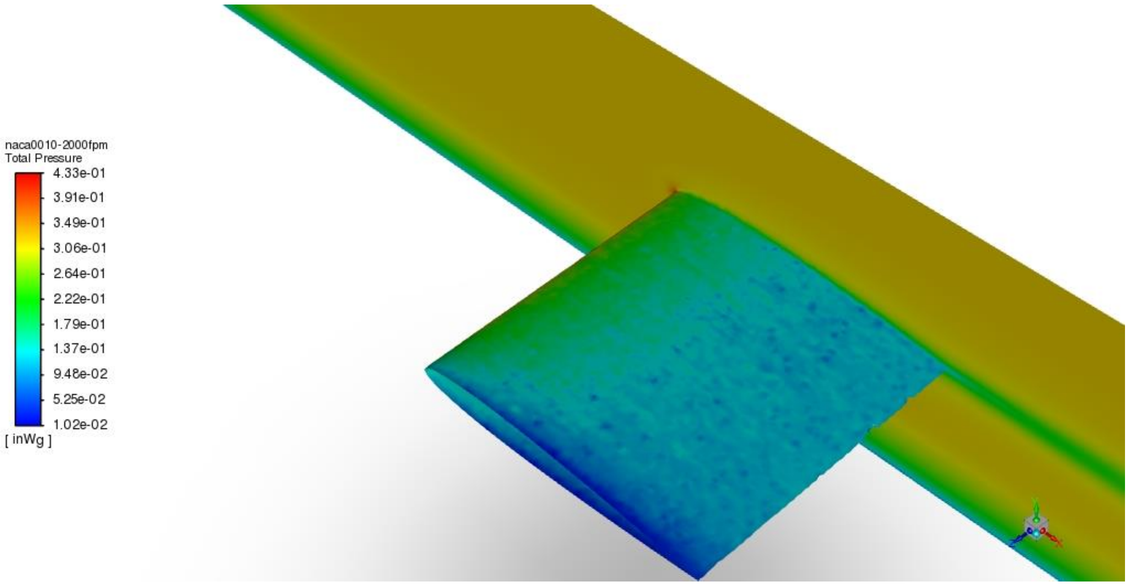

(d) 2000fpm

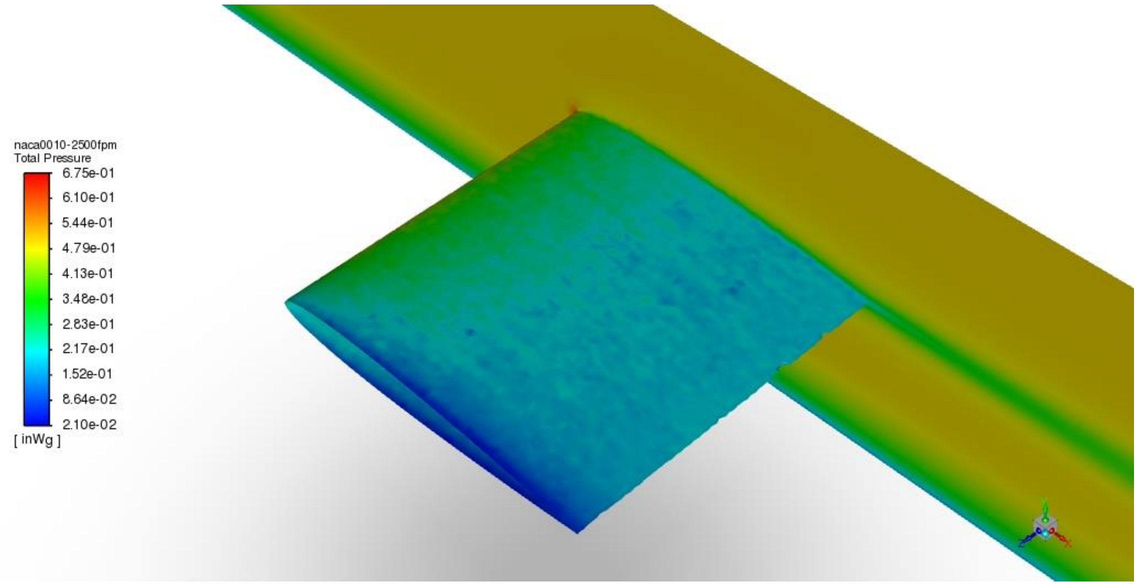

(e) 2500fpm

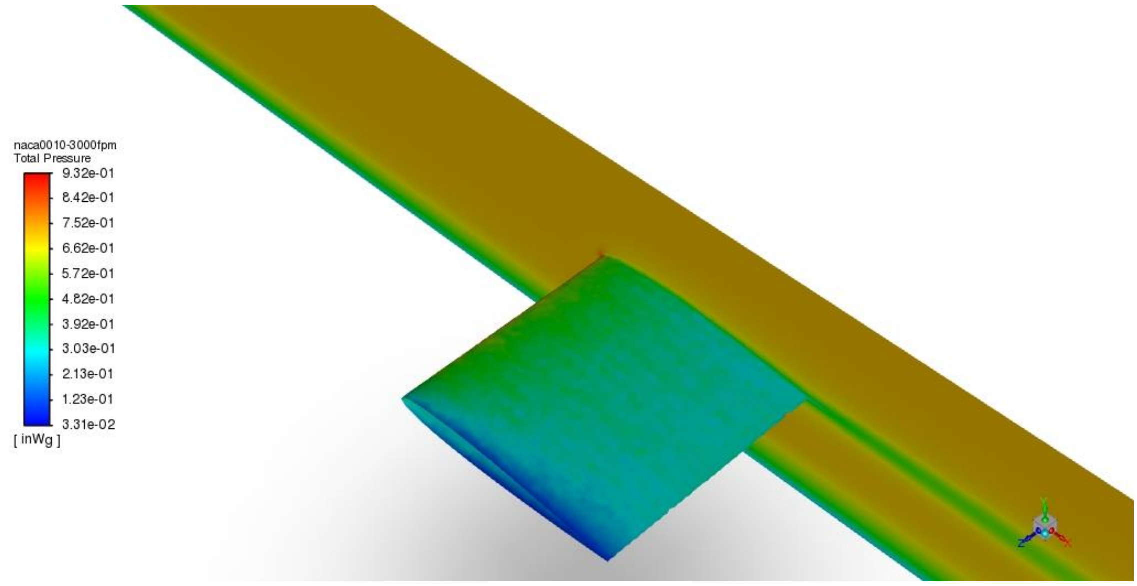

(f) 3000fpm

B3: Total Pressure contour plot of conventional airfoil with reduced thickness for different velocities

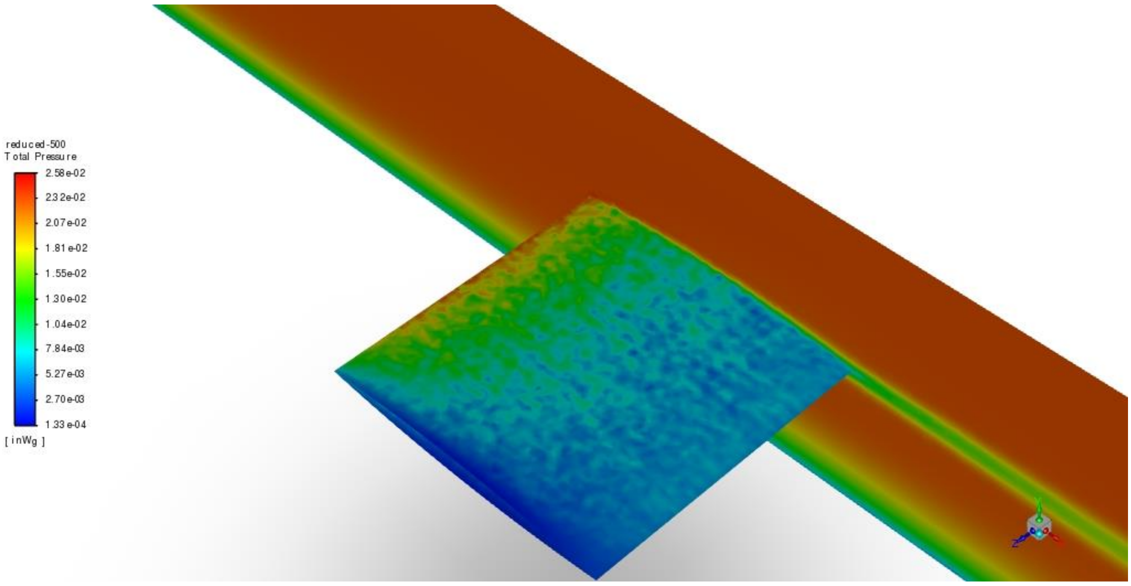

(a) 500fpm

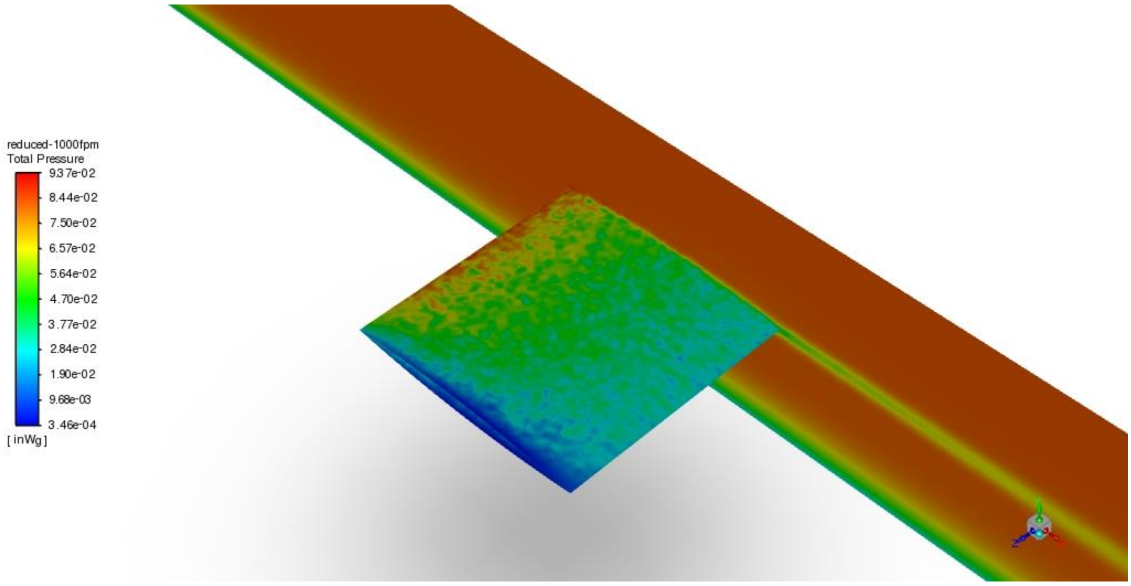

(b) 1000fpm

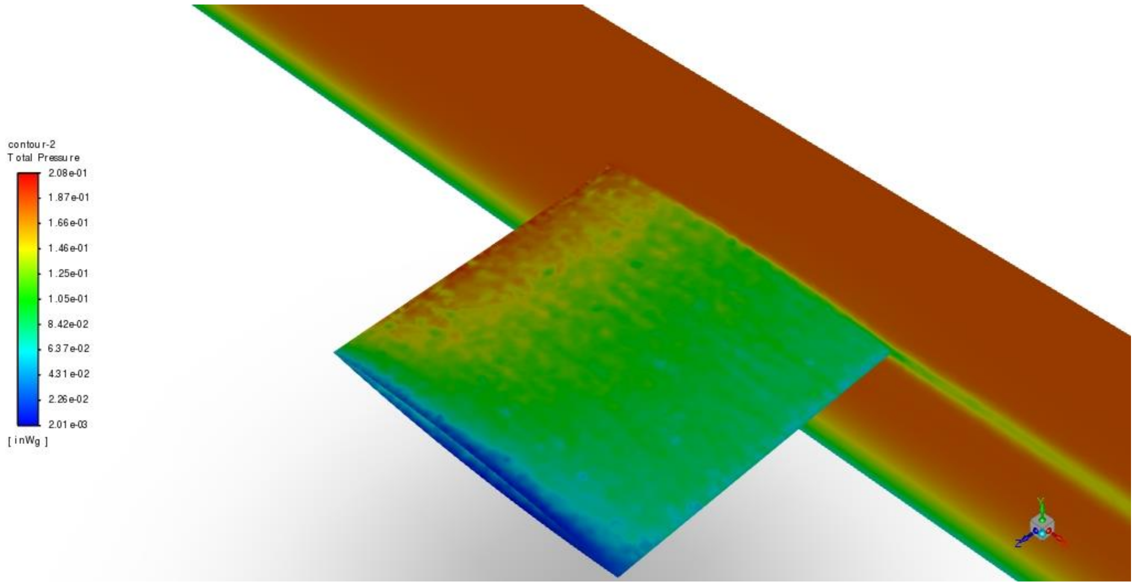

(c) 1500fpm

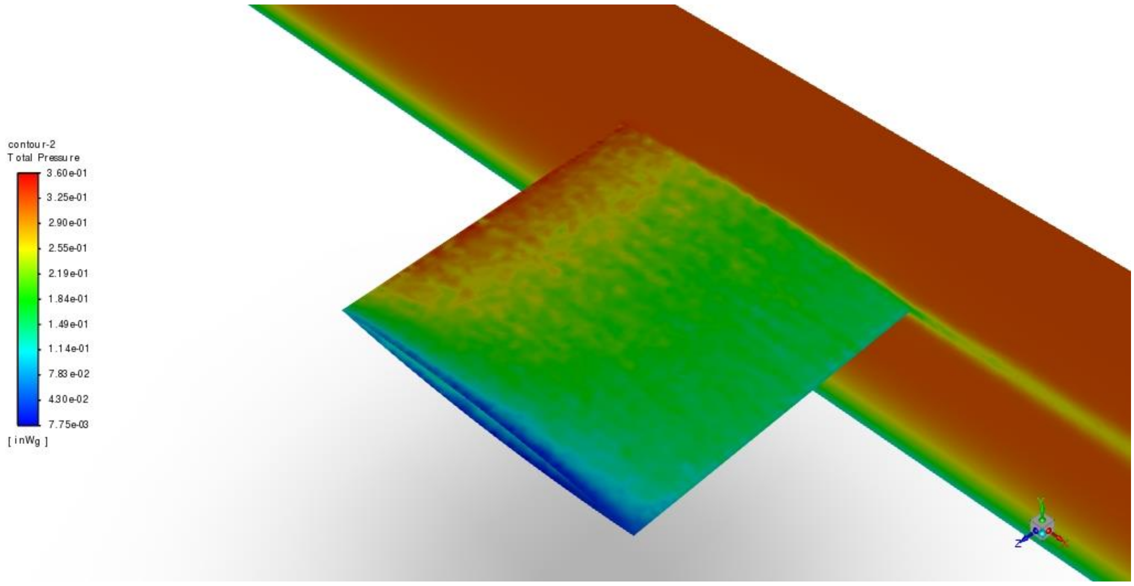

(d) 2000fpm

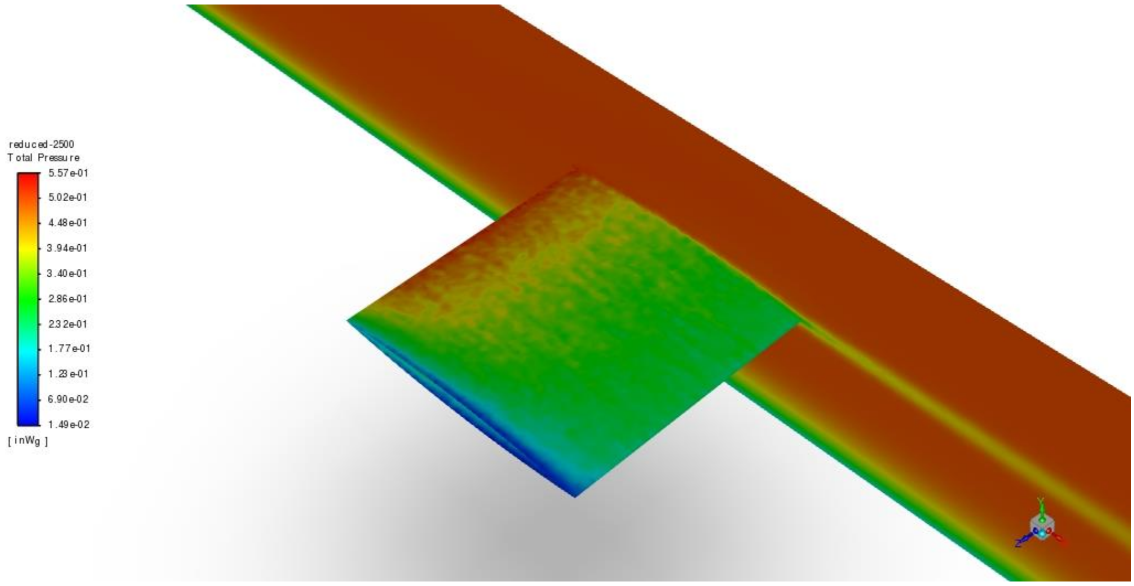

(e) 2500fpm

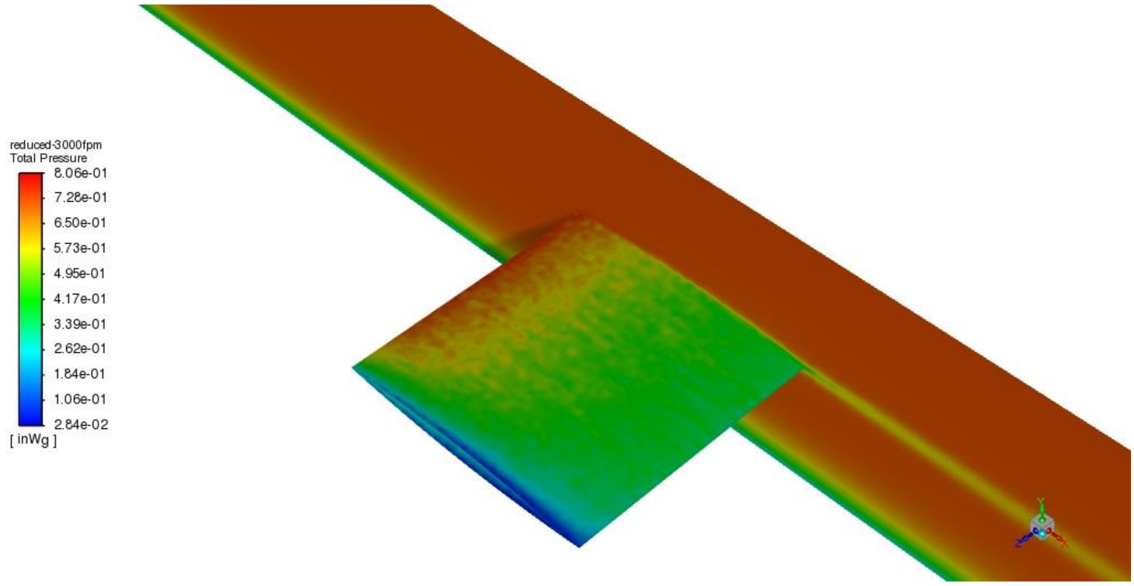

(f) 3000fpm

B4: Total Pressure contour plot of NACA0006 airfoil for different velocities

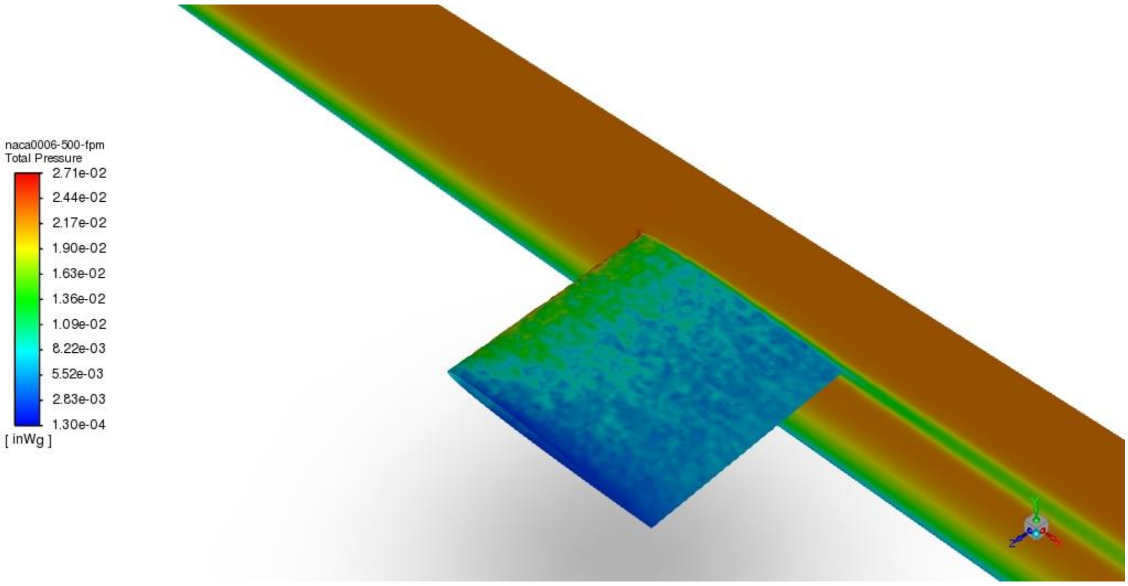

(a) 500fpm

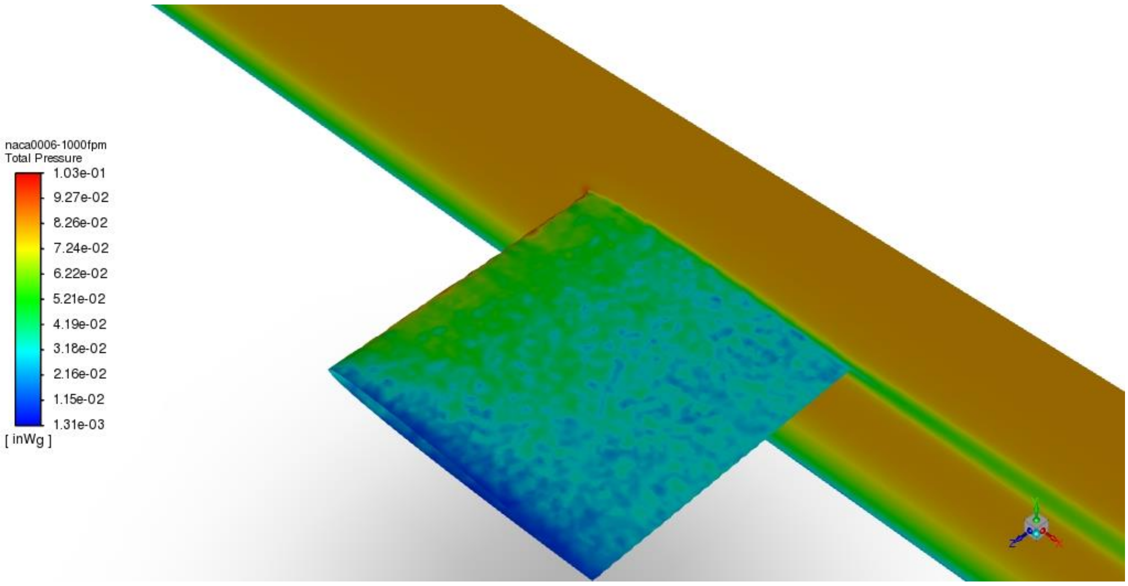

(b) 1000fpm

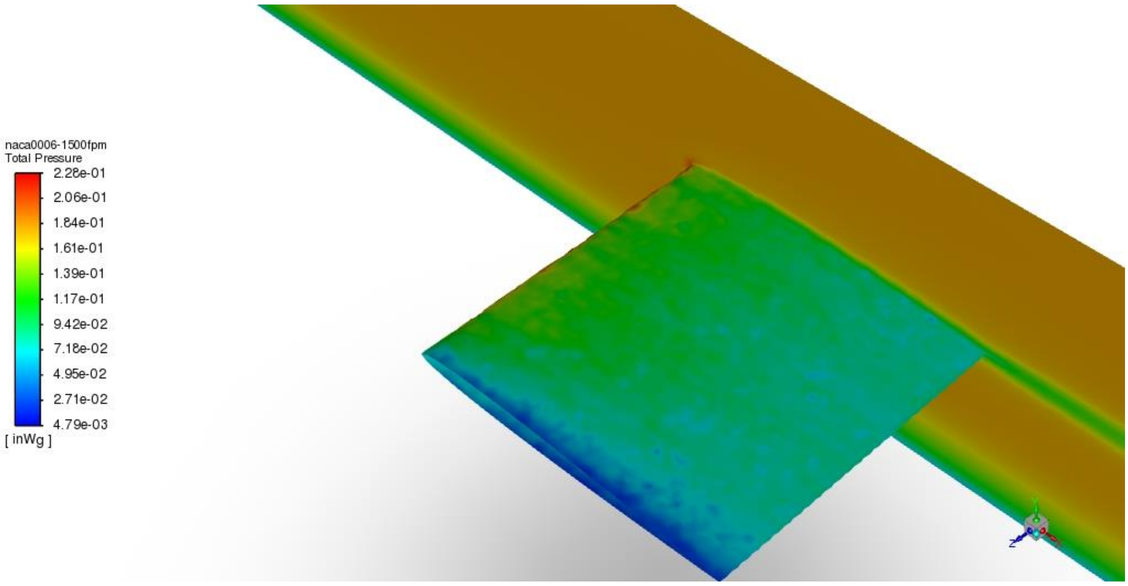

(c) 1500fpm

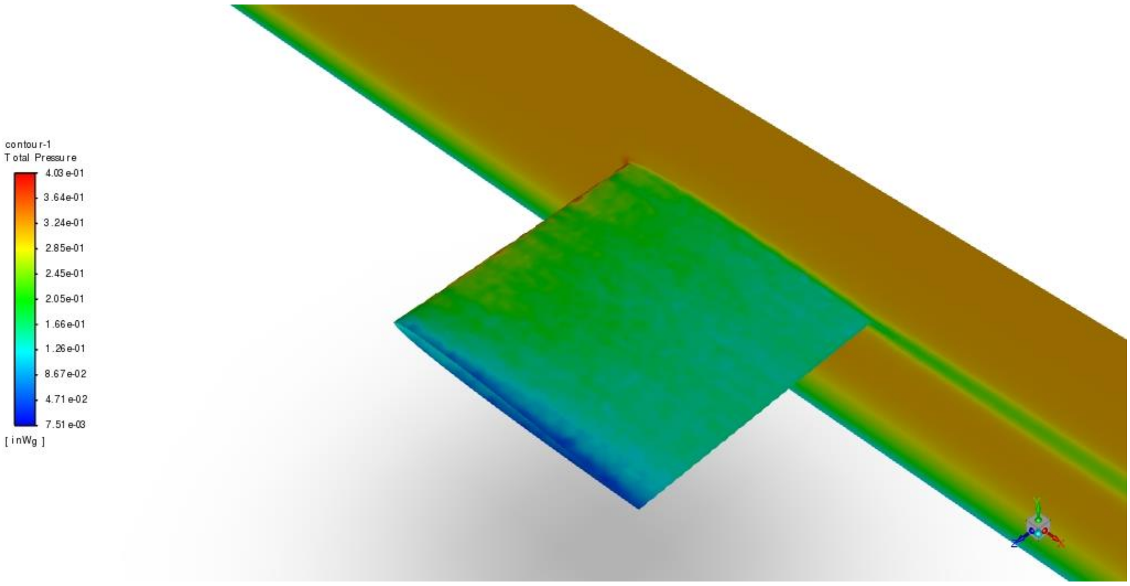

(d) 2000fpm

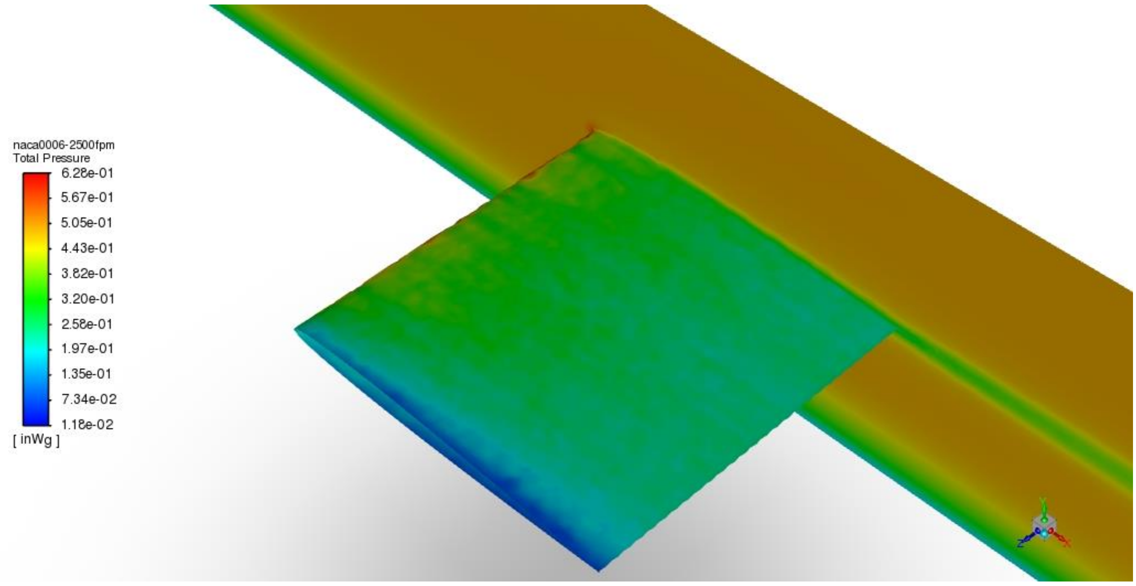

(e) 2500fpm

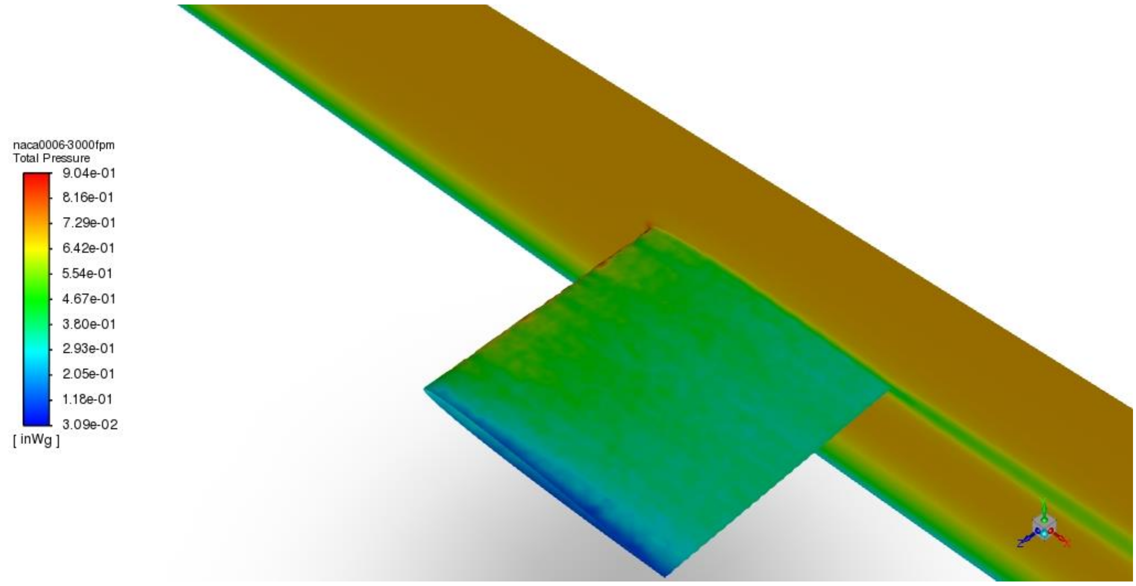

(f) 3000fpm

APPENDIX C: VELOCITY VECTOR COLORED BY TOTAL PRESSURE PLOT OF DIFFERENT PROFILES FOR DIFFERENT VELOCITIES

C1: Velocity vector colored by total pressure plot of conventional airfoil for different velocities

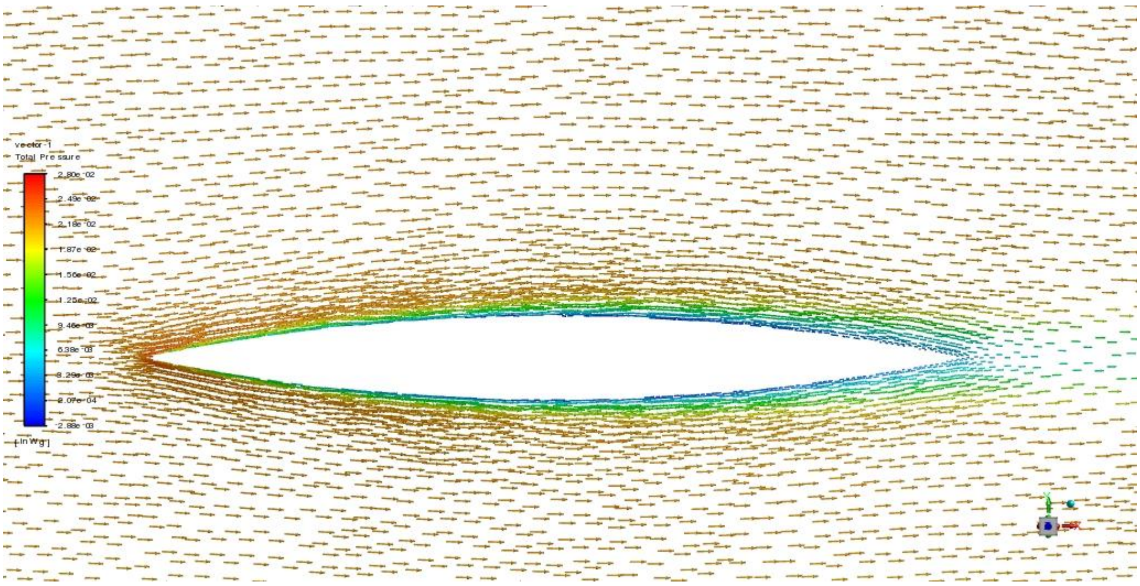

(a) 500fpm

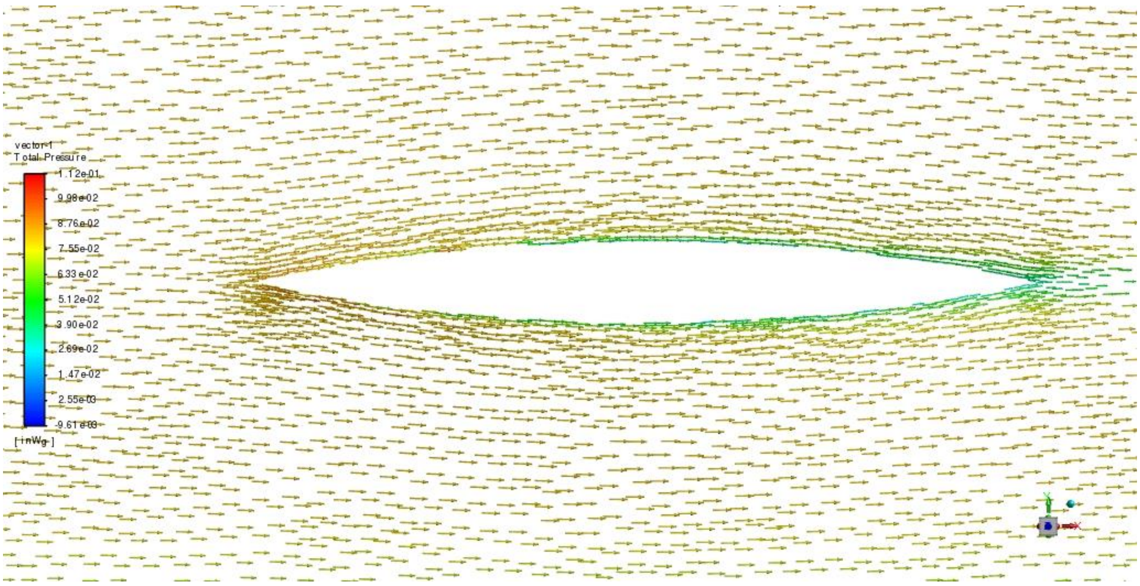

(b) 1000fpm

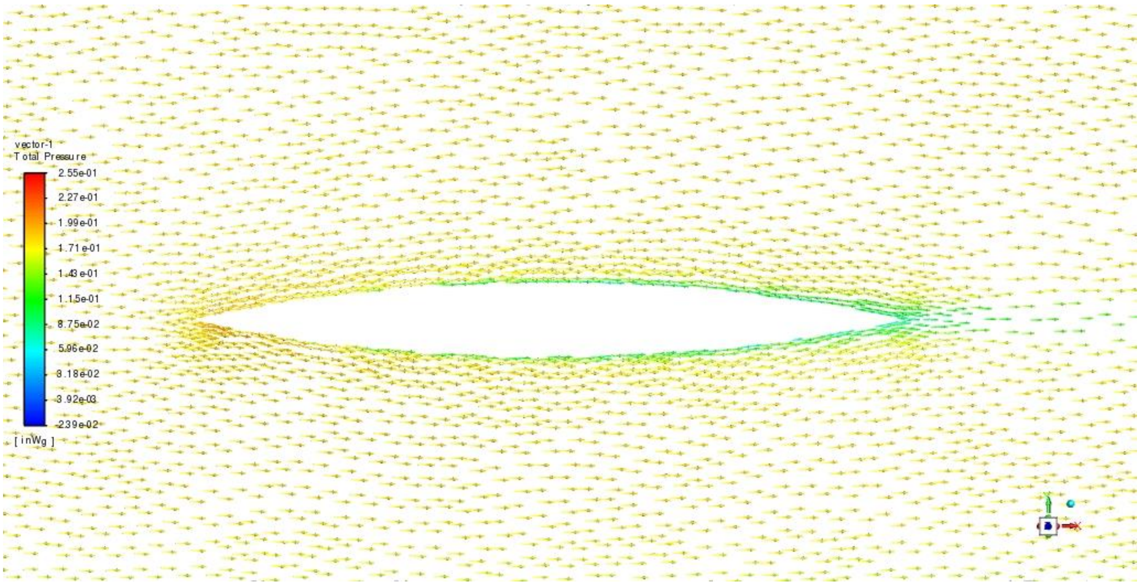

(c) 1500fpm

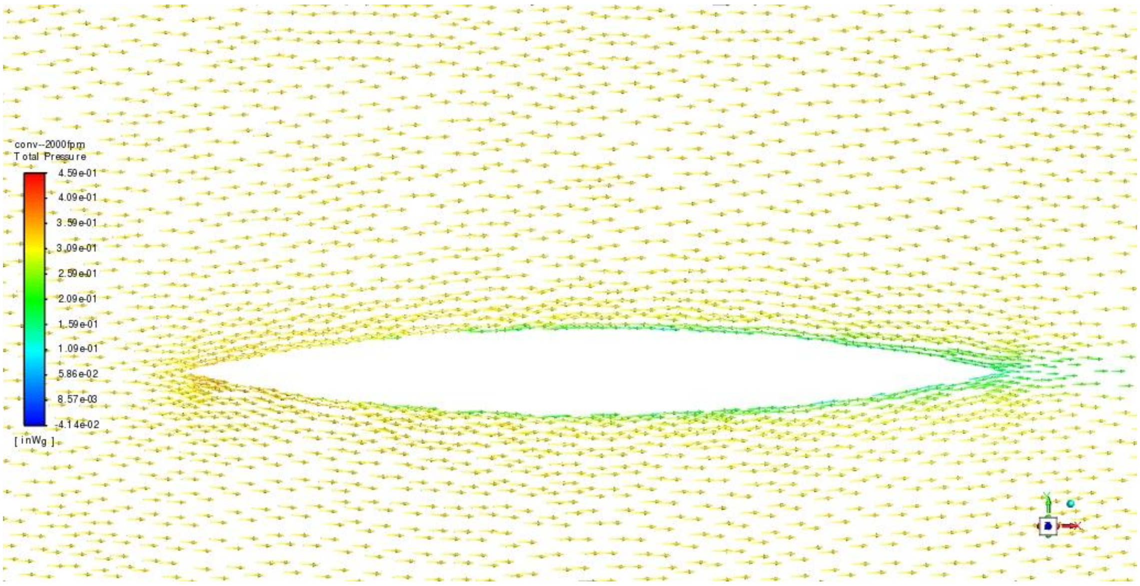

(d) 2000fpm

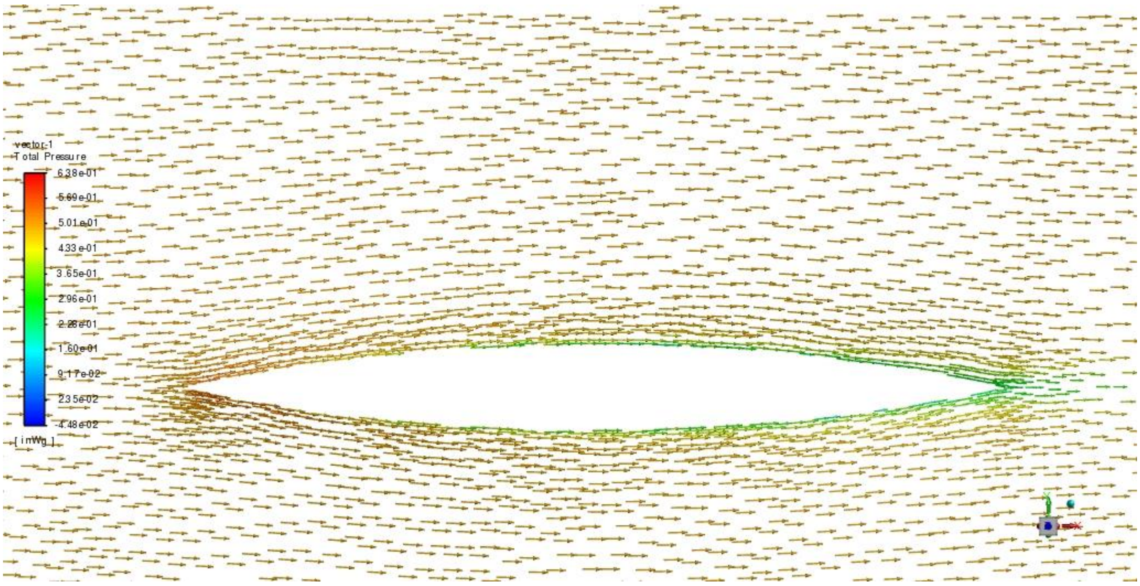

(e) 2500fpm

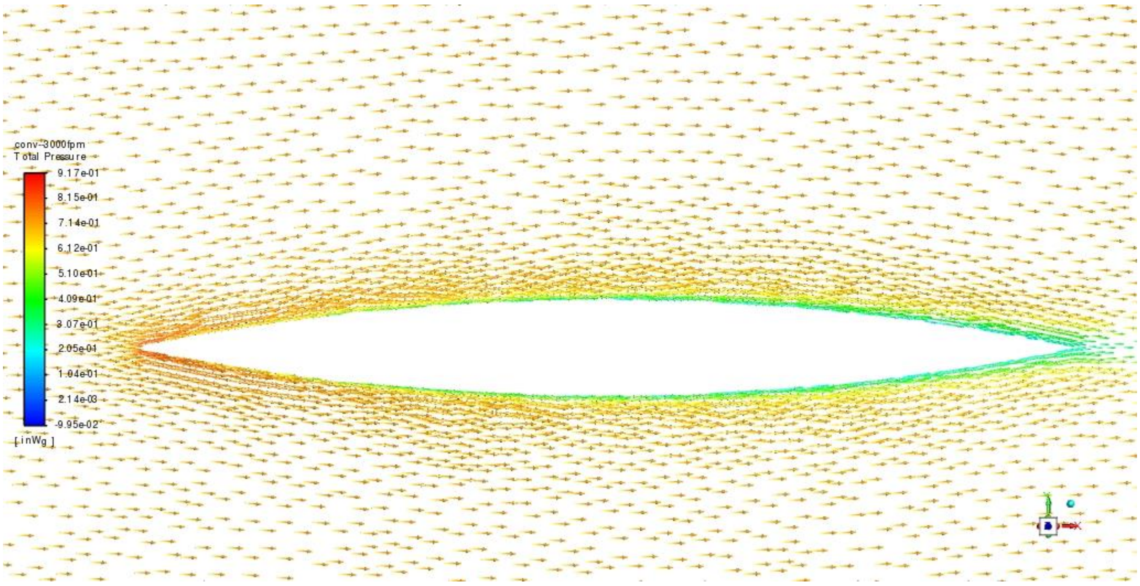

(f) 3000fpm

C2: Velocity vector colored by total pressure plot of NACA0010 airfoil for different velocities

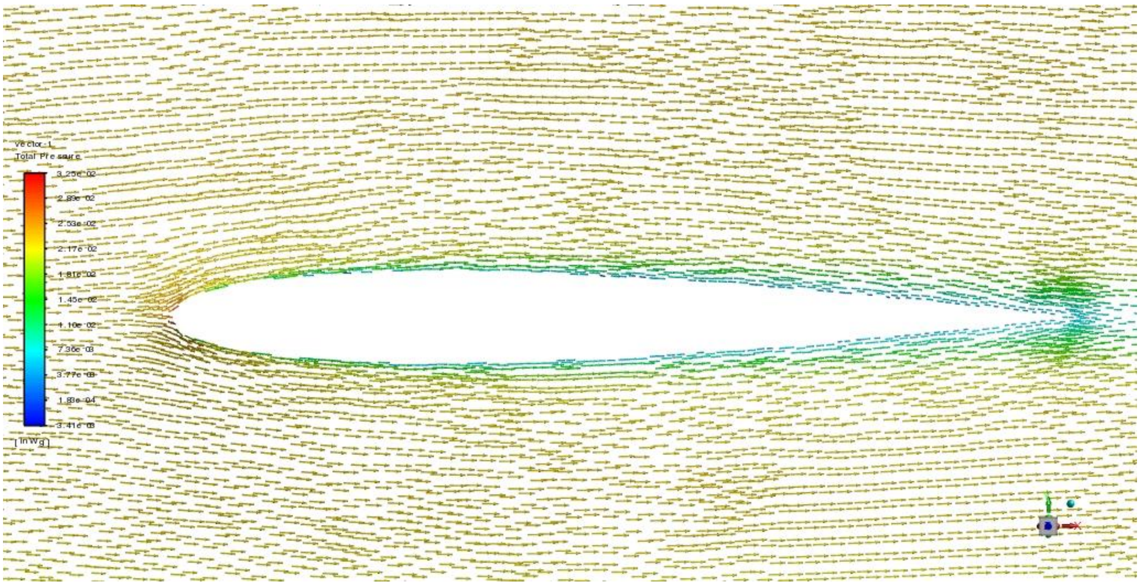

(a) 500fpm

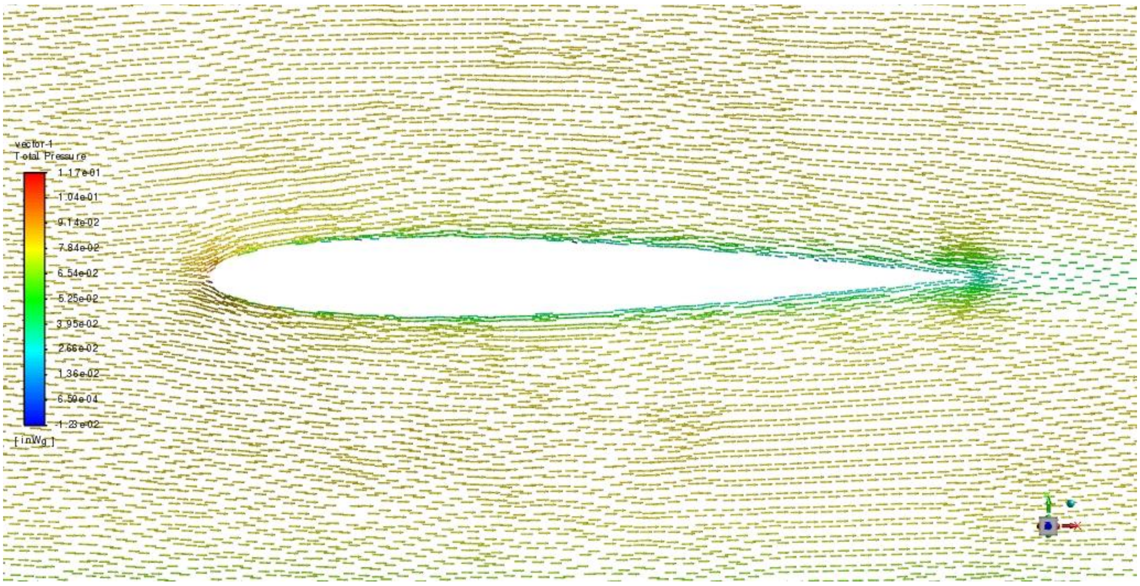

(b) 1000fpm

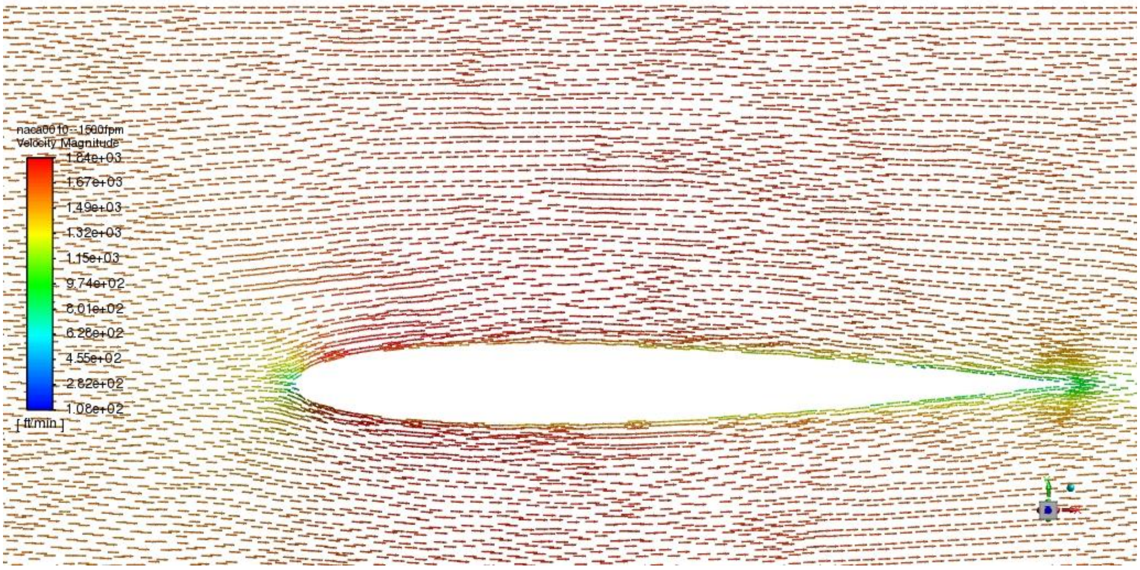

(c) 1500fpm

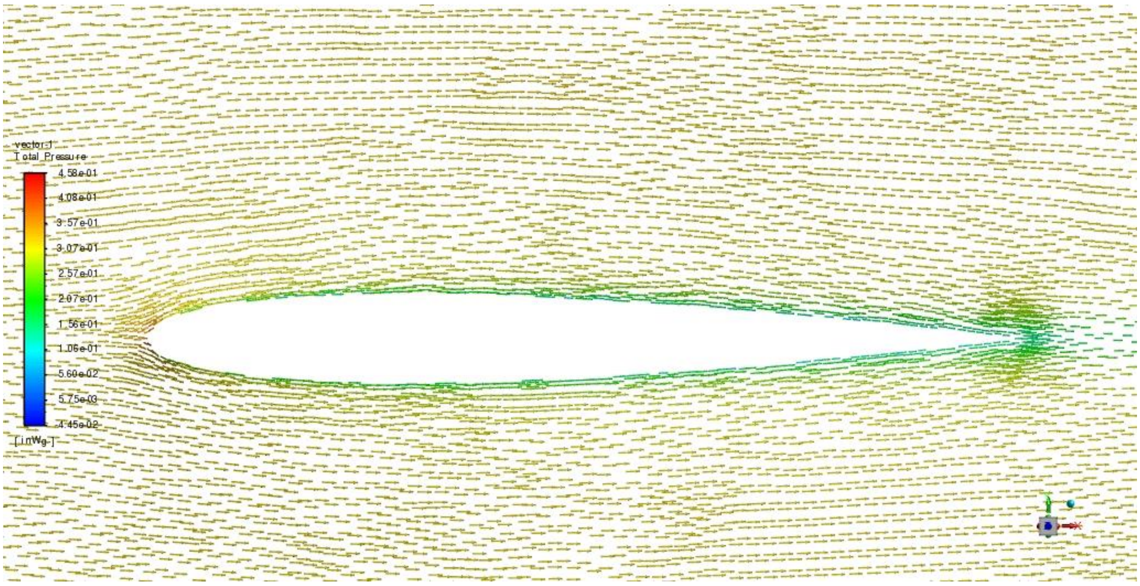

(d) 2000fpm

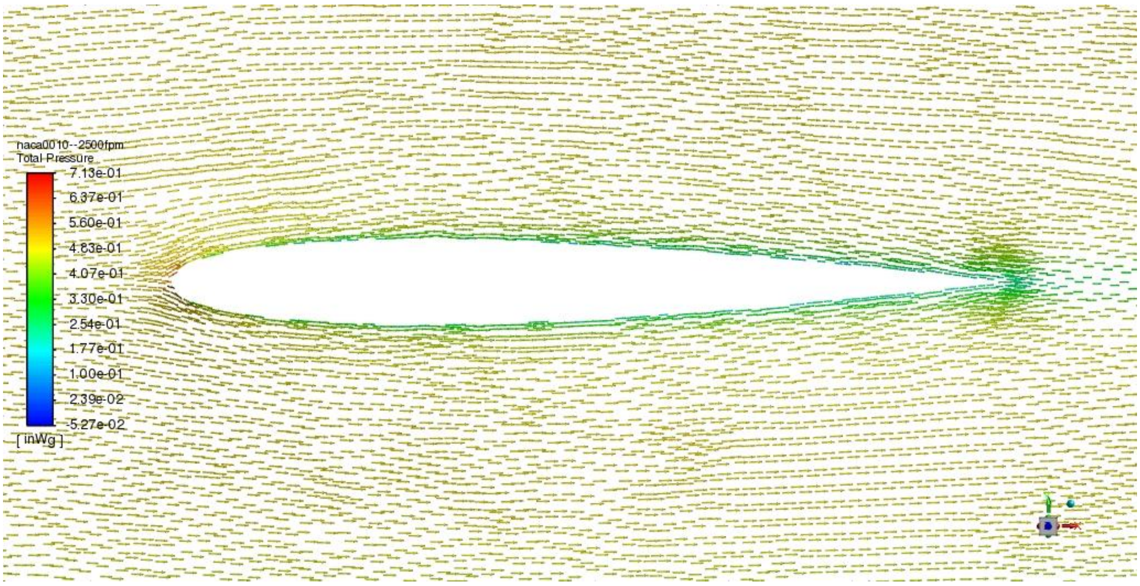

(e) 2500fpm

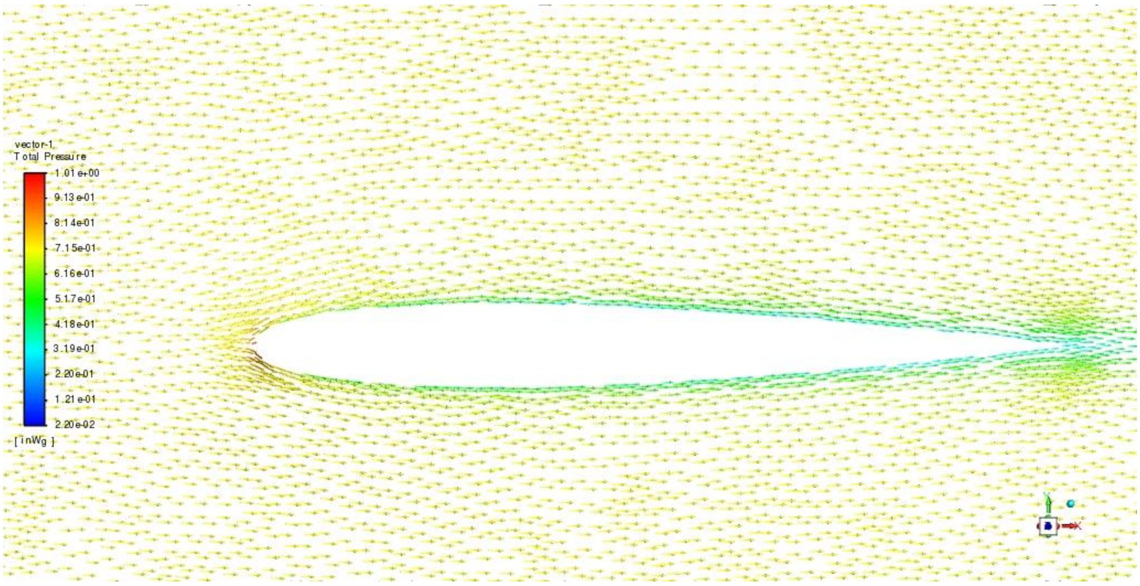

(f) 3000fpm

C3: Velocity vector colored by total pressure plot of conventional airfoil with reduced thickness for different velocities

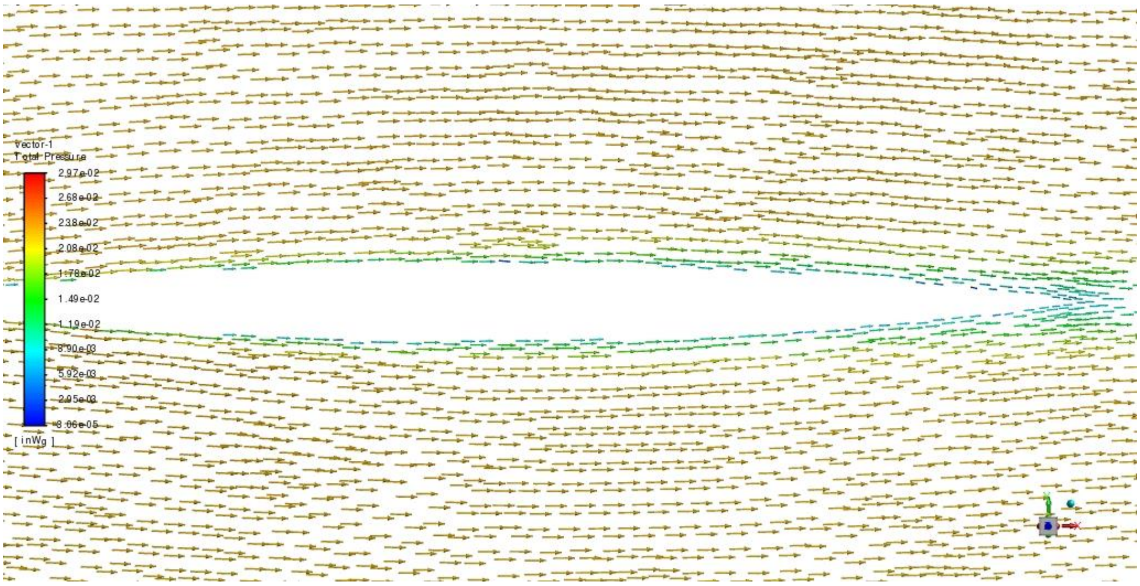

(a) 500fpm

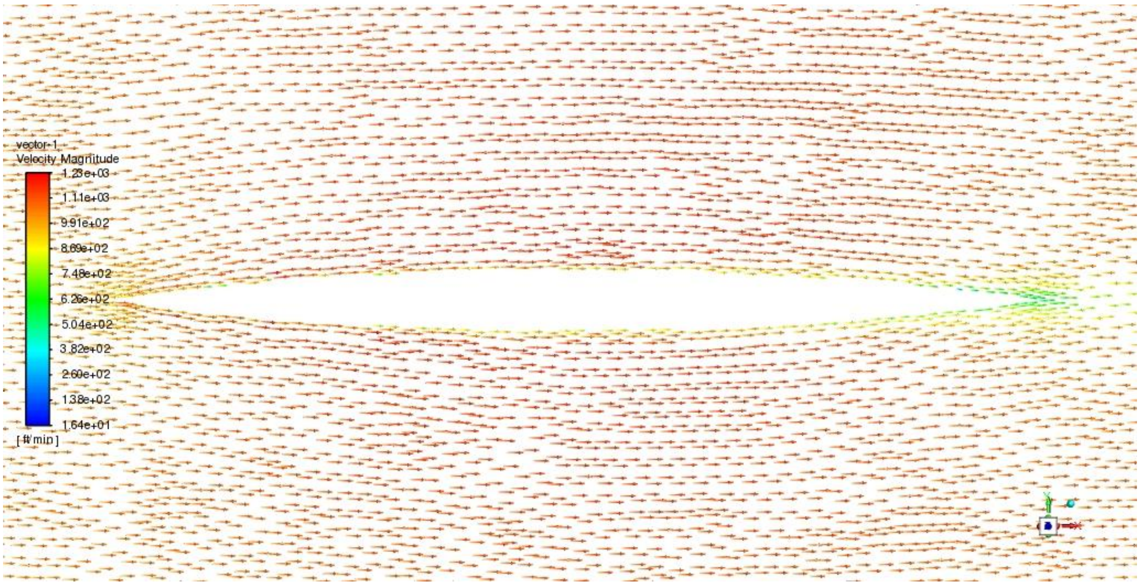

(b) 1000fpm

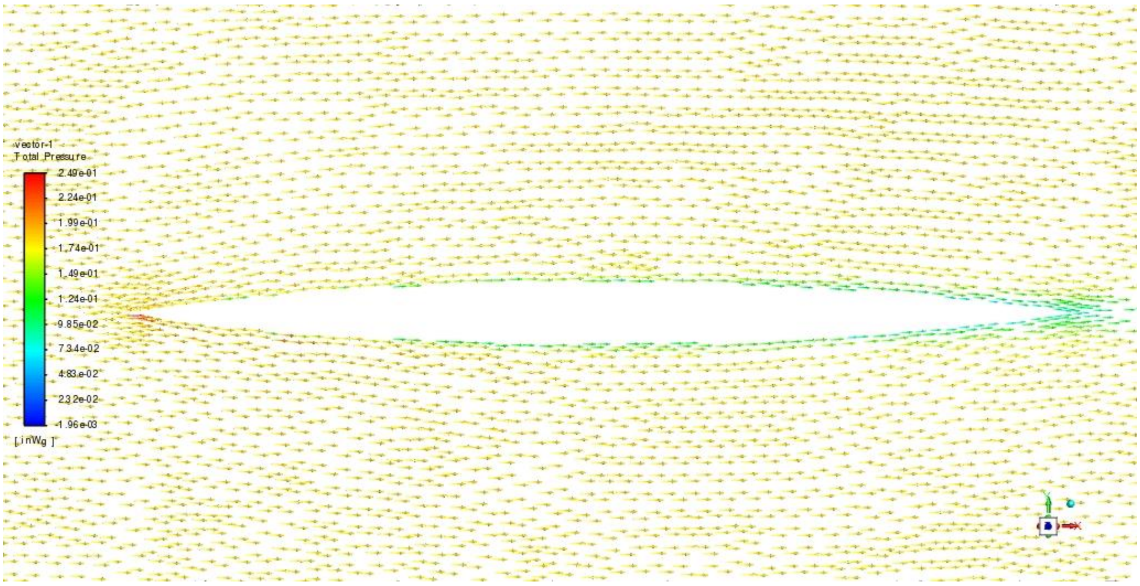

(c) 1500fpm

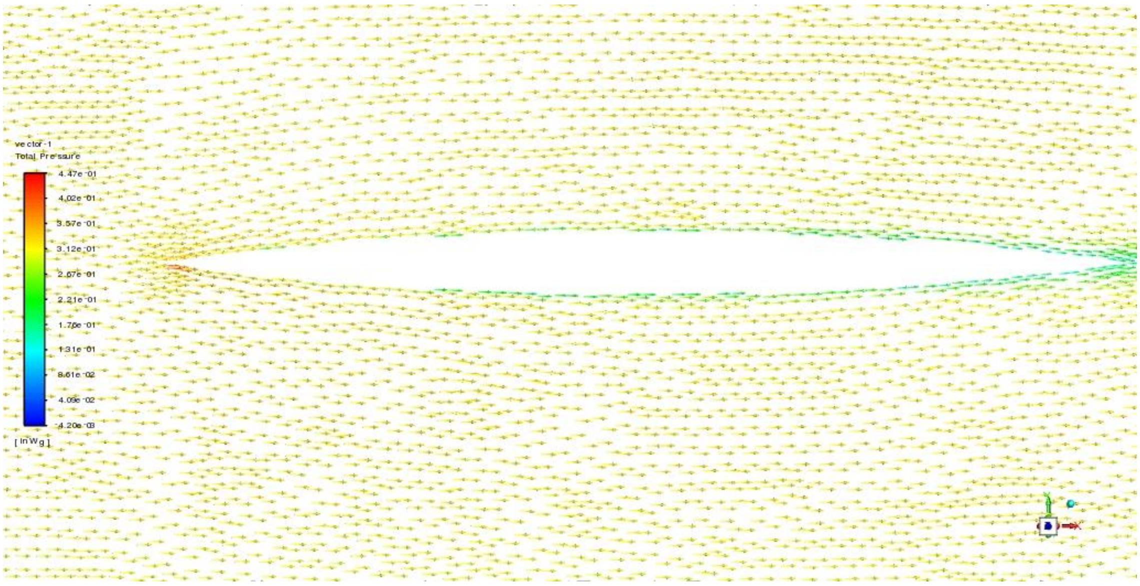

(d) 2000fpm

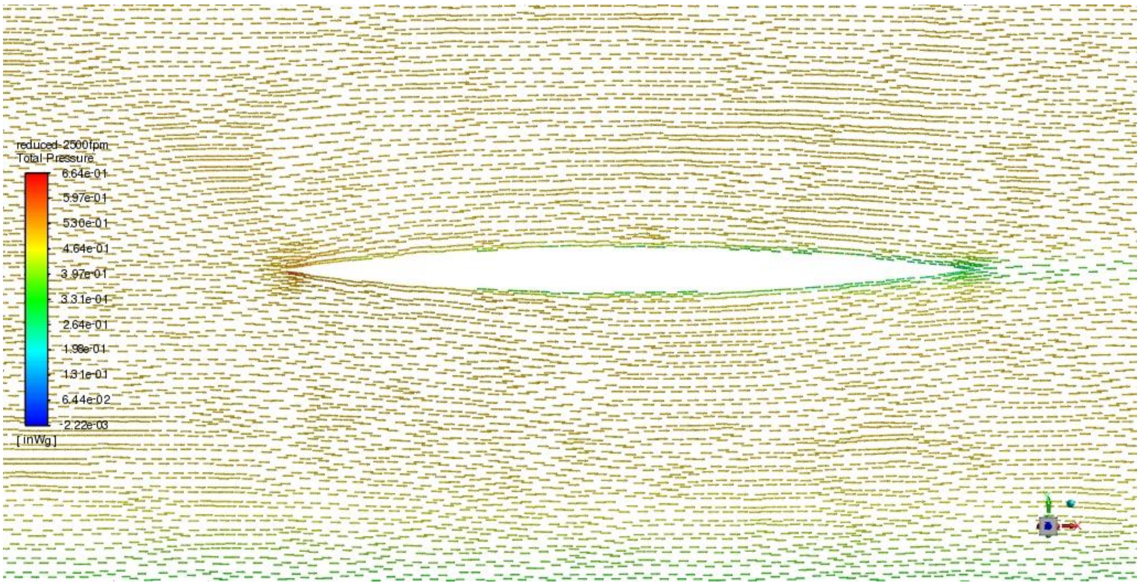

(e) 2500fpm

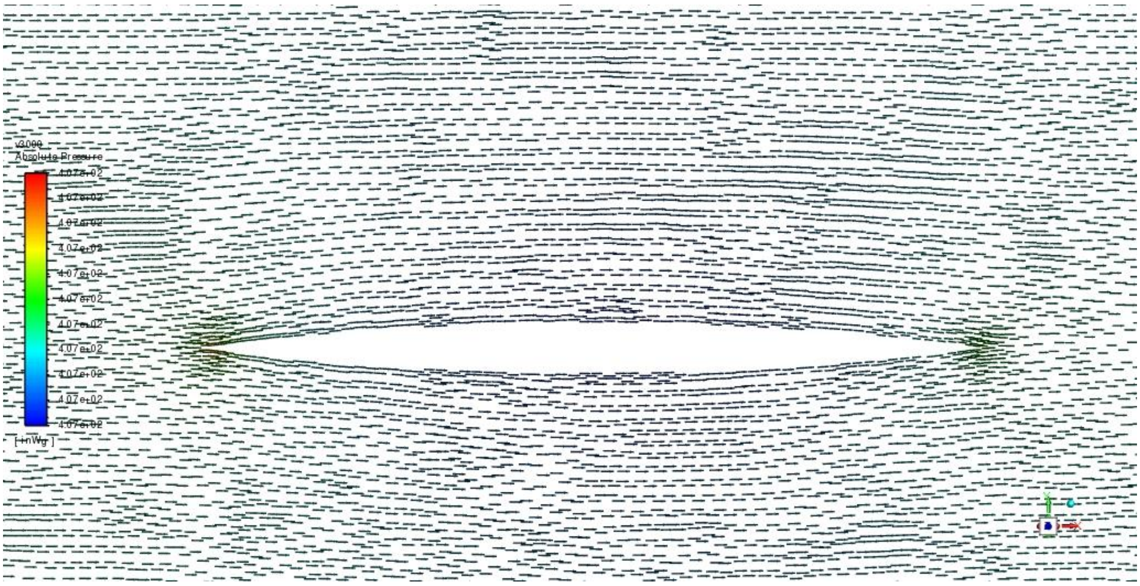

(f) 3000fpm

C4: Velocity vector colored by total pressure plot of NACA0006 airfoil for different velocities

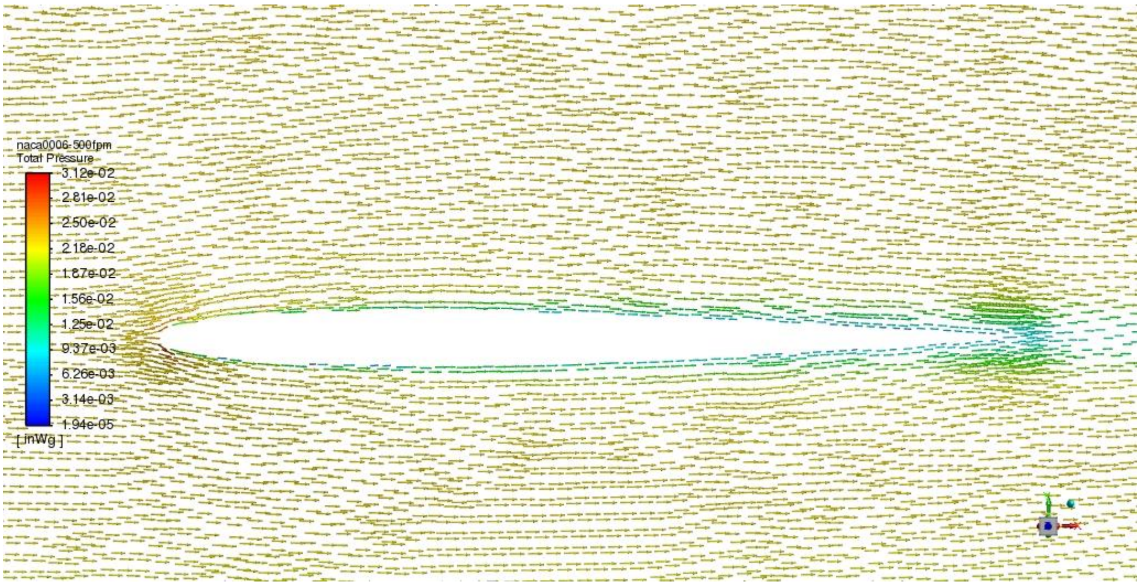

(a) 500fpm

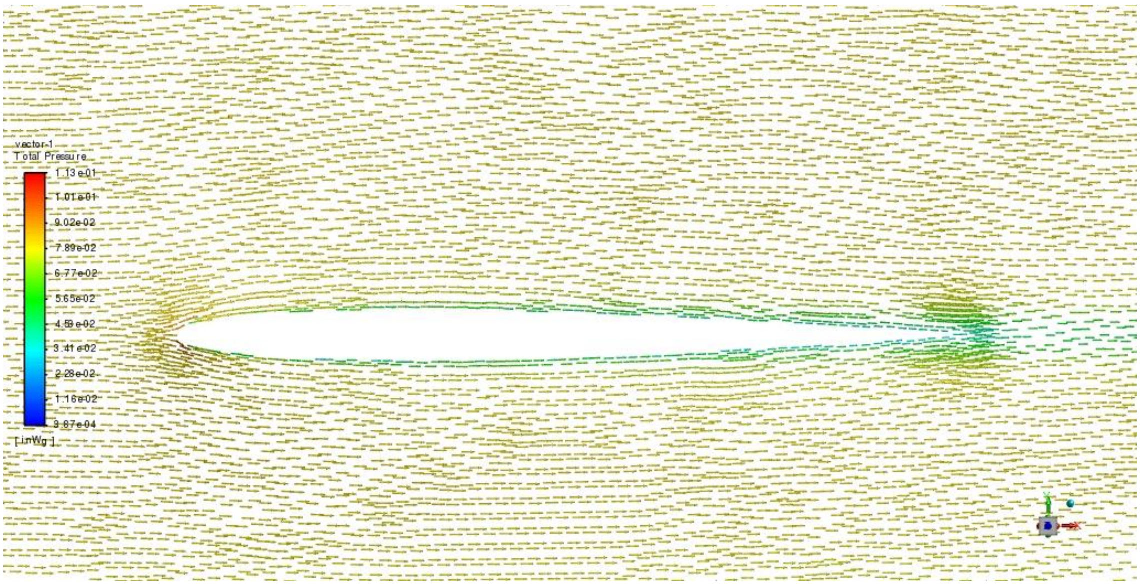

(b) 1000fpm

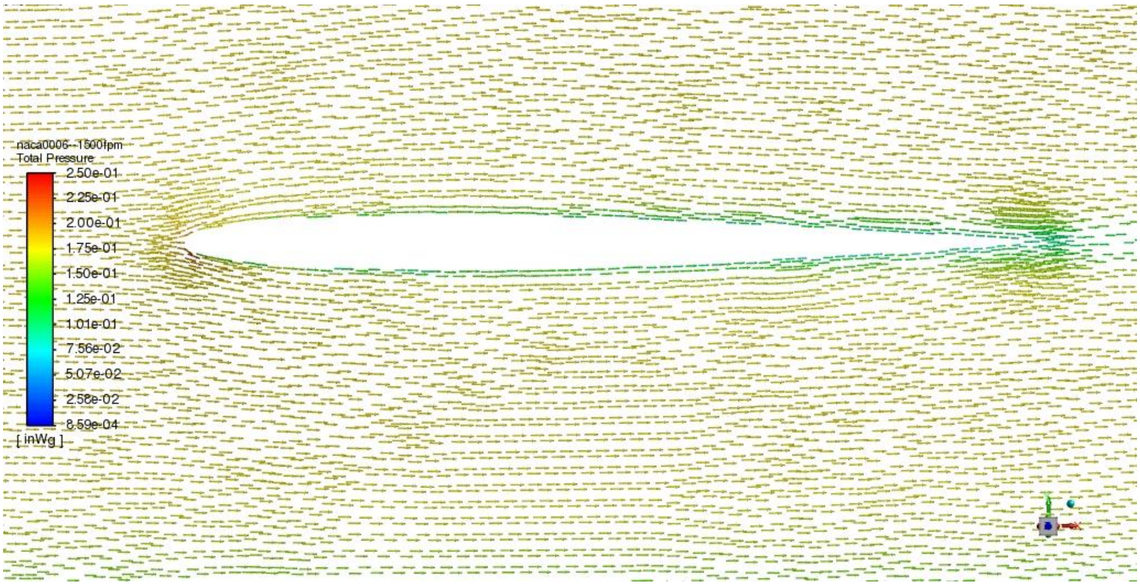

(c) 1500fpm

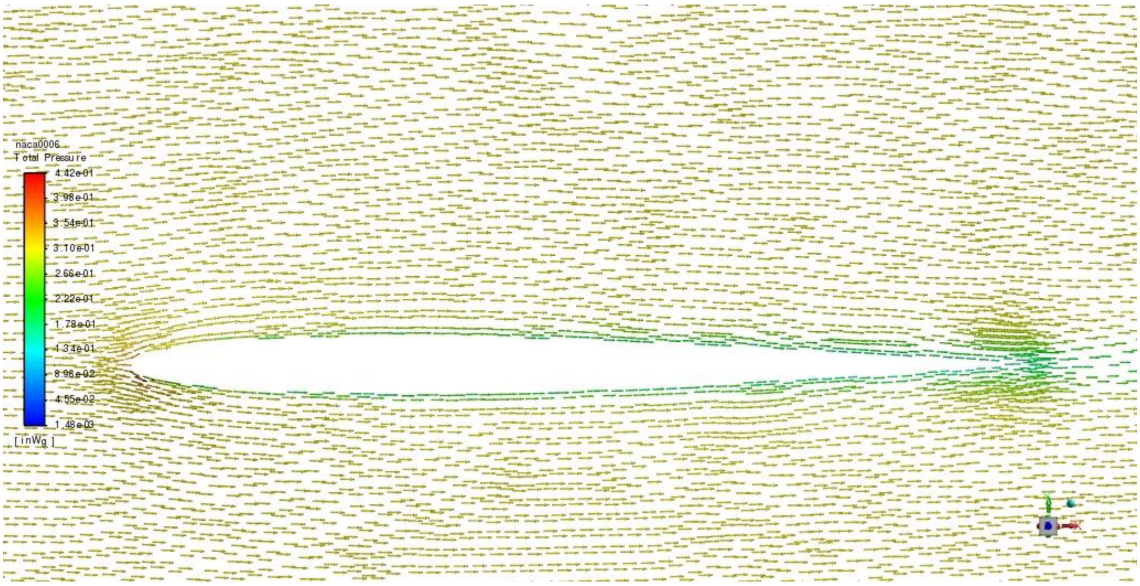

(d) 2000fpm

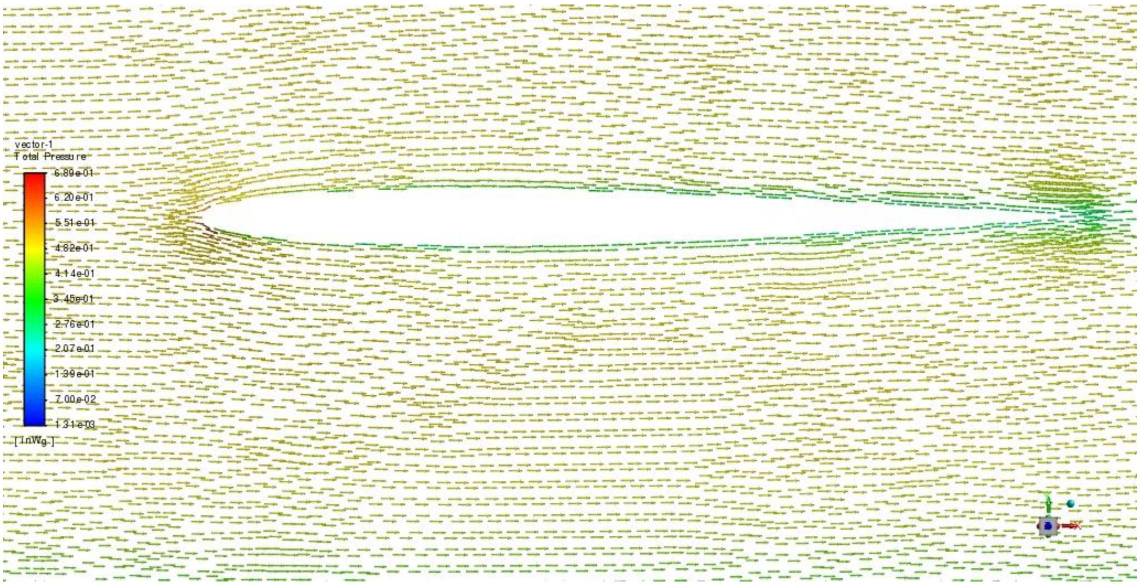

(e) 2500fpm

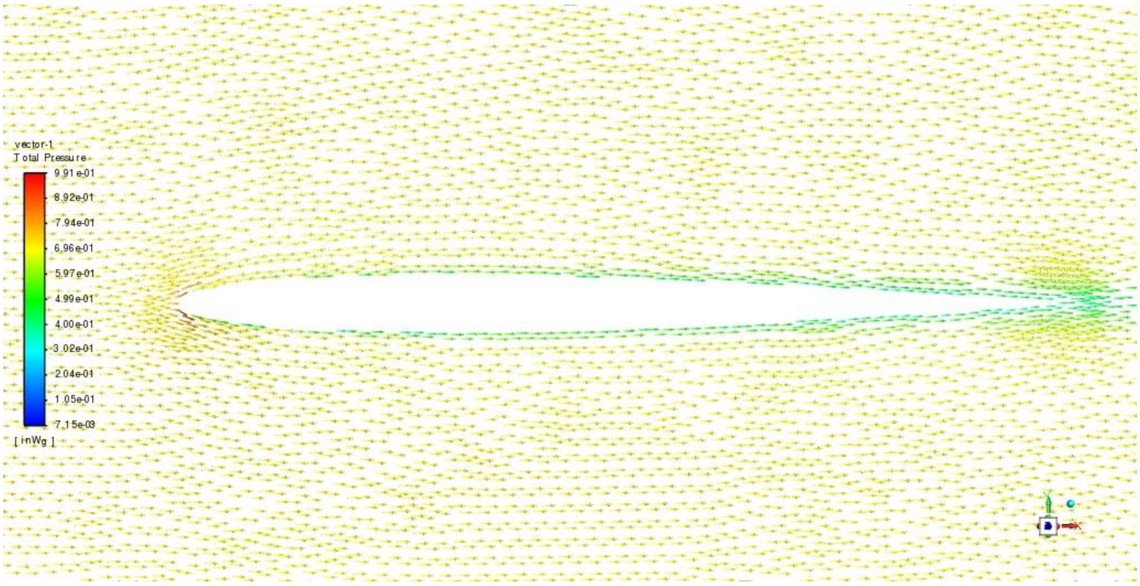

(f) 3000fpm